3DANMARKS OG GRØNLANDS GEOLOGISKE UNDERSØGELSE RAPPORT 2016/39

Geochronology of the larger Skjoldungen area, South-East Greenland (62° 30’ - 64° N)

Tomas Næraa, Thomas Find Kokfelt & Kristine Thrane

GEOLOGICAL SURVEY OF DENMARK AND GREENLAND
DANISH MINISTRY OF ENERGY, UTILITIES AND CLIMATE

GEUS

DANMARKS OG GRØNLANDS GEOLOGISKE UNDERSØGELSE RAPPORT 2016/39

Geochronology of the larger Skjoldungen area, South-East Greenland (62° 30’ - 64° N)

Tomas Næraa, Thomas Find Kokfelt & Kristine Thrane

GEOLOGICAL SURVEY OF DENMARK AND GREENLAND
DANISH MINISTRY OF ENERGY, UTILITIES AND CLIMATE

GEUS

Contents

Introduction

This geochronology report is based on samples that were collected during fieldwork in 2011 and 2012 in the Skjoldungen region of South East Greenland. Fieldwork was carried out within the framework of the “SEGMENT” project – a joint project between the National Geological Survey of Denmark and Greenland and The Ministry of Mineral Resources (MMR) in Greenland. Sample preparation and age dating was financed through the SEGMENT project and partly through a post-doc project sponsored by the Willum Foundation to Tomas Næraa.

This report presents zircon U-Pb data on 41 rock samples from the larger Skjoldungen region, which we here define as the area between Bernstorff Isfjord and Timmiarmiut Island (Figure 1), with the aim of characterizing the regional age profile of the felsic rocks. The Archaean basement rocks of this region are collectively described as the Thrym complex, as suggest by Bagas et al. (2013). The results from the 41 samples are listed in Table 1 and each sample is accompanied by a brief description with respect to lithology and field relations, as well as more detailed descriptions of the zircon textures and U-Pb data. This report excludes the rocks related to the Skjoldungen Alkaline Province (SAP) – rocks that can be found in the area around Skjoldungen Island and Kong Skjold Halvø – as these have been reported by Kokfelt et al. (2016). The U-Pb data are presented in two parts: Part 1 covers the northern section from Bernstorff Isfjord down to Helge Halvø (including this) (Figure 4). Part 2 covers the southern section from Kong Dan Halvø to Timmiarmiut Island (Figure 41). The report includes a summary and discussion of the presented age data.

Figure 1. *The larger Skjoldungen region of southern west Greenland. Red boxes outline the areas covered by the two parts in the report. Red circles indicate positions of U-Pb dated samples. Stippled box outlines the area covered by Kokfelt et al. (2016)*

Table 1. *Geographic locations and interpreted ages (Ma) for samples presented in this report. * Inherited ages are reported as the oldest documented age from each sample. I/M = igneous/metamorphic. TFN: Troels F.D. Nielsen, JKOL: Jochen Kolb, TOMN: Tomas Næraa*

					Skjoldungen orogeny			Gneiss protolith intrusion		Inherited#		Pegmatite	
Sample	**Latitude**	**Longi-tude**	**Station**	**Collec-tor**	**Age**	**2se**	**I/M**	**Age**	**2se**	**Age**	**2se**	**Age**	**2se**
Part 1 - Northern section from Thor Land to Helge Halvø													
288143	63.55503	-41.01379	-	TFN	2716	74	M	3026	11				
288145	63.55503	-41.01379	-	TFN	2702	10	M	2864	23				
527001	63.57162	-40.77822	11TOMN125	TOMN	2700	26	I			2976	33		
527006	63.56681	-40.78365	11TOMN130	TOMN	2721	7	I						
527009	63.57841	-40.78024	11TOMN134	TOMN				3046	6				
527010	63.57841	-40.78024	11TOMN134	TOMN				2797	12	3005	37		
527025	63.65995	-41.02610	11TOMN143	TOMN								2590	48
527041	63.57535	-40.77407	11TOMN155	TOMN								2601	9
527424	63.20861	-41.11895	11TOMN037	TOMN	2736	11	I			2963	23		
527425	63.20830	-41.11633	11TOMN038	TOMN	2740	14	I			2788	9		
527432	63.20996	-41.14006	11TOMN044	TOMN	2726	17	I			2886	5		
527435	63.20986	-41.14092	11TOMN047	TOMN	2733	10	I						
527454	63.28278	-41.22472	11TOMN069	TOMN	2724	8	I						
527458	63.28494	-41.18681	11TOMN074	TOMN	2718	11	I						
527460	63.28380	-41.18434	11TOMN075	TOMN	2721	12	I						
527463	63.38675	-41.34399	11TOMN079	TOMN	2731	9	I			2898	82		
527469	63.38655	-41.35038	11TOMN083	TOMN	2737	10	I			3078	80		
536001	63.37987	-41.15153	12TOMN8	TOMN	2738	18	I						
536517	63.63465	-40.79405	12TOMN27	TOMN	2701	11	I						
536525	63.60656	-40.99989	12TOMN29	TOMN						3015	13		
536526	63.60656	-40.99989	12TOMN29	TOMN	2713	31	M	2793	19				
536537	63.50894	-41.38611	12TOMN42	TOMN	2706	15	I						
536588	63.26427	-41.15231	12TOMN110	TOMN	2701	14	I						
536590	63.26440	-41.15124	12TOMN111	TOMN				2834	8				
Part 2 - Southern section, from Kong Dans Halvø to Tingmiarmiut													
523922	63.02227	-41.93940	12TOMN121	TOMN	2736	5	I						
523927	63.06282	-41.96599	12TOMN124	TOMN	2725	14	I						
523928	63.06282	-41.96599	12TOMN124	TOMN	2740	17	I			2876	29		
523941	62.83518	-41.92843	12TOMN138	TOMN	2731	7	I			2808	3		
523942	62.83518	-41.92843	12TOMN138	TOMN	2717	28	I			2793	19		
523947	62.78784	-41.96252	12TOMN139	TOMN	2724	17	I						
523949	62.80423	-42.24727	12TOMN140	TOMN	2722	7	I			2891	11		
523950	62.80423	-42.24727	12TOMN140	TOMN	2753	6	I			3235	20		
523961	62.84040	-42.37710	12TOMN143	TOMN				3231	12				
523962	62.88919	-42.37743	12TOMN147	TOMN	2728	7	I			3076	6		
523983	62.74651	-42.44880	12TOMN154	TOMN	2712	7	I			3885	10		
523991	62.46868	-42.19949	12TOMN160	TOMN	2740	5	I			2919	17		
527490	63.02900	-41.74066	11TOMN113	TOMN	2732	26	I			2833	11		
527492	63.03594	-41.74108	11TOMN116	TOMN	2735	10	I			2879	85		
527493	63.03551	-41.74688	11TOMN117	TOMN	2722	17	I			2872	9		
536574	62.89806	-41.60184	12TOMN105	TOMN						2765	7		

Methods

Zircon separation

Rock samples were crushed and sieved through a 500 µm mesh. Heavy mineral separates were either produced with a Wilfley shaking table or by pan washing. The heavy mineral fraction was transferred to disposable plastic Petri dishes using ethanol, and magnetic minerals were removed using a hand magnet. Zircon grains were subsequently hand-picked from the final heavy mineral concentrate in the Petri dish. The hand-picked zircon grains were cast into epoxy and polished to expose a central cross-section of each grain.

Zircon imaging

Prior to age analyses zircon grains were imaged for documenting internal textures. This documentation was done using petrographic light microscopy and scanning electron microscopy (SEM). All samples were imaged using SEM imaging, applying either cathodoluminescent (CL) or back scattered electron (BSE) methods. BSE images were done at GEUS using a Philips XL40 and CL imaging were done either at the Centre for Microscopy, Characterisation and Analyses at the University of Western Australia using a Zeiss 1555 VP-FESEM or at the Natural History Museum in Stockholm using a Hitachi S-4300 FE-SEM.

U-Pb analyses

LA-ICP-MS

Laser ablation - inductively coupled plasma - mass spectrometry (LA-ICP-MS) were for most part done on the Thermo Finnigan Element2 mass spectrometer coupled to a New Wave Research UP213 at the GEUS laboratory, with a setup similar to that described by Frei and Gerdes (2009). Few samples were analysed at Lund University using a Photon-machines 193nm G2 excimer laser coupled to a Bruker Aurora Elite Quadrupole. The New Wave laser was operated at a repetition rate of 10 Hz and nominal energy output of 55%, corresponding to a laser fluency of c. 8 J/cm^{-2}. The G2 excimer rate of 7 Hz and nominal energy output of 60%, corresponding to a laser fluency of c. 4 J/cm^{-2}. All data were acquired with a single spot analysis with a beam diameter of 25-30 µm and a crater depth of approximately 15–20 µm. For the spot diameter of 30 µm and ablation times of 20-30 s the amount of ablated material approximates 200–300 ng. The total acquisition time for each analysis was 50-60 s, with the first 20-30 s used to measure the gas blank. The instrument was tuned to give large, stable signals for the ^{206}Pb and ^{238}U peaks, low background count rates (typically around 150 counts per second for ^{207}Pb) and low oxide production rates (^{238}U^{16}O/^{238}U generally below 0.5 %). ^{202}Hg, ^{204}(Pb + Hg), ^{206}Pb, ^{207}Pb, ^{208}Pb, ^{232}Th and ^{238}U intensities were determined through peak jumping mode in both ICP-MS systems. Mass ^{202}Hg was measured to monitor the ^{204}Hg interference on ^{204}Pb where the ^{202}Hg/^{204}Hg

≡ 4.36, which can be used to correct significant common Pb contributions using the model by Stacey and Kramers (1975). $^{207}Pb/^{235}U$ was calculated from the $^{207}Pb/^{206}Pb$ and $^{206}Pb/^{238}U$ assuming $^{238}U/^{235}U \equiv 137.88$ (. The elemental fractionation induced by the laser ablation and the instrumental mass bias on measured isotopic ratios were corrected through standard-sample bracketing using the GJ-1 reference zircon (Jackson et al., 2004). For data obtained from GEUS, the data reduction was done using in-house data reduction software, whereas data from Lund University we reduced using the Iolite software (Paton et al., 2010; 2011). All isotope data were plotted and evaluated using ISOPLOT (Ludwig, 2008). For data quality, the natural zircon reference materials (Plešovice and 91500) were used as secondary standards (Sláma et al., 2008).

Nordic ion microprobe facility (Nordsim)

Secondary ion-mass spectrometry (SIMS) U–Th–Pb isotopic analyses were carried out using a large geometry Cameca IMS1280 instrument at the Swedish Museum of Natural History. The instrument set up follows that described by Whitehouse et al. (1999), Whitehouse and Kamber (2005) and references therein. An O_2^-primary beam was operated in aperture illumination (Köhler) mode yielding a ca. 15–20 µm spot. Pre-sputtering with a 25 µm raster for 120s, centring of the secondary ion beam in the 3000 µm field aperture (FA), mass calibration optimisation, and optimisation of the secondary beam energy distribution were performed automatically for each run. Mass calibration of all peaks in the mono-collection sequence was performed at the start of each session. A mass resolution (M/M) of ca.5400 was used to ensure adequate separation of Pb isotope peaks from nearby $HfSi^+$ species. Ion signals were detected using the axial ion-counting electron multiplier. All analyses were run in fully automated chain sequences. Data reduction assumes a power law relationship between Pb+/U+ and UO2+/U+ ratios with an empirically derived slope in order to calculate actual Pb/U ratios based on those in the 91500 zircon standard. U concentration and Th/U ratio are also referenced to the 91500 zircon standard. Common Pb correction is made if the ^{204}Pb signal statistically exceeds average background and assumes a $^{207}Pb/^{206}Pb$ ratio of 0.83 (equivalent to present day Stacey and Kramers (1975); model terrestrial Pb).

SHRIMP II

The U–Pb isotopic analyses on zircon were performed using the Sensitive High-Resolution Ion Microprobe (SHRIMP II) at the John de Laeter Centre of Mass Spectrometry, Curtin University. Isotope ratios and absolute abundances of U, Th and Pb were determined relative to the M257 zircon standard ($^{206}Pb/^{238}U$ age = 561 Ma, ^{238}U = 840 ppm; Nasdala et al. 2008), using the standard operating and data processing procedures described by Compston et al. (1984) and Claoué-Long (1995), and Zircon OGC–1 ($^{207}Pb/^{206}Pb$ age: 3465 Ma, with variable U contents) was used to monitor the $^{207}Pb/^{206}Pb$ ratio (Stern et al., 2009). Analyses of the M257 zircon standard were interspersed with those of unknown zircon grains during each measurement session. The surface of the sample was cleaned by rastering the primary ion beam over the area of the spot for a period of 3 minutes prior to each

analysis to reduce common Pb contamination. Data processing was carried out using SQUID 2.23 (Ludwig, 2009).

Regional geology

The Archaean Thrym complex in the Skjoldungen region in SE Greenland (Figure 4 and Figure 24) is dominated by amphibole- or pyroxene-bearing orthogneiss with abundant xenoliths of mafic and ultramafic lithologies and often with agmatitic textures where these propagate into belts of mafic granulites (Figure 2A; e.g. Nielsen et al., 1988; Kolb et al., 2013). The textural term “gneissic or agmatitic gneiss” is however not appropriate in many cases, as these units display a large degree of strain variation, and in many places are better described as inclusion-rich granites (Figure 2B, C). In many places the gneissic fabric is inherited from earlier basement rocks that have been infiltrated or sometimes almost totally assimilated by granitic melts in what might be described as lit-par-lit intrusions (Figure 2D, E). As a consequence the widespread gneissic fabric in the younger granitic intrusions often makes it difficult to distinguish them from earlier basement rocks, and challenge the understanding and interpretation of the observed textures and structures in the field. In general the older basement rocks are often modified heavily by influx of granitic melts at a syn-deformational stage (Figure 2D, E, Kolb et al. (2013) and Bagas et al. (2016)). These late melts also appear to have assimilated the pre-existing basement gneisses based on field evidence as well as the presence of inherited zircon populations. The age of these granitic intrusions range from ca. 2750 to 2700 Ma and the strain variation reflected in these rocks suggest that they were emplaced syn- to post tectonically (Bagas et al., 2013; Kolb et al., 2013; Berger et al., 2014)

Older rock units of grey banded gneiss and narrow supracrustal belts, up to several hundreds of metres thick and tens of kilometres long, are common in the northern part, as well as, in the southernmost part of the Thrym Complex (Bagas et al., 2013). The supracrustal belts are predominantly composed of mafic granulites, ultramafic rocks and para-gneisses that typically are infiltrated by a network of leucocratic orthopyroxene-bearing veins (Figure 2F, G). These leucocratic veins appear to date the peak granulite facies metamorphism that occurs regionally around 2750 Ma (Kokfelt et al. 2016; this report). Geochemically the felsic veins often display positive Eu-anomalies with extremely low HREE concentrations, suggesting derivation from partial melting with plagioclase as a melting phase e.g. hornblende and plagioclase melting reaction with orthopyroxene as a peritectic phase (Bagas el al., 2013).

In general the banded gneisses predate the granulite facies metamorphism throughout the Skjoldungen region. Prior to this study, the banded gneisses units were poorly documented in the Thrym complex. However a zircon U-Pb age of a banded gneiss sample (sample 516101) from Skjoldungen Island gave a protolith intrusion age of 2865 ± 7 Ma with two overprinting events recorded at 2797 ± 9 Ma and 2726 ± 14 Ma (Kolb et al., 2013). Early bulk-rock Sm-Nd data from an agmatitic gneiss from south of Sehested Fjord have been reported with a model age of c. 3130 Ma, and in the northern region from Imaersivik Island two samples of banded gneiss yield Sm-Nd model ages of 2880 and 2840 Ma, respectively (Kalsbeek and Taylor, 1993). Berger et al. (2014) published zircon U-Pb ages from two para-gneiss samples, yielding detrital zircon ages from ca. 2880 to 2800 Ma. In this report we document gneiss protolith ages in the northern part of the Thrym Complex ranging from c. 3050 to 2800 Ma and a single protolith age in the south at ca. 3230 Ma. These old proto-

lith ages, combined with age data from inherited zircons, show that the “old” basement of the Thrym complex is dominated by ages ranging from c. 3100 to 2800, however with the southern part also including even older ages of up to c. 3880 Ma.

Figure 2. *Field images highlighting the rock textures of Neoarchean leucocratic veins that intruded in the region from c. 2760 to 2700 Ma. Photos: a) Mafic belt in the northern part of the Thrym complex infiltrated by leucocratic granite; b) and c) strain variations in granitoid basement rocks from the southern part of the region; d) lit-par-lit intrusions and infiltration of leucocratic melts into mafic and felsic gneiss; e) and f) orthopyroxene-bearing leucocratic veins infiltrating mafic granulite; and g) banded-gneiss alternating with mafic granulite infiltrated by leucocratic undeformed leucocratic veins.*

The last major components of the Archaean basement are mafic and ultramafic to more evolved alkaline intrusions constituting the Skjoldungen Alkaline Province (SAP) that define a c. 30 km wide SE-trending belt in the northern part of the region around Skjoldungen Island (Blichert-Toft et al., 1995; Kokfelt et al., 2016). As discussed in this report and as shown by Bagas et al. (2013) and Kolb et al. (2013), the alkaline intrusions are synchronous with the granulite metamorphism and the granite influx (lit-par-lit intrusions). In this report we further include U-Pb data from undeformed network of leucocratic veins within a hornblendite in Thor Land (sample 527006), which arguably also belongs to the SAP.

Structural foliation trajectories in the southern part of the region are by Kolb et al. (2013) interpreted as early foliations (S_T), ascribed to the foliation in xenoliths and larger semi coherent belts of mafic rocks or from an inherited gneiss foliation that is clearly older than the granitic intrusions. However as described above strain variation in the inclusion-rich granitic intrusions from this part of the region induce a younger foliation trajectory within the granitoids (*Figure 2B, C*) and the foliation development in the southern part of the region is syn- to post magmatic in origin (belonging to the Skjoldungen orogeny). In the northern part of the region the main foliation trajectory is ascribed to isoclinal folding (F_{S1}) with associated penetrative foliation development (S_{S1}) (Kolb et al., 2013). The S_{S1} foliation is observed within mafic belts and banded gneiss. Both the S_{S1} and S_T foliation trajectories are situated in open to closed F_{S2} folds and late tectonic intrusions are described as intruding into the limbs of F_{S2} folds (Kolb et al., 2013). The syn- to post-magmagtic foliation in the southern region has therefore likely developed during F_{S2} shearing. These structural fabrics have been assigned to distinct deformation stages, where the S_T related deformation in the southern region has been assigned to the Timmiarmiut Orogeny. The S_{S1} foliation has been assigned to a younger deformation, which has been named the Skjoldungen Orogeny (Kolb et al., 2013).

Summary of geochronological data presented in this report

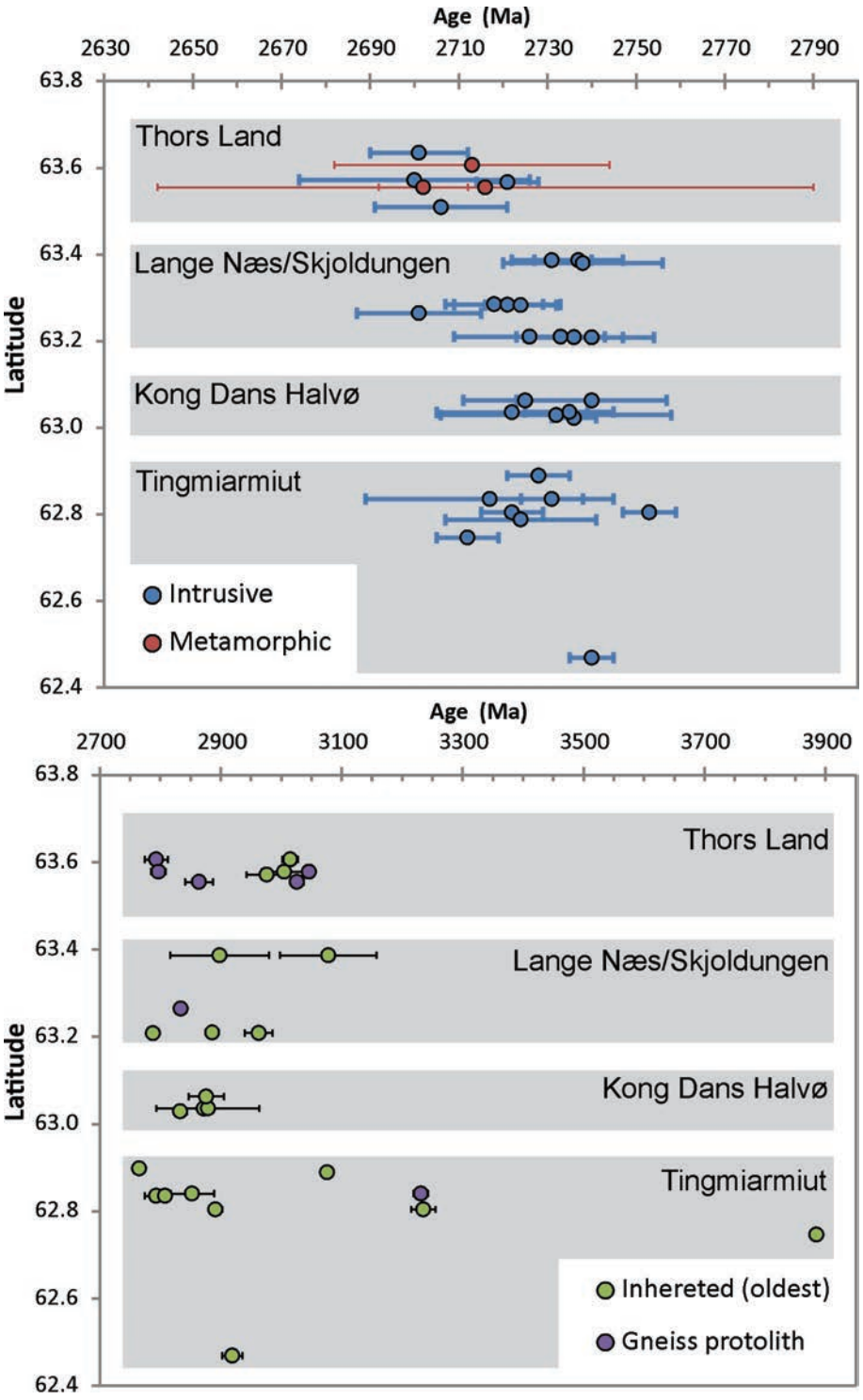

Figure 3. *Summary of ages presented in this report. A) Intrusive and metamorphic ages. B) Inherited and gneiss protolith ages.*

Throughout the Thrym complex the overall dominant rock type is a granitoid rock either undeformed or with a nebulitic or agmatitic texture and with abundant xenoliths of mafic and ultramafic lithologies. Leucocratic granitoids are abundant as veins and sheets within these mafic belts. The granitoids display strain variations and are likely intruded syn- to post tectonic, however the leucocratic melts within the mafic belts are rarely deformed. The strain is often focused in regions dominated by less competent felsic granitoid units, and between units of different strain competence, as often observed in the granitoid dominated southern part of the Thrym complex. Age dating presented in this report show that these units have crystallisation ages between 2700 ± 26 and 2753 ± 6 Ma (Figure 3A) and generally contain abundant zircon inheritance (Figure 3B). The intrusion ages of the granitoid rocks overlap in time with the intrusion age of the SAP, thus the major crustal remelting event within the region was associated with numerous intrusions of alkaline mafic to ultramafic magmas, however the relation (if any) between the crustally- and mantle derived melts are unknown. A northern possible extension of the SAP to the northern part of Thor Land is suggested in this report, based on the occurrence of a mafic-ultramafic intrusion with chemical composition similar to Vend Om Gabbro and with overlapping U-Pb age to the SAP. Here the new intrusion is represented by two samples of leucocratic veins/sheets related to an intrusive hornblendite (sample 527001 and 527006).

Older basement rocks represented by banded gneiss units mainly occur in the northern part of the region (Figure 4). Only one was visited in the southern region (sample 523961; Figure 42). The gneiss protolith intrusion ages for the banded gneisses in the northern region range from ca. 3050 Ma (sample 527009 and 288143) to c. 2860 Ma (sample 288145). A layered mafic rock with an age of c. 2800 Ma (sample 536526) is also documented. One banded gneiss outcrop in the south has a protolith age of c. 3230 Ma, distinctively older than observed in the gneisses from the northern region, although such ages here exist as inherited populations. The age range obtained from the banded gneisses is broadly matched by the inherited zircon ages contained within the granitoid intrusions throughout the whole area, suggesting that the older gneisses once constituted a much larger coherent part, but were to a large extend reworked to produce the later granitoid intrusions. In the southern part of the region, zircon inheritance in a few samples suggests that older Eoarchaean (up to 3885 Ma) basement rocks were present. That higher percentage of older basement (older than ca. 3200 Ga) is present in the southern part of the region is supported by zircon ages in stream sediments (Thrane and Keulen, 2015) and by Hf isotope signatures in zircons (Kokfelt et al., 2016).

Discussion

Age constraints on regional magmatism and metamorphism

Kolb et al. (2013) suggest that high-grade metamorphism was synchronous with emplacements of igneous orthopyroxene-bearing granites (charnockites) where one such example was dated to 2785 ± 9 Ma (unpublished data mentioned in Nutman and Rosing, 1994), and further suggest that migmatites dated at c. 2760-2740 Ma and associated foliation parallel lit-par-lit intrusions with magmatic fabric reflect a continuation of the high-grade metamorphism.

Several samples documented in this report have ages between 2800-2780 Ma. Rocks of this age in the northern part of the Thrym complex are observed as sheared or isoclinally folded leucocratic veins (samples 527010, 536526). Also present are inherited zircon grains of this age hosted by undeformed granitic sheets and veins within mafic units (samples 527425, 527432). In the southern part of the complex c. 2800 Ma ages are found in leucocratic granites expressed in zircon grains as inner rim domains (sample 536574, 523941, 523942, 523949, 523983 and 523991) surrounded by outer rim domains with ages around 2750-2720 Ma. The textures of the c. 2800-2780 Ma inner rims are mainly growth or sector zoned, suggesting that the age domains reflect a magmatic stage. Many of the grains with 2800 Ma inner rims have older xenocrystic core domains, one sample with ages up to c. 3880 Ma. Data presented in this report cannot confirm whether or not these inherited zircon grains crystallised in charnockitic rocks, as mentioned by Nutman and Rosing (1994) and advocated by Kolb et al. (2013). It is however clear that the zircon age domains (c. 2800-2780 Ma) reflect a magmatic event that includes remelting of crustal rocks, as seen from the xenocrystic zircon cores.

The regional intrusion of granitoid melts into the Thrym complex is dated to take place from c. 2760 to 2700 Ma with abundance of ages around 2730 Ma, the emplacement of the alkaline rocks of the SAP covers the same time span (Blichert-Toft et al., 1995; Kokfelt et al., 2016). It seems likely that this 60 myr long period can be divided into distinct stages; an early 2760 to 2750 Ma stage is documented by syenitic gneisses in the Kong Dans Halvø area, whereas subsequent stages at c. 2740, 2710 and 2700 Ma are localised in the Skjoldungen Island area (Kokfelt et al., 2016). Age data documenting the granulite facies overprinting within the mafic belts suggest that high-grade metamorphism occurred around 2740 Ma (Bagas et al., 2013, 2016; Berger et al., 2014; Tusch et al., 2014). Berger et al. (2014) reported zircon ages from a paragneiss within a mafic unit on Helge Halvø in the northern part of the Thrym complex and argue that there is evidence for two metamorphic rims with ages of 2742 ± 7 and 2701 ± 5 Ma. Another study (Tusch, 2014) from the same area focused on Lu-Hf isotope dating of garnet. The garnets were present as porphyroblasts in a metamorphic matrix containing mainly sillimanite and quartz. The rock unit was sheared during sillimanite growth and have later been heavily overprinted by the emplacement of undeformed granitic melts (dated at 2701 ± 14 Ma in this report; sample 536588). The garnet Lu-Hf isotope data yields an isochron age of 2742 ± 26 Ma (MSWD = 0.45), however the Lu-Hf isochron age could have been partly reset during this emplace-

ment of the granitic melts. The garnets have homogeneous major element compositions and it seems likely that garnet growth took place during a prograde path and were homogenised at peak conditions (c. 800 °C) and that shearing occurred during retrograde conditions as observed from growth of sillimanite (Tusch, 2014). Further estimates on peak metamorphism are based on zircon rims found in a sample of a mafic granulite, from which Bagas et al. (2016) suggest that metamorphic peak conditions occurred at 2744 ± 9 Ma, in good agreement with the previous data. Thus several lines of evidence suggest consistently that granulite facies overprinting occurred between 2735 and 2753 Ma.

Several samples in this report are from leucocratic veins (leucosome) within the mafic granulites (sample 527432, 527435, 527424, 527425, 527454, 527463, 527469) and as such these could be related to partial melting during granulite facies conditions. These samples yield ages from 2724 ± 8 Ma to 2740 ± 14 Ma, with a weighted mean age of **2732 ± 5** Ma (n = 7; MSWD = 1.2). This suggests that zircon crystallisation in the leucosome occurred after peak granulite facies conditions during the retrograde path. In the southern part of the Thrym complex mingling of mafic and felsic rocks are observed at two localities (described under sample 523922, 523927 and 523928) and the mean crystallisation age of these units are **2735 ± 11** Ma (n = 3; MSWD = 1.3; ranging from 2725 ± 14 Ma to 2740 ± 17 Ma), it is uncertain whether these rocks belong the SAP. In the same part of the complex, the granitoid rocks from the area south of Kong Dans halvø are mainly amphibole-bearing granites with some examples of assemblages that were retrogressed from granulite facies conditions as witnessed by orthopyroxene overgrown by hornblende (brown agmatites in Nielsen, 1988). Age data from these samples (527490, 527492, 527493, 523941, 523942, 523947, 523949, 523950, 523962, 523983 and 523991) range from 2712 ± 7 Ma to 2735 ± 10 Ma (excluding sample 523950 that has an age of 2753 ± 6 Ma), with an average of **2730 ± 6 Ma** (n = 10; MSWD = 3.4).

Kolb et al. (2013) report ages of orthogneiss in the Thor Land area (sample 516150) and from a undeformed leucocratic vein (sample 516151) within the orthogneiss. Data from both samples have main zircon age populations that yield mean upper intercept ages of c. 2706 ± 11 Ma. This age is interpreted as reflecting the crystallisation age of the leucocratic vein, and is suggested (by Kolb et al., 2013) to reflect a second deformation stage (D_{S2}) of the Skjoldungen Orogeny. Data presented in this report from the same area document undeformed leucocratic and gabbroic melts veins (sample 536517) with ages ranging from **2721 ± 7 Ma** to **2700 ± 26 Ma**. In addition, the leucocratic net-veining of the hornblendite yields an age of 2721 ± 7 Ma (mentioned under sample 527001 and 527006), which likely reflects back-veining or residual melts, suggesting that this time period was associated with the intrusion of mafic- to ultramafic melts. This magmatism could likely be related with the magmatism in SAP (Blichert-Toft et al., 1995; Kokfelt et al., 2016). Late intrusive undeformed granitoids are also documented as intrusive sheets at Helge Halvø and Lange Næs (sample 527458, 527460, 536588 and 537537) with ages ranging from 2701 ± 14 Ma to 2721 ± 12 Ma with a weighted mean of **2713 ± 15 Ma**.

Overall the zircon age data suggest that the main influx of granitic melts in the mafic belts intruded either during or slightly after the granulite facies metamorphic event. Two main stages of magmatism have been identified:1) an early stage at c. 2740 to 2725 Ma at peak to post-peak granulite metamorphism, and 2) a later stage at c. 2700 to 2720 Ma, which

seems to be closely related to the intrusion of the mafic and ultramafic units of the SAP (Kokfelt et al., 2016). Furthermore, the shearing observed in the rocks of the southern part of the region (Figure 2C) could imply that foliation trajectories in the southern region developed syn-magmatically, this foliation development could likely have been developed during F_{S2} fold development and associated shearing at 2712 ± 7 to 2753 ± 6 Ma (Kolb et al., 2013).

Part 1: Northern section from Thor Land to Helge Halvø

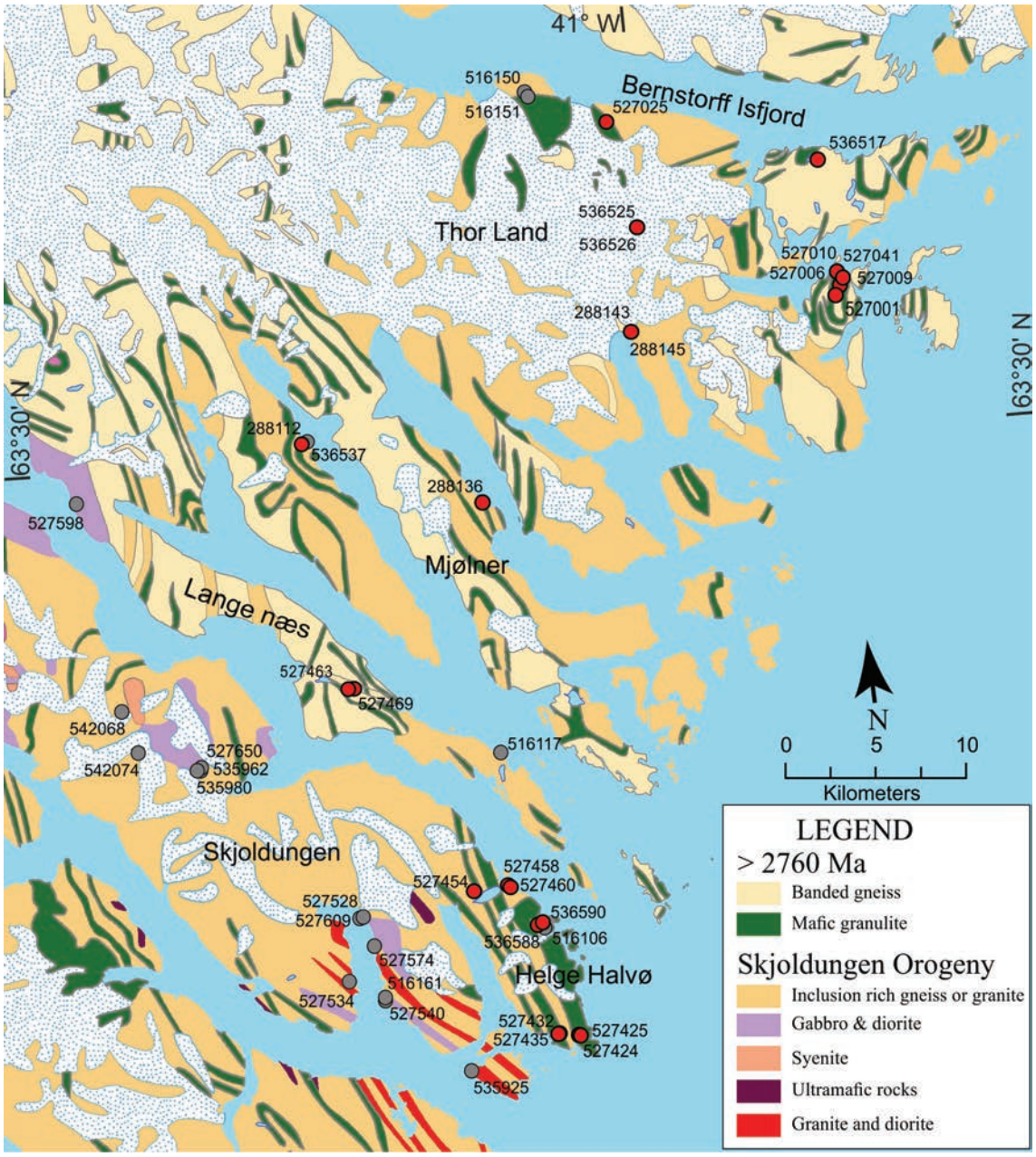

Figure 4. *Simplified geological map of the northern part of the region. Red circles are locations for samples presented in this report. Grey dots are locations for samples where geochronology is reported either in Kolb et al. (2013), Berger et al. (2014) or Kokfelt et al. (2016).*

Banded gneiss in Thor Land

Banded gneiss with isoclinal folded leucocratic horizons (sample 527009 and 527010)

Description: Locally occurring banded gneiss consisting of a melanocratic component with two generations of granitic veins; one that is foliated and isoclinal folded and a younger undeformed variety (Figure 5). The melanocratic part of the gneiss (sample 527009) was sampled to exclude as much of the later leucocratic veining as possible. Sample 527010 was sampled from a foliated leucocratic part of the gneiss. The undeformed leucocratic granite veins have not been age dated.
Purpose: Protolith age of banded grey gneiss and age of the early intrusive leucocratic veins.
Analytical methods: BSE-imaging; GEUS LA-ICP-MS data.

Figure 5. *Outcrop photographs displaying the different components of the gneiss in Thor Land. Sample 527009 is taken from the grey part of the gneiss, sample 527010 is from the isoclinal folded leucocratic veins. The late undeformed leucocratic granite veins are also present at the locality, but are not obvious in the shown photographs.*

Melanocratic part of gneiss (sample 527009)
Data description and interpretation: Zircon grains are prismatic to oblate and vary in size from 100 to 300 µm in length (Figure 6C). Internal textures are composed of growth zoned core domains and thin (mainly less than 10 µm) homogeneous rims. Zircon U-Pb age data are mainly concordant and plot in one group (Figure 6A) with $^{207}Pb/^{206}Pb$ ages ranging from 2981 ± 58 Ma to 3079 ± 40 Ma. Th/U values cluster between 0.5 and 1 with no relationship with age (Figure 6B). By selecting all data that are less than 10 % discordant we obtain a weighted mean $^{207}Pb/^{206}Pb$ age of **3046 ± 6 Ma** (n = 35; MSWD = 0.64), which are interpreted to reflect the crystallisation age of the melanocratic gneiss protolith.

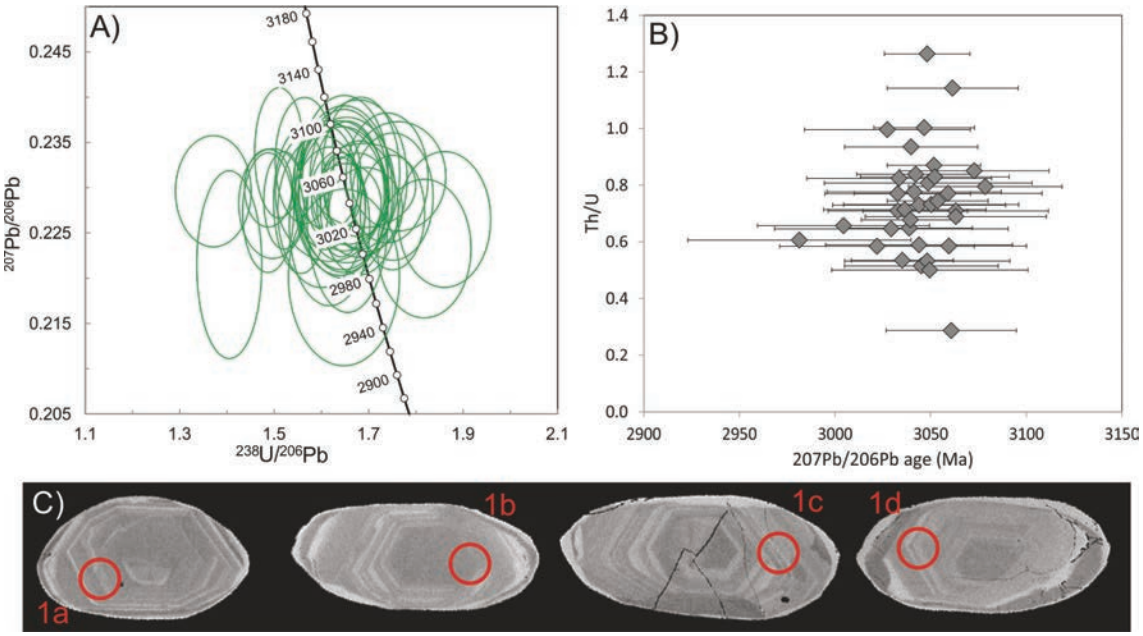

Figure 6. *Sample 527009. A) Tera-Wasserburg diagrams with all data plotted, B) Th/U vs. $^{207}Pb/^{206}Pb$ age, C) zircon textures with wide rather diffuse growth zoning patterns. Red circles indicate laser spot (30 µm diameter), $^{207}Pb/^{206}Pb$ ages, 1a: 3048 ± 43 Ma, 1b: 3054 ± 26 Ma; 1c: 3052 ± 39; 1d: 3060 ± 41 Ma. Errors are on 2σ level.*

Leucocratic foliated gneiss (sample 527010)

Data description and interpretation: Zircon grains are mostly prismatic ranging between 100 and 400 µm in length, but also include oblate grains. Internal textures are variable, often including core and rim domains. The core domains are variously altered, and often homogeneous, only a few grains being growth zoned. Rim domains are mainly homogeneous and often separated from core domains by an inclusion-rich narrow zone (Figure 7C). Zircon U-Pb age data are >90% concordant with ages ranging from 2636 to 3046 Ma. The analyses define two age groups, the main one around 2800 Ma and a smaller one around 3000 Ma (Figure 7A, B). Th/U values range from 0.1 to 2.1, for the 2800 Ma age group whereas the older group has Th/U values between 1 and 1.4. By selecting analyses with ages above 2700 Ma and below 2890 Ma (the main population) we obtain a weighted mean $^{207}Pb/^{206}Pb$ age of **2797 ± 12 Ma** (n = 29; MSWD = 1.7), which we interpret as the crystallisation age of foliated leucocratic veins. The three oldest analyses (>90% concordant) have a weighted mean $^{207}Pb/^{206}Pb$ age of 3005 ± 37 Ma (n = 3; MSWD = 1.3), which is similar as the age of the intruded gneiss (527009) and as such likely to be xenocrystic grains from the melanocratic host gneiss.

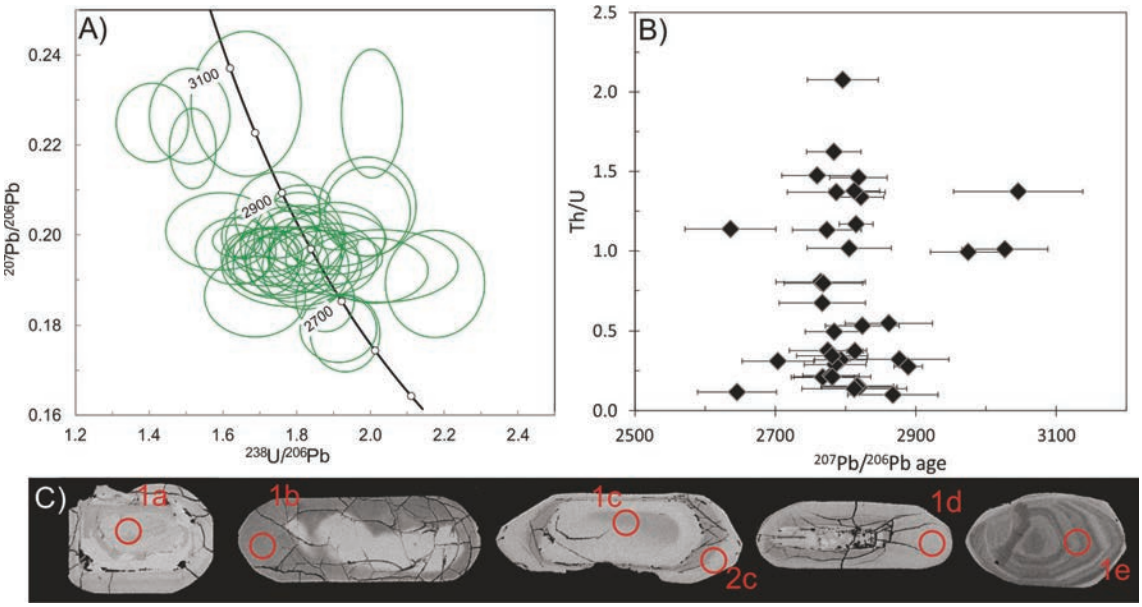

Figure 7. *Sample 527010. A) Tera-Wasserburg diagram with all data plotted. B) Th/U versus $^{207}Pb/^{206}Pb$ age diagram. As observed the main population plots with an age around 2800 Ma interpreted as the crystallisation age of the leucocratic veins. C) Zircon textures; the ca. 2800 grains have homogenous textures (1a-1d), whereas few grains with growth zoned textures (1e) have ages up to 3046 Ma. Red circles indicate location of laser spots, $^{207}Pb/^{206}Pb$ ages, 1a: 2784 ± 41 Ma, 1b: 2767 ± 62 Ma, 1c: 2768 ± 45 Ma, 2c: 2645 ± 56 Ma, 2785 ± 44 Ma, 3046 ± 92 Ma. Spot size 30 microns. Errors are on 2σ level.*

Grey migmatitic gneiss (sample 288143)

Description: Grey migmatitic gneiss
Purpose: Age of gneiss protolith inheritance and metamorphic overprinting.
Analytical methods: BSE-imaging; GEUS LA-ICP-MS data.

Data description and interpretation: Many zircon grains are growth zoned, however overprinting textures, e.g. homogeneous rims or internal domains are common (Figure 8C). The analyses are relatively concordant and plot in two groups with $^{207}Pb/^{206}Pb$ ages ranging from 2692 ± 65 Ma to 3058 ± 56 Ma (Figure 8A). Th/U values range from 0.16 to 1.0 and do not show any relationship with age (Figure 8B). The main age population based on analyses that are < 2 % discordant yields a weighted $^{207}Pb/^{206}Pb$ age of **3026 ± 11 Ma** (MSWD = 0.25). This age is interpreted to reflect the minimum intrusive age of the gneiss protolith. An age of the overprinting is poorly constrained, however, the three analyses with the youngest ages give an imprecise average of **2716 ± 74 Ma** (MSWD = 1.4).

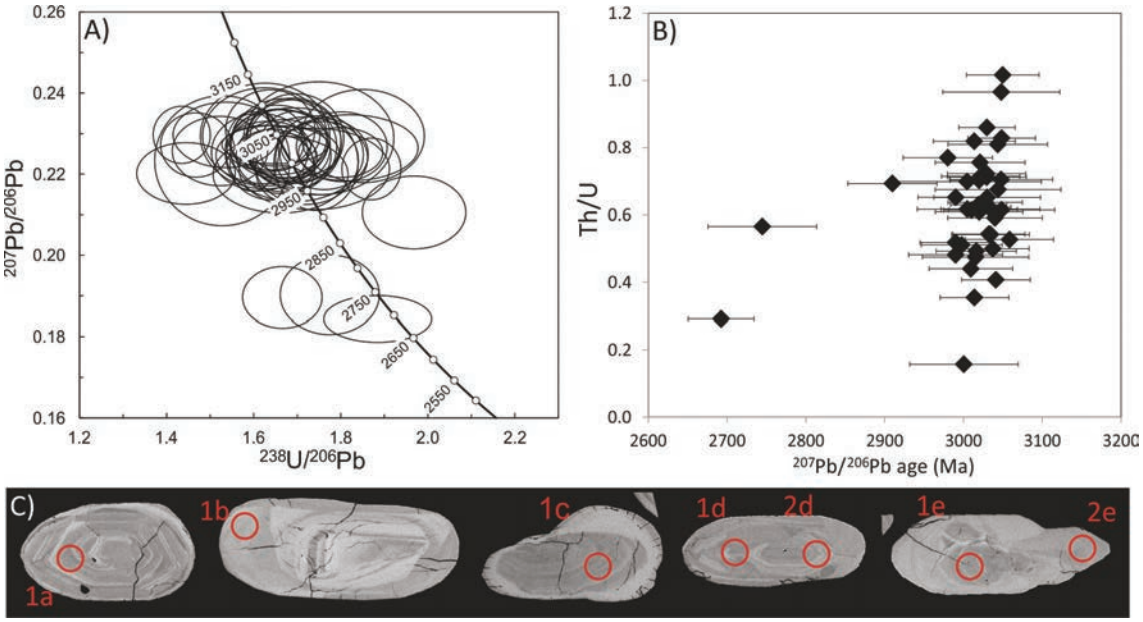

Figure 8. *Sample 288143. A) Tera-Wasserburg diagram with all data. B) Th/U versus $^{207}Pb/^{206}Pb$ age diagram. C) Zircon BSE images, with a clear distinction between growth zoned core domains and homogeneous rim domains. Red circles indicate location of laser spots, $^{207}Pb/^{206}Pb$ ages, 1a: 3034 ± 63 Ma, 1b: 2745 ± 69 Ma; 1c: 3058 ± 56 Ma; 1d: 3041 ± 44 Ma, 2d: 3044 ± 63 Ma; 1e: 3015 ± 67 Ma, 2e: 2692 ± 42 Ma. Spot size 30 µm. Errors are on 2σ level.*

Reddish gneiss (sample 288145)

Description: Reddish gneiss intrusive into grey gneiss (sample 288143)
Purpose: Age of the intrusion and inheritance
Analytical methods: BSE-imaging; GEUS LA-ICP-MS data.

Data description and interpretation: Zircon grains often have growth-zoned cores and homogeneous rims, and many grains have metamict inner domains, often as inner rims (Figure **9**C). Zircon U-Pb age data are generally concordant and plot in a group that smears out along concordia, with $^{207}Pb/^{206}Pb$ ages ranging from 2659 ± 99 Ma to 2883 ± 88 Ma (Figure **9**A). Th/U values range from 0.1 to 0.9 and show no obvious correlation with $^{207}Pb/^{206}Pb$ age (Figure **9**B). By selecting analyses from growth zoned core domains a mean age of **2864 ± 23 Ma** (MSWD = 0.15) is obtained, this age is interpreted to reflect the intrusive age of the gneiss protolith. Selecting spots from the homogeneous rim domains a weighted mean age of **2702 ± 10 Ma** (MSWD = 0.9) is obtained. As the unit is intrusive into the grey gneiss represented by sample 288143, there seems to be two possibly interpretations of the obtained data: 1) The core age reflects the intrusion age of the red gneiss into the grey gneiss, and the rim domains record metamorphic overprinting. 2) The rim domains of the zircon grains in the red gneiss reflect the intrusion of the red gneiss into the grey gneiss; in this interpretation the core domains are inherited. Our preferred interpretation is that the core domains reflect the intrusion age of the protolith of the red gneiss.

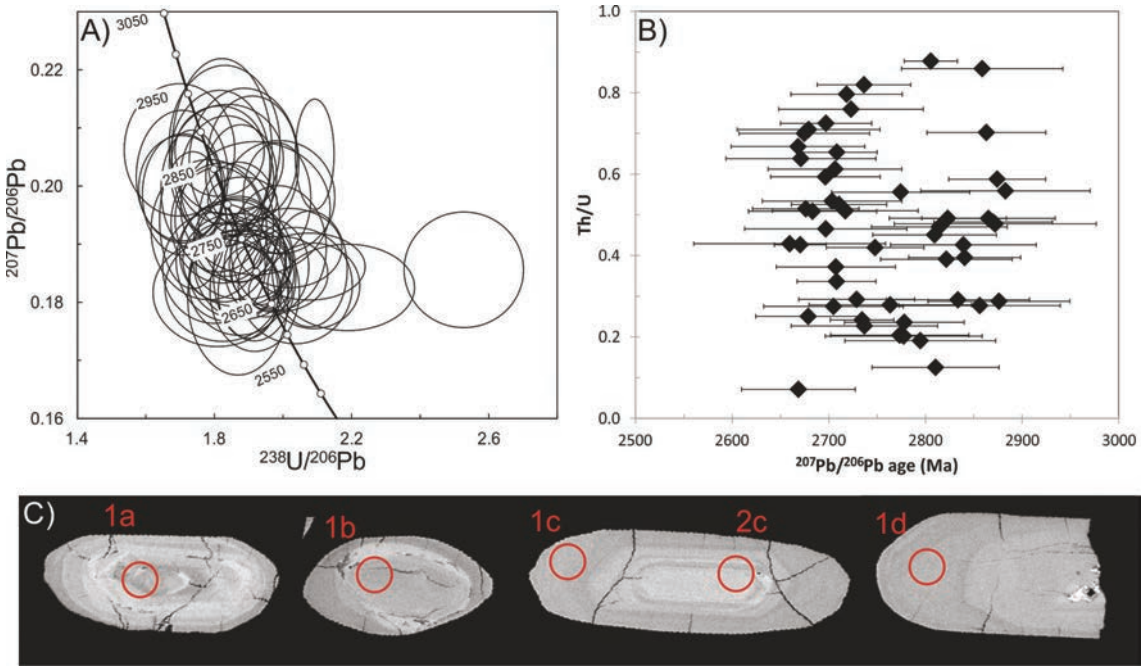

Figure 9. *Sample 288145. A) Tera-Wasserburg diagram with all data. B) Th/U versus $^{207}Pb/^{206}Pb$ age diagram. C) Zircon BSE images. Red circles indicate location of laser spots, $^{207}Pb/^{206}Pb$ ages, 1a: 2859 ± 83 Ma, 1b: 2865 ± 69 Ma; 1c: 2718 ± 58 Ma; 2c: 2839 ± 75 Ma, 1d: 2683 ± 66 Ma. Spot size 30 microns. Errors are on 2σ level.*

Banded gneiss (sample 536526)

Description: Banded gneiss with foliation parallel leucocratic veins and deformed mega-crystic feldspar augens (Figure 10A). The unit is intruded by undeformed leucocratic veins (Figure 10B).
Purpose: Age of gneiss protolith, age of metamorphic overprinting.
Analytical methods: CL-imaging; GEUS LA-ICP-MS data.

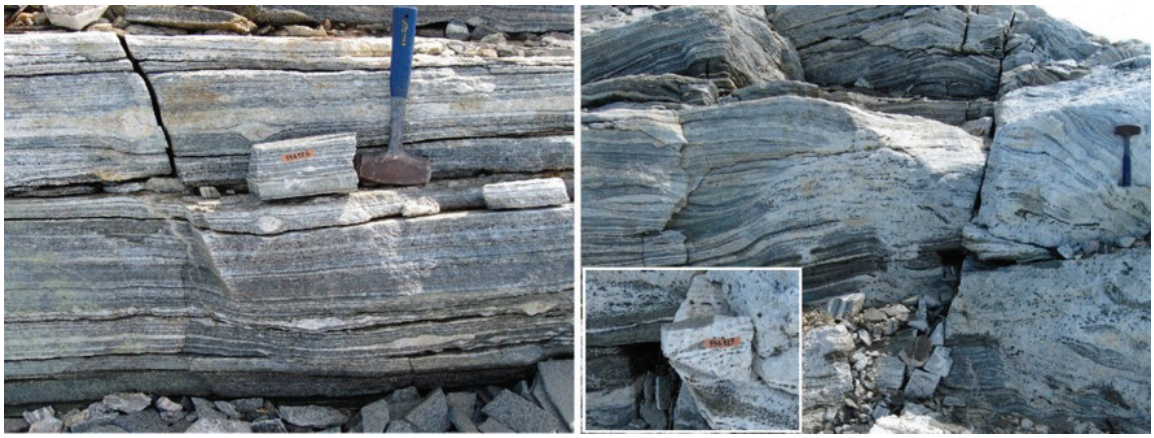

Figure 10. *A) Banded gneiss with compositional variation and deformed feldspar megacrysts (sample 536525). B) Same banded gneiss unit as A) a few meters away along strike where undeformed leucocratic melts infiltrate the banded gneiss (sample 536526).*

Data description and interpretation: Zircon grains are prismatic to oblate and vary from 100 to 250 µm in length. Internal textures are dominated by growth-zoned cores of variable CL intensity and thin homogeneous rim domains (Figure 11C). Zircon U-Pb age data are mainly concordant with $^{207}Pb/^{206}Pb$ ages ranging from 2184 ± 28 Ma to 2822 ± 73 Ma (Figure 11A). In a Th/U vs. $^{207}Pb/^{206}Pb$ age plot, the data display decreasing Th/U ratios for decreasing ages, and seem to fall into one relatively tight group with high ages and Th/U ratios and another group with lower and larger spread in Th/U and generally lower ages (Figure 11B). Texturally the group with low ages and Th/U ratios includes the rim domains and growth zoned domains with low CL intensity. Selecting the analyses with high Th/U ratios and including three analyses with clear CL zoning (high ages but low Th/U) we obtain a weighted mean **$^{207}Pb/^{206}Pb$ age of 2793 ± 19 Ma** (n = 15, MSWD = 0.50) which is interpreted to reflect felsic veining within the mafic protolith. Selecting the remaining analyses, excluding three with low ages, we obtain a weighted mean $^{207}Pb/^{206}Pb$ age of **2713 ± 31 Ma** (n = 9; MSWD = 1.4), which likely reflects a metamorphic overprinting age.

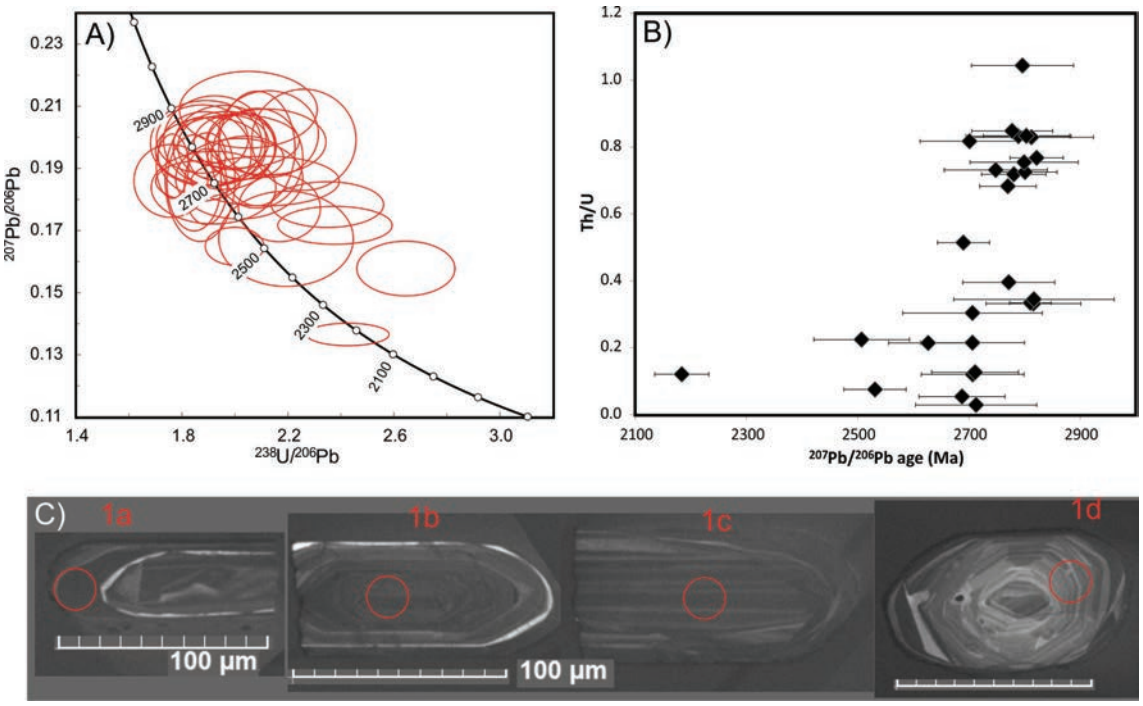

Figure 11. *Sample 536526. A) Tera-Wasserburg diagram with all data. B) Th/U versus $^{207}Pb/^{206}Pb$ age diagram. C) Zircon BSE images. Red circles indicate position of laser spots, $^{207}Pb/^{206}Pb$ ages, 1a: 2706 ± 47 Ma, 1b: 2817 ± 97 Ma; 1c: 2811 ± 93 Ma, 1d: 2789 ± 74 Ma. Spot size 30 microns. Errors are on 2σ level.*

Leucocratic melts in banded gneiss (sample 536525)

Description: Undeformed leucocratic veins intruding into banded gneiss (sample 536526)
Purpose: To obtain the intrusive age of the leucocratic veins and to obtain information about inheritance.
Analytical methods: CL-imaging; GEUS LA-ICP-MS data.

Data description and interpretation: Zircon grains are prismatic and from 100 to 250 µm in length. The internal textures include domains with bright CL-zoning and domains with dull CL-zoning. Grains with bright CL-zoned rims are often CL-dull (Figure 12C). The CL-bright domains are growth-zoned, whereas the CL-dull domains display a variety of textures from growth-zoned to diffusely zoned. Zircon U-Pb age data are mainly concordant, except for a few analyses that define two separate Discordia arrays (Figure 12A). Concordant grains (± 90%) range in age from 2019 ± 127 Ma to 3072 ± 101 Ma. There is an overall decrease in Th/U with decreasing $^{207}Pb/^{206}Pb$ age, both for the CL-bright and Cl-doll domains, each group defining separate groups (Figure 12B). Domains with bright CL zoning have the highest ages with a weighted mean **$^{207}Pb/^{206}Pb$ of 3015 ± 13 Ma** (n = 28; MSWD = 0.63). These grain domains are xenocrystic/inherited. Analyses from the CL dull domains show a large spread in ages, and it is difficult to obtain unambiguous age constraints from these grains. However, as ages below 2600 Ma are unknown from the basement in the region taken together with altered character of the zircon domains, it is very uncertain if these analyses reflect a Proterozoic overprinting event. Calculating an age from analyses of the CL-dull domains with Th/U ratios above 0.5 yields a weighted mean $^{207}Pb/^{206}Pb$ age of 2750 ± 100 Ma (n = 5; MSWD = 3.0). Calculating an intercept age from the discordant analyses within CL-bright domains yields a weighted mean $^{207}Pb/^{206}Pb$ age of 2785 ± 130 Ma (n = 3). Despite the large errors, the overlap in these ages could suggest that they both reflect the timing of the intrusion of the leucocratic melts.

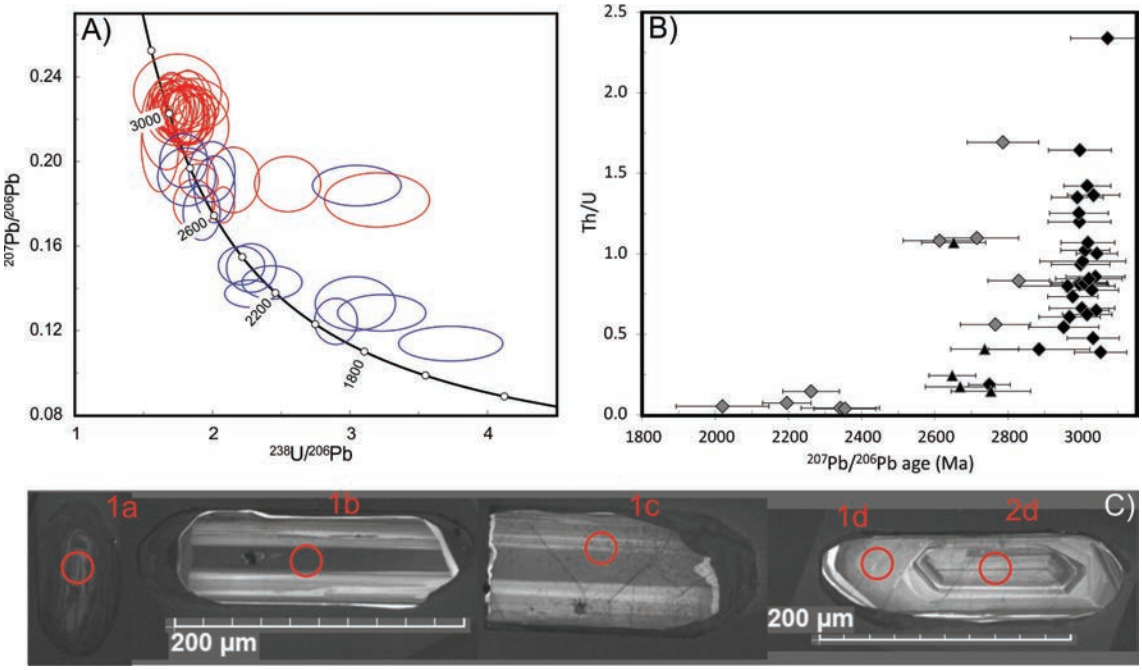

Figure 12. *Sample 536525. A) Tera-Wasserburg diagram with all data. B) Th/U versus $^{207}Pb/^{206}Pb$ age diagram, black diamonds: CL-bright and concordant, black triangles: CL-bright and discordant; grey diamonds: CL-dull; C) Zircon CL images. Red circles indicate position of laser spots (30 µm diameter), $^{207}Pb/^{206}Pb$ ages, 1a: 2765 ± 95 Ma, 1b: 3018 ± 73 Ma; 1c: 3043 ± 56 Ma, 1d: 3032 ± 71 Ma, 2d: 2993 ± 80 Ma. Errors are on 2σ level.*

Late intrusive granitoids sheets related to a gabbroic hornblendite

Leuco-gabbroic melt veins (sample 536517)

Description: Leucogabbroic melt vein in mafic granulite (Figure 13). The mafic granulites are also intruded by leucocratic veins that are associated with the leucogabbroic veins (Figure 13B).
Purpose: Age of intrusive gabbroic melt vein.
Analytical methods: CL-imaging; GEUS LA-ICP-MS data.

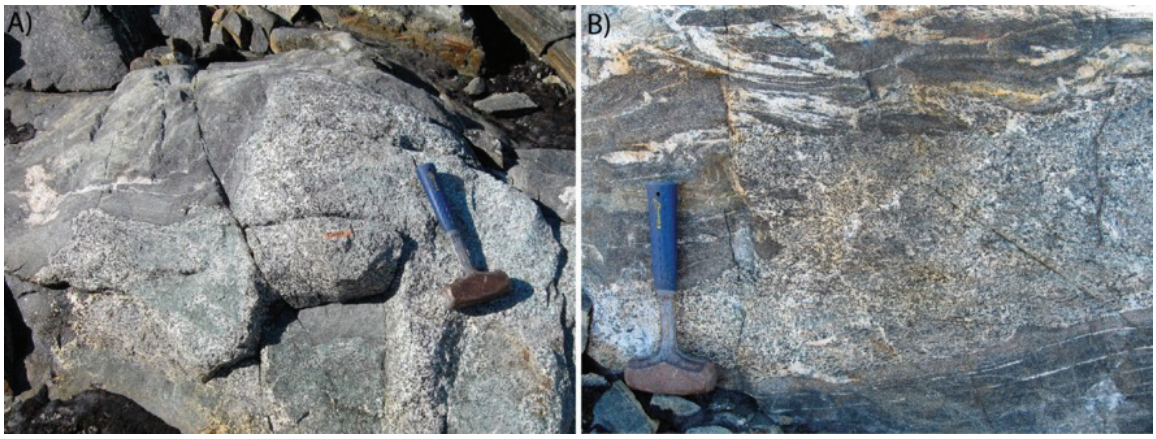

Figure 13. *Sample 536517. A) and B) Foliated mafic granulite/amphibolite intruded by undeformed leuco-gabbroic vein and associated leucocratic veins.*

Data description and interpretation: Zircon grains are prismatic and oblate and from 100 to 200 µm in length. Internal textures are characterised by diffusely zoned or altered core domains and sector zoned rim domains (Figure 14C). Zircon U-Pb age data are mainly concordant and plot in one group with $^{207}Pb/^{206}Pb$ ages ranging from 2659 ± 51 Ma to 2738 ± 92 Ma, there is no measurably age difference between rim and core domains (Figure 14A). Th/U ratios range from 0.1 to 0.7 and display no relation with age (Figure 14B). By selecting analyses from the least altered core and rim domains we obtain a weighted mean **$^{207}Pb/^{206}Pb$ age of 2701 ± 11 Ma** (n = 34; MSWD = 0.28), which is interpreted as the crystallisation age of the leucogabbro.

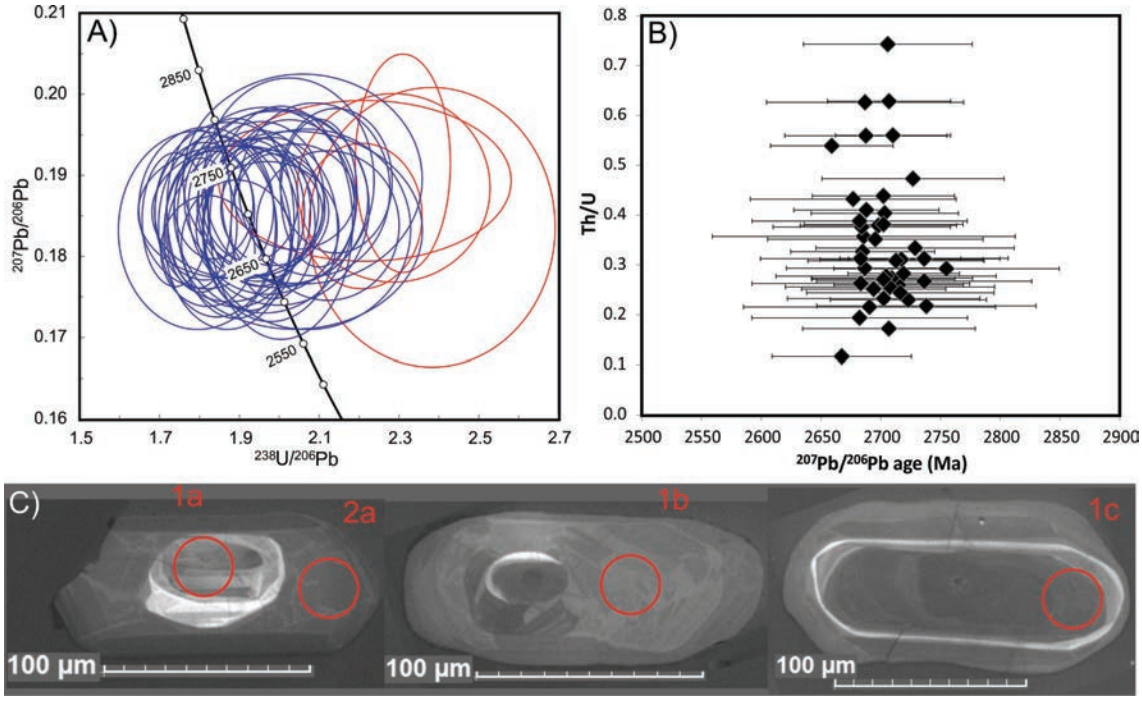

Figure 14. *Sample 536517. A) Tera-Wasserburg diagram with all data. B) Th/U versus $^{207}Pb/^{206}Pb$ age diagram. C) Zircon CL images. Red circles indicate position of laser spots (30 µm diameter), $^{207}Pb/^{206}Pb$ ages, 1a: 2694 ± 60 Ma, 2a: 2677 ± 86 Ma, 1b: 2715 ± 54 Ma, 1c: 2702 ± 81 Ma. Errors are on 2σ level.*

Undeformed felsic vein network within meta-gabbro (sample 527006)

Description: Sample 527006 is from felsic undeformed veins forming a network within a meta-gabbro/hornblendite unit (Figure 15B). The meta-gabbro/hornblendite occurs as several km long lenses with thickness up to several 100 meters (Figure 15A).
Purpose: Age of intrusive leucocratic veins, minimum age of meta-gabbro.
Analytical methods: BSE-imaging; GEUS LA-ICP-MS data.

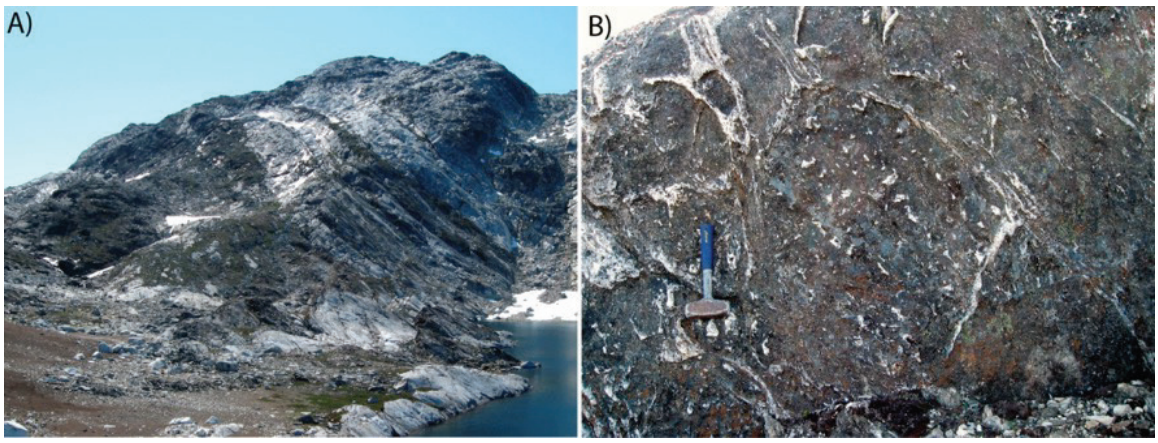

Figure 15. *A) Meta-gabbro/hornblendite intrusive units (black) as km-scale sheets in a banded gneiss basement. B) Felsic veins, interpreted as late residual melts or as back-veining from wall rock lithologies are abundant in the hornblendite. Photograph shows cm-wide felsic (plagioclase-dominated) veins cutting meta-gabbro with large hornblende crystals.*

Data description and interpretation: Zircon grains are mainly prismatic with a large size variation from 10 to 400 µm in length. Internally grains display core and rim domains both with homogeneous textures, and the rim domains being BSE-brighter than the core domains (Figure 16C). Grains are often highly fractured with cracks radiating from the core regions. Zircon U-Pb data plot in one concordant group with ages that range from 2689 ± 57 Ma to 2761 ± 56 Ma (Figure 16A) without any distinct difference between core and rim domains. Th/U ratios range between 0.2 and 0.8 without any correlation with age (Figure 16B). The weighted mean $^{207}Pb/^{206}Pb$ age of all analyses is **2721 ± 7 Ma** (n = 53; MSWD = 0.36). In comparison, a Concordia age calculated from analyses that are more than 98% concordant yields a less precise, but overlapping age of 2730 ± 11 Ma (MSWD = 2.1). This age is interpreted as the crystallisation age of the leucocratic veins and also represents a minimum age of the meta-gabbro.

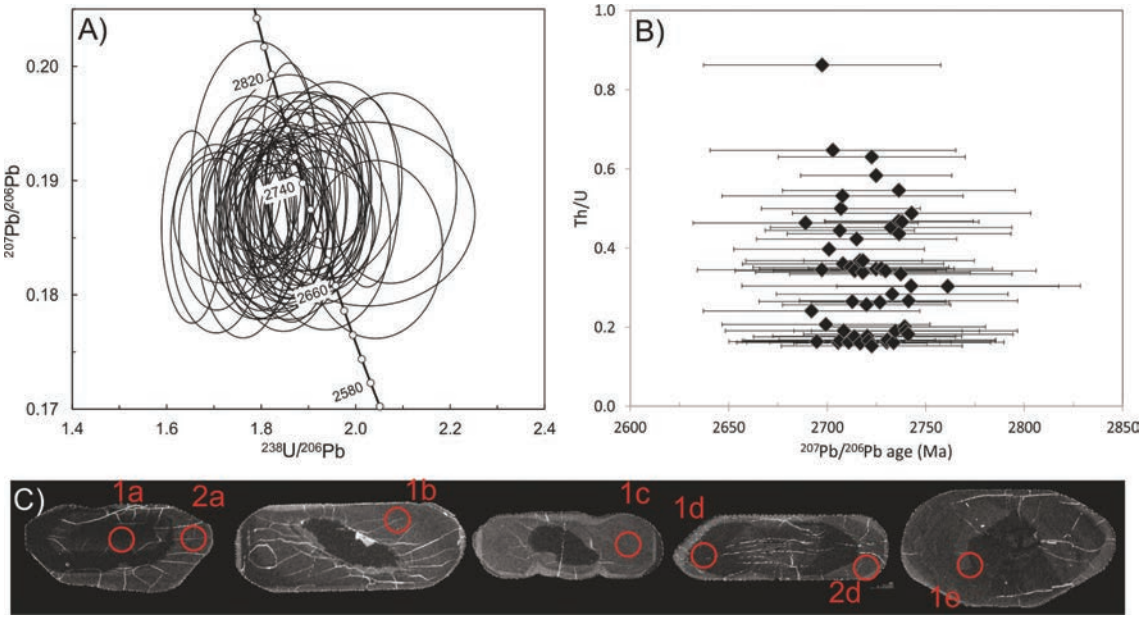

Figure 16. *Sample 527006. A) Tera-Wasserburg diagram with all data. B) Th/U versus $^{207}Pb/^{206}Pb$ age diagram. C) Zircon BSE images. Red circles indicate position of laser spots (30µm diameter), $^{207}Pb/^{206}Pb$ ages, 1a: 2720 ± 43 Ma, 2a: 2743 ± 60 Ma, 1b: 2712 ± 50 Ma, 1c: 2725 ± 38 Ma, 1d: 2706 ± 52 Ma, 2d: 2736 ± 38 Ma. Errors are on 2σ level.*

Granitic sheet in border zone of meta-gabbro, Thor Land (sample 527001)

Description: Undeformed granitic sheet in the boundary between the meta-gabbro and the basement gneisses (Figure 17). The melt could likely relate to the infiltrating melts within the meta-gabbro (527006).
Purpose: Age of intrusion and inheritance
Analytical methods: BSE-imaging; GEUS LA-ICP-MS data.

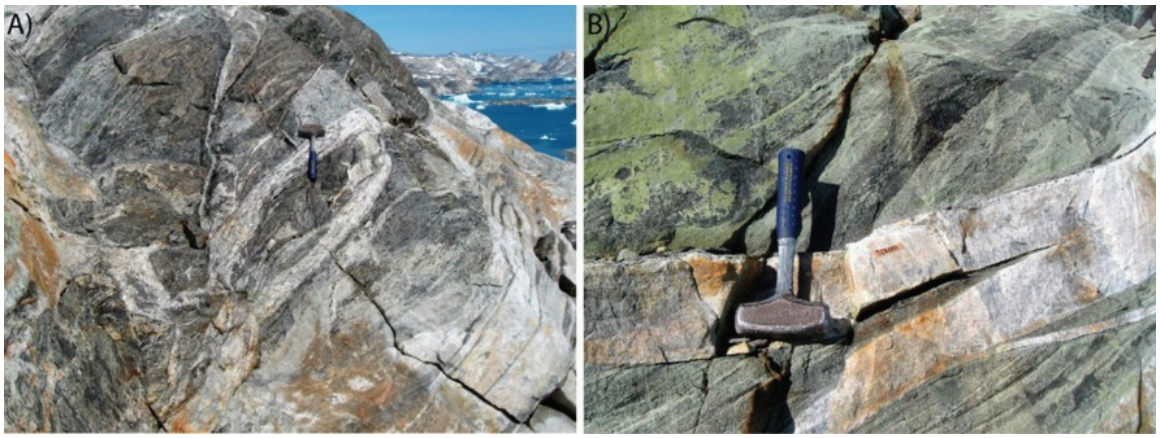

Figure 17. *Outcrop sample 527001. A) and B) Intrusive felsic sheets at the border of the meta-gabbro (hornblendite) in A) it can be observed that some sheets at the boundary are sheared and mylonitic in texture (sheets below hammer and lower right corner of image).*

Data description and interpretation: Zircon grains are mainly prismatic however form and size varies considerably; grain size ranges from 100 to 500 µm in length. Internal zircon textures are primarily composed of BSE-bright homogeneous rim domains and darker, mainly homogeneous core domains (Figure 18C). Irregular domains of different BSE intensity are common. Few grains have core or internal domains with growth-zoned textures. Zircon U-Pb data are concordant except for a few analyses, and display a spread along Concordia with $^{207}Pb/^{206}Pb$ age ranging from 2694 ± 51 Ma to 3003 ± 53 Ma (Figure 18A). Th/U ratios vary mainly between 0.07 and 0.6, with one outlier at 1.35, and decrease with decreasing age until ca. 2800 Ma; younger domains have higher Th/U up to 0.6 (Figure 18B). U concentrations display an overall increase with decreasing age. It is somewhat ambiguous to obtain meaning full geological ages, however the U and Th/U relations with age suggest two inherited populations, an old ca. 3000 Ma population and a younger ca. 2800 Ma population. The youngest rim domains at ca. 2700 Ma are interpreted as the intrusion age of the granitic sheet. In detail we calculate the following ages: 1) a weighted mean of the three oldest grains: **2976 ± 33 Ma** (n = 3, MSWD = 0.89), 2) a weighted mean of 11 analyses with low Th/U (highlighted in Figure 18B) yields and age of **2815 ± 12** Ma (n = 11; MSWD = 0.56), and 3) a weighted mean of the 4 youngest analyses with high Th/U ratios (highlighted in Figure 18B) yields an age of **2700 ± 26 Ma** (n = 4, MSWD = 0.13).

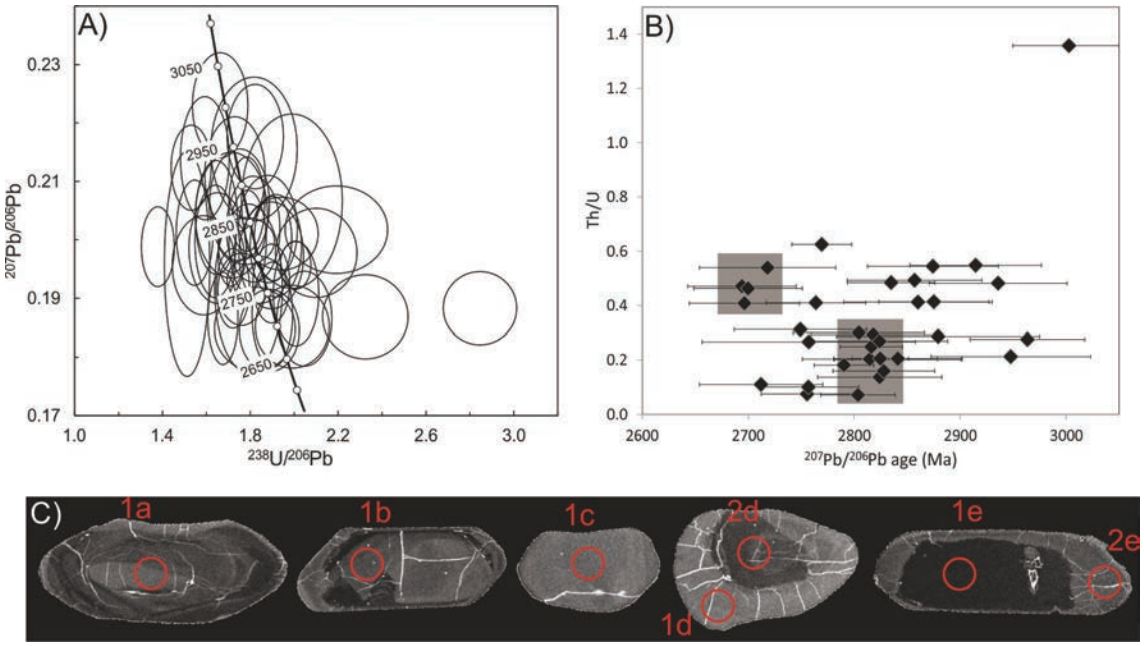

Figure 18. *Sample 527001. A) Tera-Wasserburg diagram with all data. B) Th/U versus $^{207}Pb/^{206}Pb$ age diagram, grey shaded squares highlight the analyses selected for age calculation of the two young populations. C) Zircon BSE images. Red circles indicate position of laser spots (spot size is 30 µm), $^{207}Pb/^{206}Pb$ ages, 1a: 3003 ± 53 Ma, 1b: 2824 ± 69 Ma, 1c: 2700 ± 51 Ma, 1d: 2718 ± 64 Ma, 2d: 2713 ± 57 Ma, 1e: 2818 ± 59 Ma, 2e: 2764 ± 47 Ma. Errors are on 2σ level.*

Mainly undeformed granitoid intrusions within foliated mafic granulites as sheets and leucocratic veins

Garnet-bearing leucosome, Helge Halvø (sample 536588)

Outcrop description: This sample is from a spectacular outcrop in the region exposing garnet-sillimanite schist and mylonite that are infiltrated by undeformed leucocratic melts (Figure 19). These melts are often found within pressure shadow regions in the garnet-sill schist, which have acted as a competent unit and as a result have been boudinaged. Sample 536588 is from an undeformed garnet-bearing (entrained) leucocratic granite sheet (Figure 19A).
Purpose: Age of leucocratic intrusion
Analytical methods: CL-imaging; GEUS LA-ICP-MS data.

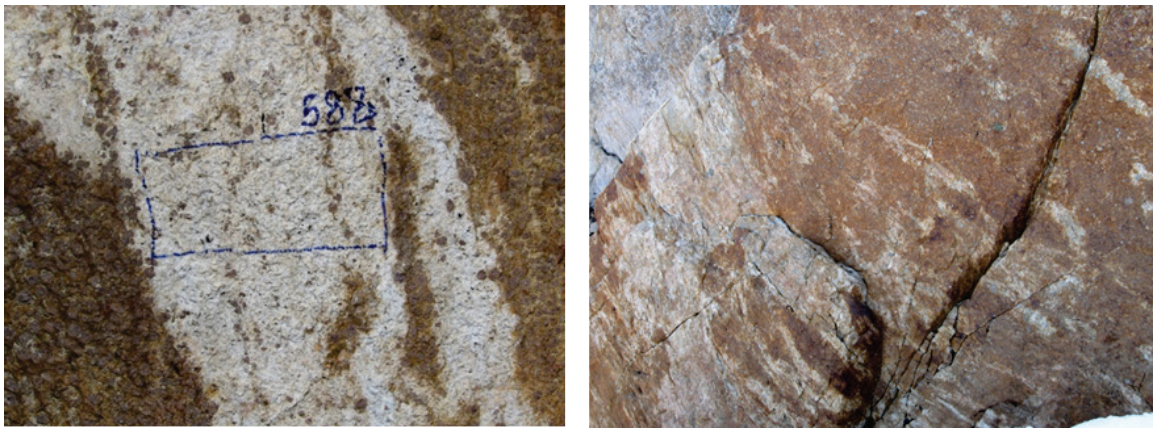

Figure 19. *A) Sample 536588 of a leucocratic granite sheet within garnet-sillimanite schist. B) Emlarged view of the relation between infiltrating leucocratic veins and the garnet-sillimanite schist, the garnet-sillimanite schist occurs as boudinaged units within silica-rich mylonite.*

Data description and interpretation: Zircon grains are rounded and mainly sector-zoned and ca. 100 µm in diameter (Figure 20C). Zircon U-Pb data plot in one concordant and coherent group with $^{207}Pb/^{206}Pb$ ages ranging from 2601 ± 66 Ma to 2735 ± 76 Ma (Figure 20A). Th/U ratios range from 0.05 to 0.35 and in general the analyses with low age have low Th/U ratios. Selecting 21 analyses with highest $^{207}Pb/^{206}Pb$ age yields a weighted mean of **2701 ± 14 Ma** (n = 21; MSWD = 0.13), which is interpreted as the crystallisation age of the intrusive granitic sheets (Figure 20B).

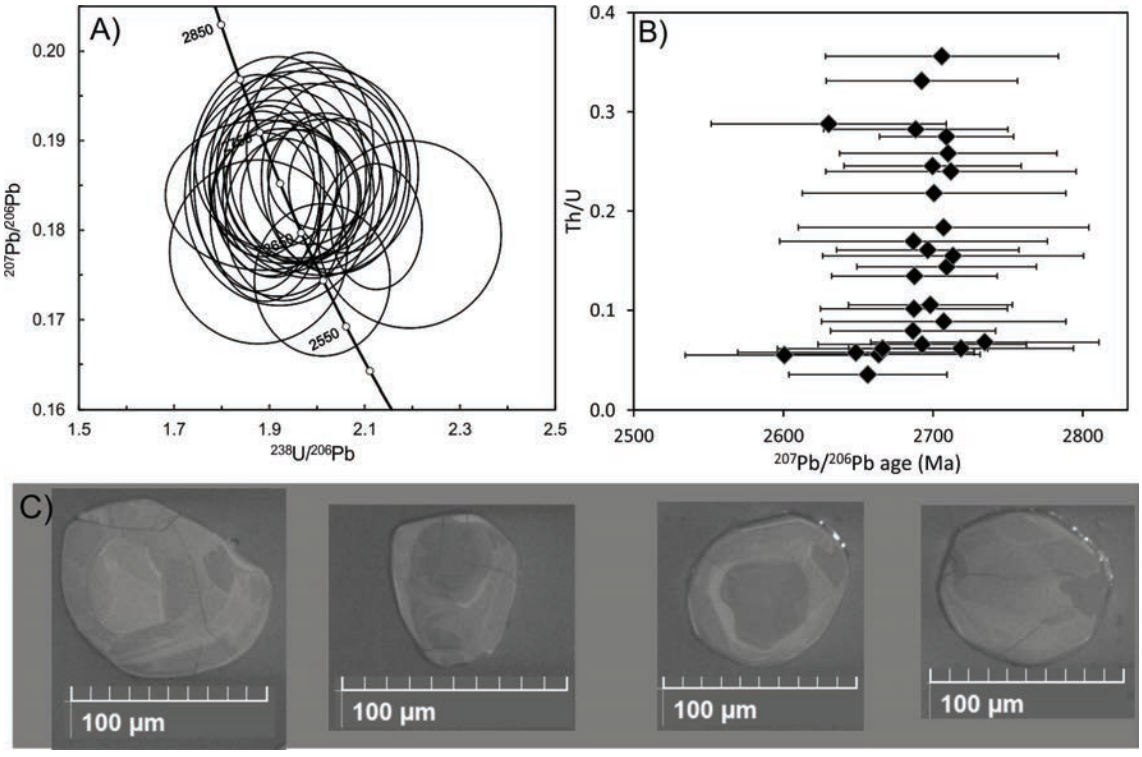

Figure 20. *Sample 536588. A) Tera-Wasserburg diagram with all data. B) Weighted mean $^{207}Pb/^{206}Pb$ age. C) Zircon BSE images, showing rounded sector-zoned grains interpreted to be igneous in origin. Errors are on 2σ level.*

Leucocratic granite sheet (sample 527458)

Description: This sample is from a late undeformed leucocratic granitic sheet that intrudes and infiltrates the host basement, which mostly comprises mafic granulite (Figure 21).
Purpose: Latest intrusive phase in the area and documentation of zircon inheritance.
Analytical methods: BSE-imaging; GEUS LA-ICP-MS data.

Figure 21. *Outcrops of the rock units from where sample 527458 is taken. Late leucocratic melts infiltrate the gneiss basement that is mainly composed of foliated mafic granulites.*

Data description and interpretation: Zircon grains are prismatic and from 200 to 500 µm in length. Internally the grains are dominated by BSE-grey, homogeneous domains (Figure 22C). Often grains have core and rim domains, which is best seen in transmitted light. Core domains appear altered, are inclusion-rich and often mantled by BSE-brighter domains. Zircon U-Pb age data consist one group of concordant analyses, and another group of discordant analyses with a rough upper Discordia intercept age of 2711 ± 32 Ma and a lower intercept age of 291 ± 39 Ma (Figure 22A). Concordant analyses (< 10 % discordant) are mainly from rim domains and have ages ranging from 2696 ± 52 Ma to 2739 ± 77 Ma and Th/U ratios from 0.1 to 0.7. The discordant analyses have Th/U ratios < 0.1 (Figure 22B). The concordant analyses (< 5 % discordant) yield a weighted mean $^{207}Pb/^{206}Pb$ age of **2718 ± 11 Ma** (n = 23, MSWD = 0.14), which is interpreted as the intrusion age of the leucocratic granite sheet.

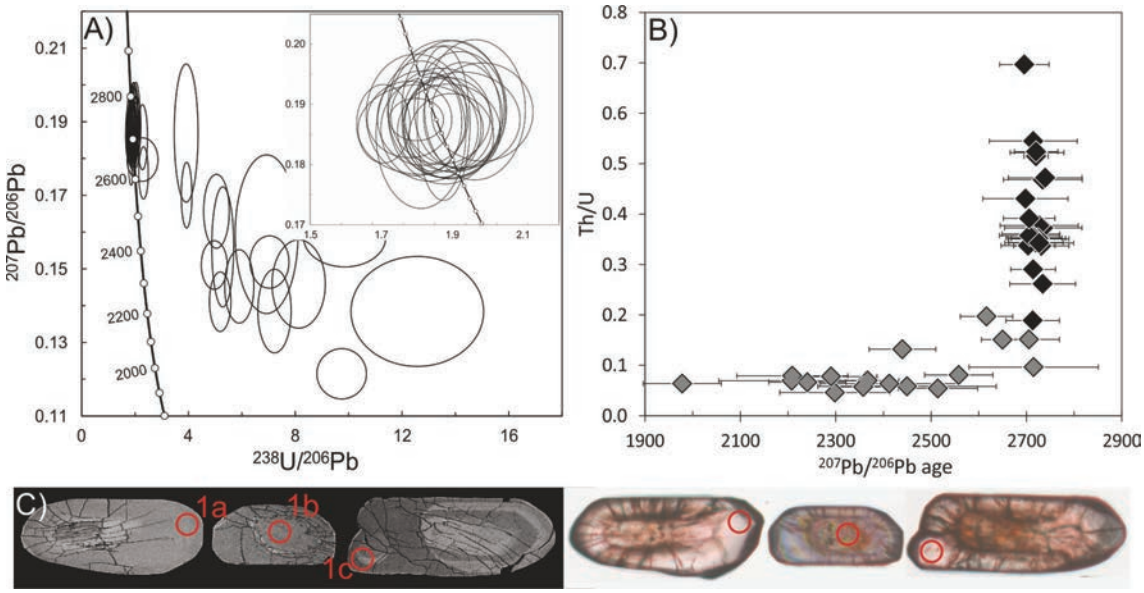

Figure 22. *Sample 527458. A) Tera-Wasserburg diagram with all data displayed, discordant analyses are mainly from core domains. Insert diagram shows data that are >90 % concordant. B) Th/U versus $^{207}Pb/^{206}Pb$ age diagram, black diamonds >90 % concordant, grey diamonds <90 % concordant. C) Zircon BSE and polarised light images, textures reveal altered core and wide rim domains. Red circles indicate position of laser spots (30 µm diameter), $^{207}Pb/^{206}Pb$ ages, 1a: 2731 ± 58 Ma, 1b: 2558 ± 72 Ma (72 % conc.), 1c: 2735 ± 81 Ma. Errors are on 2σ level.*

Leucocratic granite sheet (sample 527460)

Description: This sample is from a late undeformed leucocratic granitic sheet intrusing and infiltrating the host gneiss that is constituted by mafic granulites.
Purpose: Intrusive age of leucocratic veins.
Analytical methods: BSE imaging; GEUS LA-ICP-MS and Nordsim data.

Data description and interpretation: Zircon grains are mainly prismatic with fewer grains being oblate or rounded and vary from 200 to 400 µm in length. Internally grains mainly have inclusion- rich, BSE-dark cores and homogeneous BSE-grey and BSE-bright rim domains (Figure 23C). Overall grains appear strongly altered especially the core domains. Zircon U-Pb age data plot in one concordant group (core and rim analyses) with a few discordant analyses, $^{207}Pb/^{206}Pb$ ages range from 2692 ±96 Ma to 2802 ± 99 Ma (Figure 23A). Zircon grains that are <5 % discordant yield a weighted mean $^{207}Pb/^{206}Pb$ age of **2721 ± 12 Ma** (n = 27, NSWD = 0.29), which is interpreted as the crystallisation age of the intruding leucocratic veins.

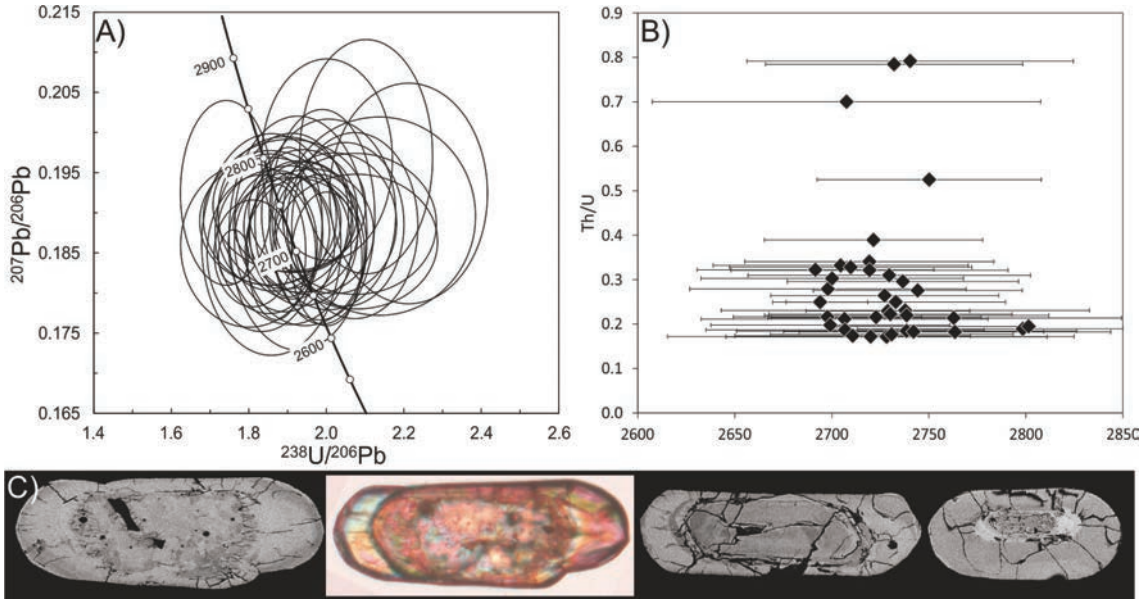

Figure 23. *Sample 527560 A) Tera-Wasserburg diagram with all data. B) Th/U versus $^{207}Pb/^{206}Pb$ age diagram. C) Zircon BSE and polarised light images, textures reveal altered core and wide rim domains. Spot documentation unfortunately lost. Errors are on 2σ level.*

Leucocratic granite veins within mafic granulite (sample 527432 and 527435)

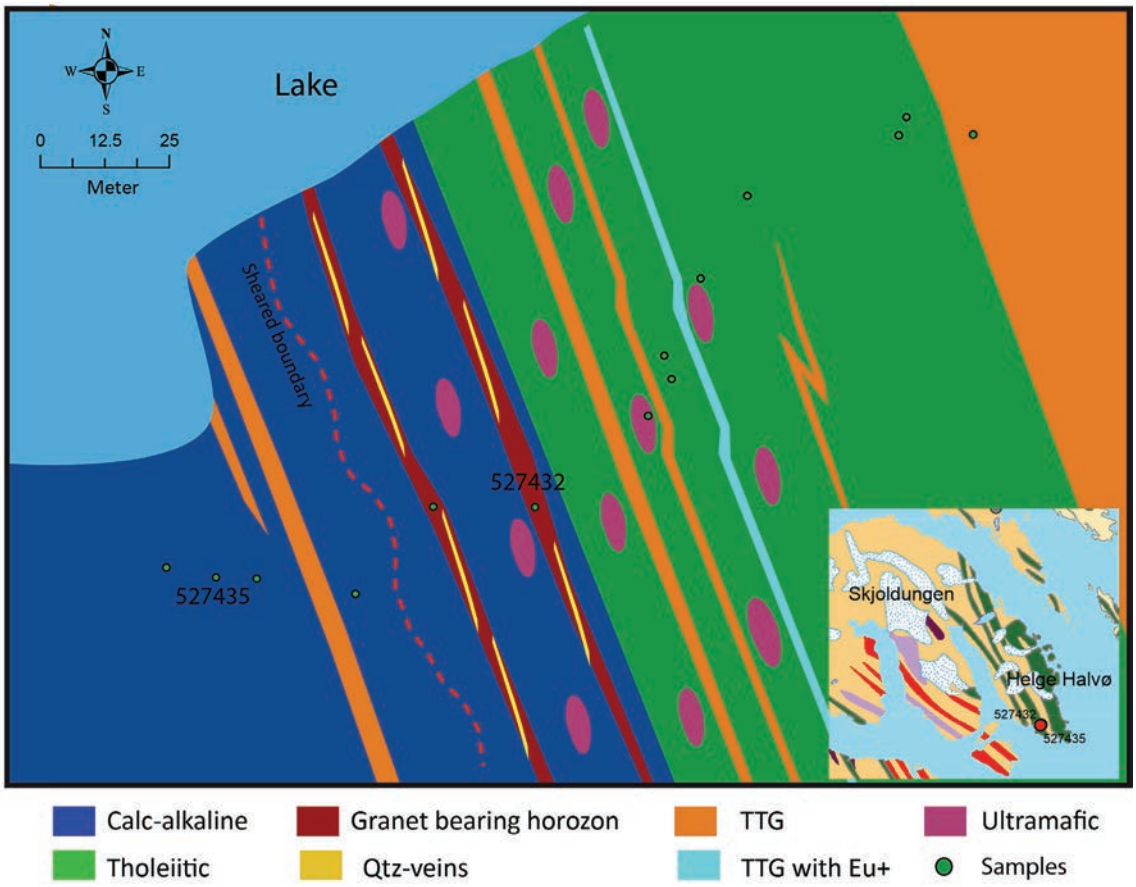

Figure 24. *Simplified map showing the geological relationship between foliated mafic units (amphibolite to mafic granulite) with abundant ultramafic enclaves and intruding leucocratic sheets. The main difference between the "calc-alkaline" and "tholeiitic" units is based on geochemistry and in the field where the "calc-alkaline" units contain a network of leucocratic veins, which is missing in the "tholeiitic" units.*

Description: These samples come from a thick mafic unit (>150 m wide) composed of predominantly of mafic "calc-alkaline" and "tholeiitic" rocks preserved as granulites (Figure 24). These mafic granulites are typically cut by orthopyroxene-bearing leucocratic veins. The unit of mafic rocks has been sampled in some detail and based on whole rock geochemistry data it can be divided into an eastern "tholeiitic" sequence and a western "calc-alkaline" sequence (Bagas et al., 2013). It is apparent from field observations that the mafic rocks of the "calc-alkaline" sequence are characterised by containing a network of leucocratic veins (Figure 25) and it is thus unclear whether the calc-alkaline nature of these veined mafic rocks is a geological artefact.
Purpose: Intrusive age of leucocratic veins and minimum age of the mafic units.
Analytical methods: BSE-imaging; GEUS LA-ICP-MS data.

Figure 25. *Mafic granulites with an irregular network of leucocratic veins, samples 527432 and 527435 were collected at this outcrop using a rock saw.*

Data description and interpretation, sample 527432: Zircon grains are mainly oblate with anhedral morphology and ca. 200 to 300 µm in length. Internally grains have complex texture, often with growth-zoned core domains and homogeneous rim domains. Many grains show signs of alteration with BSE-bright internal domains either as mantles separating core and rim domains, as rims or irregular domains (Figure 26C). Zircon U-Pb data have been obtained both by SIMs (Nordsim) and LA-ICP-MS methods. The LA-ICP-MS U-Pb analyses mainly plot in one concordant and relatively coherent group with ages ranging from 2867 ± 65 to 2690 ± 60 Ma with two analyses at 3017 ± 83 and 3010 ± 91 Ma (Figure 26A). Th/U ratios range between 0.1 and 1.3 with no obvious trend against age, however U concentration shows an overall increase with decreasing age from ca. 120 to 920 ppm (Figure 26B). The main $^{207}Pb/^{206}Pb$ age peak is focused at ca. 2800 Ma. Only six SIMs U-Pb analyses were carried out, except for one analyses, data are concordant and range in age from 2738 ± 3 to 2887 ± 5 Ma and plot into four resolvable ages (Figure 26A). Of these the oldest is best defined with a weighted mean of **2886 ± 5 Ma** (n = 2, MSWD = 0.33). Selecting analyses with mainly low U concentration and with ages above 2765 Ma (outline marked b) in Figure 26B) yields an age of **2796 ± 6 Ma** (n = 18; MSWD = 0.54). This age is considered geologically relevant as the main inherited population. Selecting analyses with high U concentration (outline marked a in Figure 26B) and ages below 2765 Ma yields a weighed mean of **2726 ± 17 Ma** (n = 11, MSWD = 0.68), which is considered to be representative of the crystallisation age of the leucocratic veins.

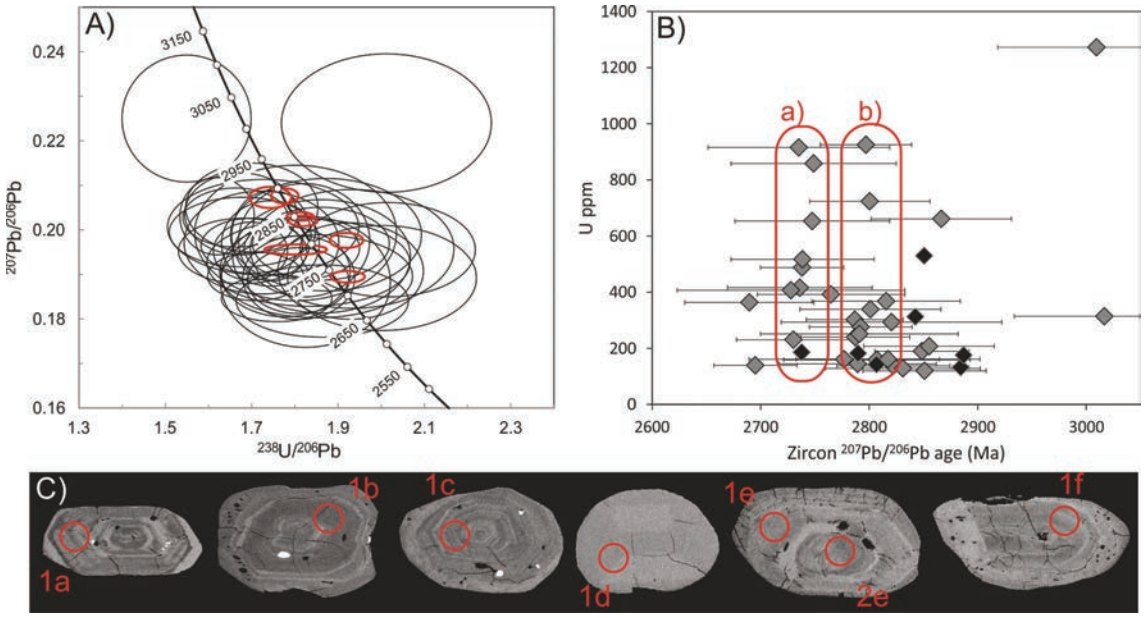

Figure 26. *Sample 527432. A) Tera-Wasserburg diagram with Nordsim (small red ellipses) and LA-ICPMS data. B) U (ppm) vs. $^{207}Pb/^{206}Pb$ age Ma. C). Zircon BSE and polarised light images, textures reveal altered core and wide rim domains. Red circles indicate location of laser spots, $^{207}Pb/^{206}Pb$ ages, 1a: 2803 ± 78 Ma; 1b: 2822 ± 52, 1c: 2848 ± 43 Ma, 1d: 2690 ± 60 Ma, 1e: 2728 ± 105 Ma, 2e: 2791 ± 91 Ma, 1f: 3017 ± 83 Ma. Errors are on 2σ level.*

Data description and interpretation, sample 527435: Zircon grains are mainly prismatic and range from 200 to 400 µm in length. Internally grains are dominated by core and rim domains, both homogeneous and BSE-grey; these domains are separated by BSE-bright regions that show evidence of alteration (**Figure 27**C). Core and rim domains often contain radial fractures that are absent in the BSE-bright domains. Zircon U-Pb age data are concordant and plot in one coherent group with $^{207}Pb/^{206}Pb$ ages ranging from 2566 ± 50 Ma to 2761 ± 39 Ma. A selection including all concordant (< 10 % discordance) analyses yields a weighted mean of 2733 ± 10 Ma (n = 37; MSWD = 0.34), which is interpreted as the crystallisation age and the age of the intrusion of the leucocratic veins.

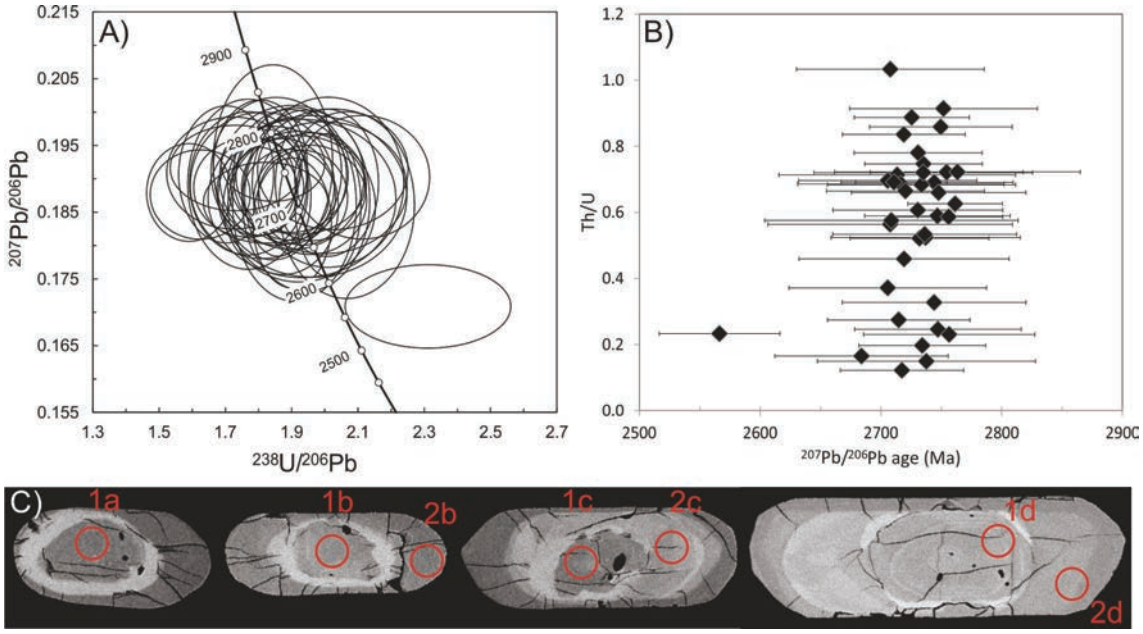

Figure 27. *Sample 527435 A) Tera-Wasserburg diagram with all data displayed. B) Th/U versus $^{207}Pb/^{206}Pb$ age diagram. C) Zircon BSE images, textures reveal variably altered cores and wide rim domains. Red circles indicate location of laser spots, $^{207}Pb/^{206}Pb$ ages, 1a: 2735 ± 91 Ma, 1b: 2734 ± 78 Ma, 2b: 2719 ± 87 Ma, 1c: 2735 ± 49 Ma, 2c: 2719 ± 51 Ma, 1d: 2715 ± 59 Ma, 2d: 2744 ± 65 Ma. Errors are on 2σ level.*

Granite sheets, Helge Halvø (sample 527424)

Description: Weakly deformed granite sheet.
Purpose: Age of protolith intrusion and inheritance
Analytical methods: BSE-imaging; GEUS LA-ICP-MS data.
Data description and interpretation: Zircon grains are mainly prismatic and from 200 to 400 µm in length. Internally the grains are highly altered as exemplified in Figure 28C, alteration are mainly observed in core regions or as BSE-bright mantles separating core and rim domains. The altered domains are inclusion-rich and BSE-bright, sometimes mixed with BSE-dark domains (Figure 28C). Rim domains are homogeneous and often highly fractured. Few grains contain unaltered core domains characterised by diffuse growth-zoning. Zircon U-Pb age data are concordant except for a few analyses and range in age from 2581 ± 63 Ma to 2975 ± 32 Ma (Figure 28A). There is a general increase in Th/U ratios for younger analyses (Figure 28B). Two age populations can be distinguished from the obtained data, one consists of unaltered core domains with a $^{207}Pb/^{206}Pb$ age of **2963 ± 23 Ma** (n = 4, MSWD = 0.55), which is regarded as an inherited population. Another population is made up from rims and internal BSE-grey, homogeneous domains yielding an age of **2736 ± 11 Ma** (n = 14, MSWD = 1.7), which is taken as the crystallisation age of the leucogranite.

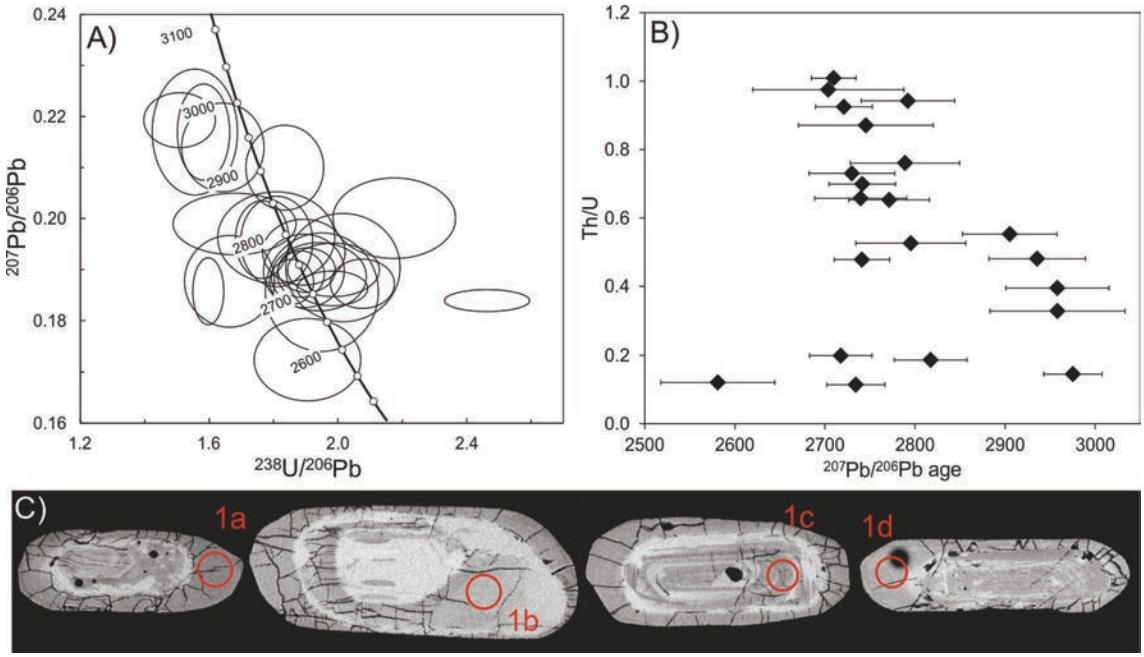

Figure 28. *Sample 527424 A) Tera-Wasserburg diagram with all data displayed. B) Th/U versus $^{207}Pb/^{206}Pb$ age diagram. C) Zircon BSE images, red circles indicate laser spots (30 µm spot size), $^{207}Pb/^{206}Pb$ ages, 1a: 2792 ± 52 Ma, 1b: 2741 ± 31 Ma, 1c: 2975 ± 32 Ma, 2730 ± 48 Ma. Errors are on 2σ level.*

Granitic sheets, Helge Halvø (sample 527425)

Description: Weakly deformed granite sheets containing assimilated older felsic and mafic gneiss units (Figure 29A, B).
Purpose: Age of protolith intrusion and inheritance
Analytical methods: BSE-imaging; GEUS LA-ICP-MS data.

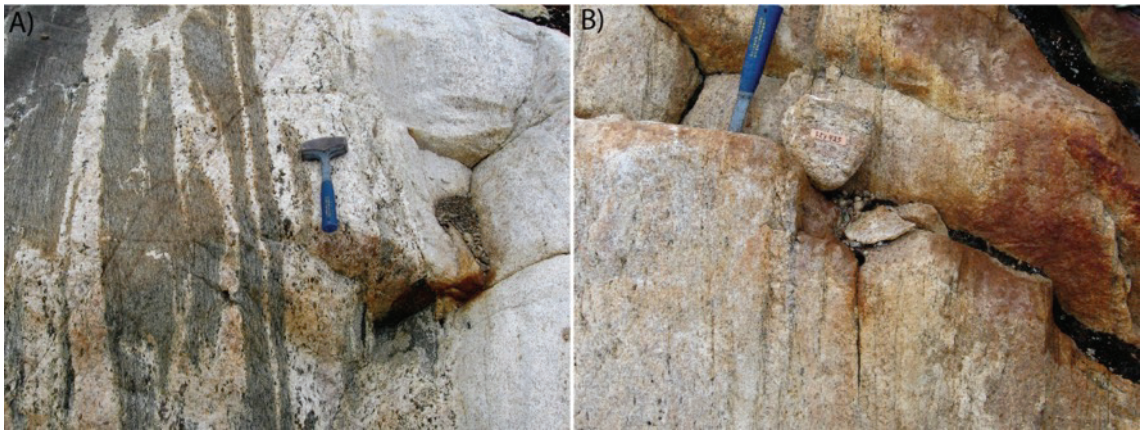

Figure 29. *Sample 537425. A) Leucocratic granite veins infiltrating mafic granulite, B) leucocratic granite veins.*

Data description and interpretation: Zircon grains are mainly prismatic from 200 to 500 µm in length. Internally most grains appear strongly altered often with BSE-bright, inclusion-rich core domains and homogenous BSE-grey rims (Figure 29C). Many core domains however also reveal diffuse, growth-zoned patterns that are often easier observed in transmitted light. Zircon U-Pb age data are concordant and spread out along the Concordia (Figure 29A) with $^{207}Pb/^{206}Pb$ ages ranging from 2698 ± 54 Ma to 2817 ± 40 Ma. Th/U ratios range from 0.2 to 1.0 and display no obvious correlation with $^{207}Pb/^{206}Pb$ age (Figure 29B). Selected analyses from core domains yield a weighted mean $^{207}Pb/^{206}Pb$ age of **2788 ± 9 Ma** (n = 25, MSWD = 0.38), which is interpreted as the crystallisation age of a single inherited population. The analyses from rim domains yield a weighted mean $^{207}Pb/^{206}Pb$ age of **2740 ± 14 Ma** (n = 14, MSWD = 0.61), which is interpreted as the granite intrusion age.

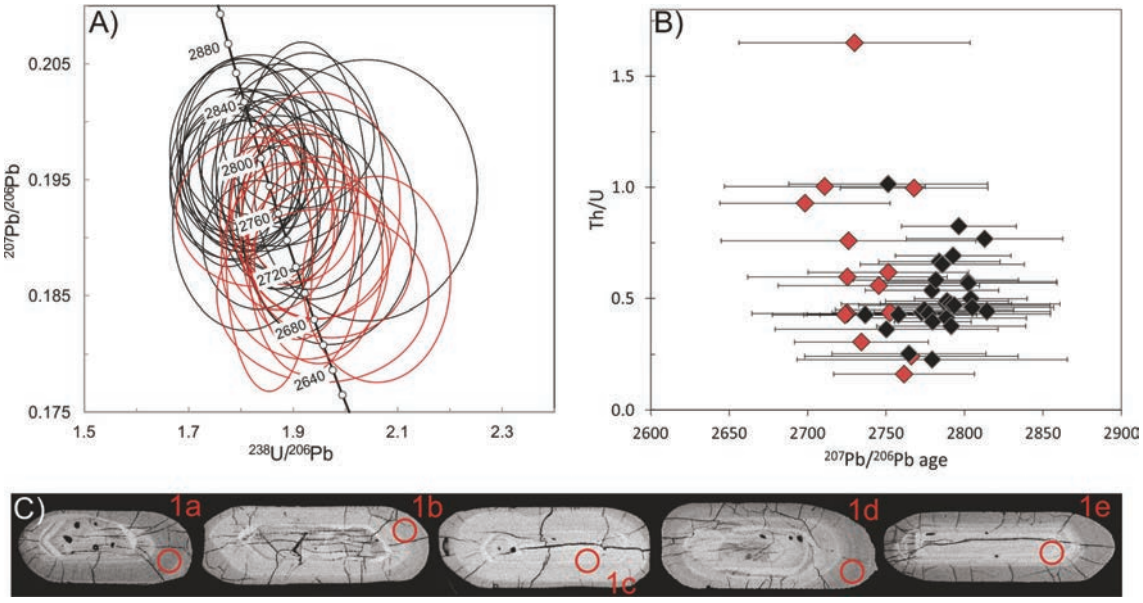

Figure 30. *Sample 527425 A) Tera-Wasserburg diagram with all data displayed, black ellipses: core domains, red ellipse: rim domains. B) Th/U versus $^{207}Pb/^{206}Pb$ age diagram, black diamonds: core domains, red ellipses: rim domains. C) Zircon BSE images, red circles indicate laser spots (30 µm in diameter), $^{207}Pb/^{206}Pb$ ages, 1a: 2768 ± 47 Ma, 1b: 2725 ± 64 Ma, 1c: 2788 ± 42 Ma, 1d: 2711 ± 64 Ma, 1e: 2805 ± 52 Ma. Errors are on 2σ level.*

Granitic sheets and veins within mafic granulites, Helge Halvø (sample 527454)

Description: 0.5 to 3 m wide leuco-granite sheets and associated orthopyroxene-bearing leucocratic veins within mafic granulite. The widest of the felsic sheets are generally foliation parallel to the foliation displayed by the mafic granulites. The smaller leucocratic veins infiltrate both the mafic and felsic granulites (Figure 31).
Purpose: Age of leucocratic melts infiltration, protolith intrusion age and inheritance.
Analytical methods: BSE-imaging; GEUS LA-ICP-MS data.

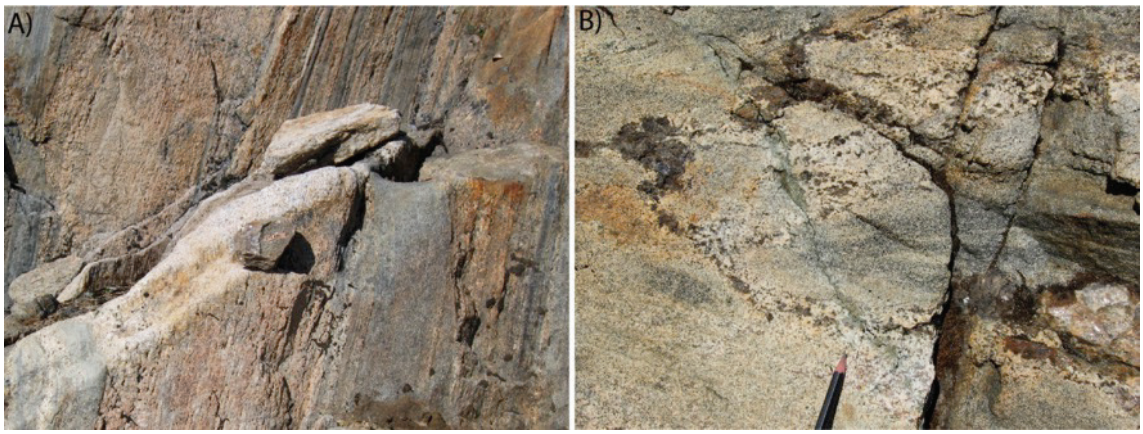

Figure 31. *A) Alternating felsic and mafic granulite. B) Leucocratic, undeformed, orthopyroxene-bearing veins intrude into both the felsic and mafic granulites.*

Data description and interpretation: Zircon grains are mainly prismatic and from 200 to 500 µm in length. Internally most grains are dominated by homogeneous domains with different BSE intensity. Most grains have BSE-grey outer rims, BSE-bright inner rims and inclusion-rich core domains (Figure 32C). Growth-zoning is not observed in BSE images, but is apparent in the normal transmitted light, where zoning occurs in the inner rim domains. Zircon U-Pb age data are concordant (except for one analyses) and plot in one coherent group (Figure 32A) with $^{207}Pb/^{206}Pb$ ages ranging from 2602 ± 103 Ma to 2764 ± 63 Ma. Th/U ratios range from 0.2 to 1.4 with no apparent correlation to age (Figure 32B). Excluding three analyses with the lowest $^{207}Pb/^{206}Pb$ ages yields a weighted mean $^{207}Pb/^{206}Pb$ age of **2724 ± 8 Ma** (n = 44, MSWD = 0.68), which is interpreted as the zircon crystallisation age and the intrusion of leucocratic orthopyroxene-bearing veins.

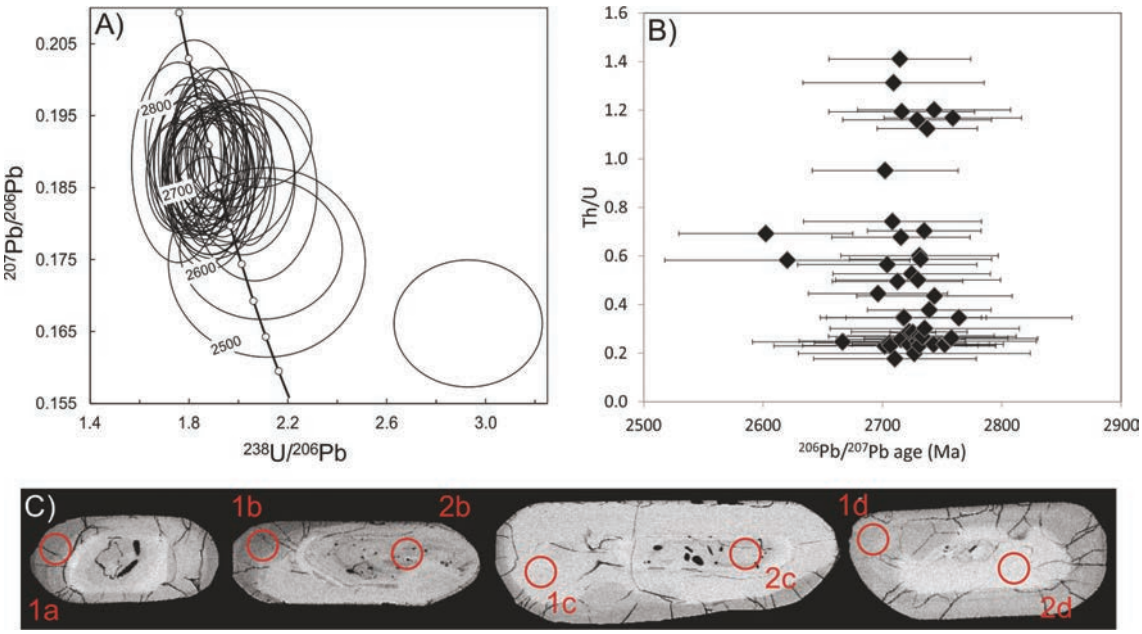

Figure 32. *Sample 527454. A) Tera-Wasserburg diagram with all data displayed. B) Th/U versus $^{207}Pb/^{206}Pb$ age diagram. C) Zircon BSE images, red circles indicate laser spots (30 µm spot size), $^{207}Pb/^{206}Pb$ ages, 1a: 2764 ± 63 Ma, 1b: 2708 ± 76 Ma, 2b: 2667 ± 58 Ma, 1c: 2706 ± 74 Ma, 2c: 2715 ± 54 Ma, 1d: 2735 ± 79 Ma, 2d: 2744 ± 49 Ma. Errors are on 2σ level.*

Leucocratic granitic veins within mafic granulite, Lange Næs (sample 527469)

Description: Leucocratic granitic veins within mafic granulite (Figure 33).
Purpose: Intrusive age of leucocratic veins.
Analytical methods: BSE-imaging; GEUS LA-ICP-MS data.

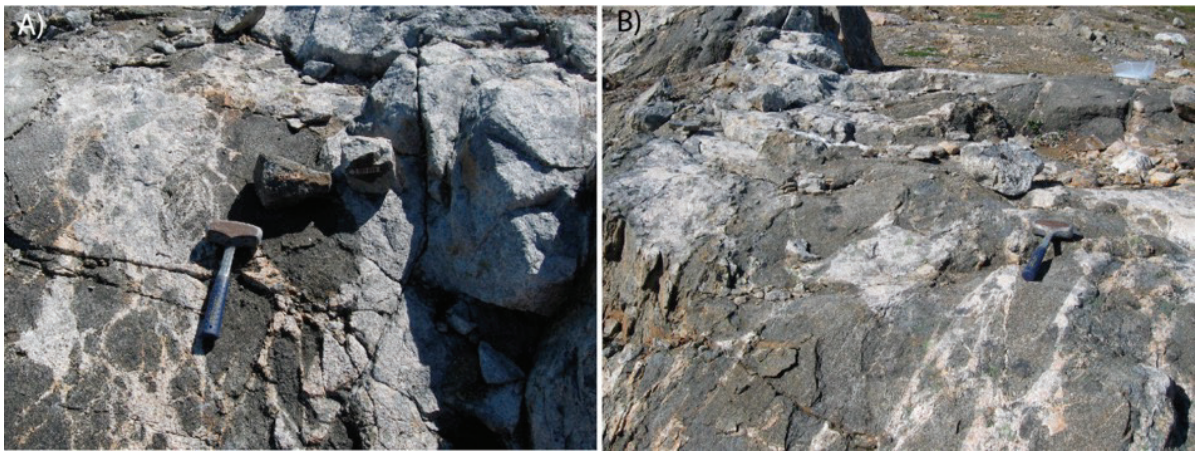

Figure 33. *Outcrop image showing a mafic granulite infiltrated by leucocratic granitic veins. Sample 527469 are from the granitic veins.*

Data description and interpretation: Zircon grains are mainly prismatic and from 200 to 500 µm in length. Internally most grains appear strongly altered, some with BSE-bright inclusion-rich core domains and often homogenises BSE-grey rims (Figure 34C). Core domains are homogeneous to faintly growth-zoned. Zircon U-Pb age data are generally concordant with $^{207}Pb/^{206}Pb$ ages ranging from 2684 ± 66 Ma to 3078 ± 80 Ma (Figure 34A). Core domains with preserved growth-zoning are generally older. Th/U ratios range between 0.1 and 2.1. The core domains older than ca. 2800 Ma display increasing Th/U for increasing age, whereas the younger rim domains display a larger variation in Th/U (Figure 34B). Selecting analyses from rim, or internal homogeneous domains, yields a mean $^{207}Pb/^{206}Pb$ age of **2737 ± 10 Ma** (n = 34; MSWD = 0.64), which is interpreted as the intrusion age of the leucocratic granite vein. Older domains are interpreted as inherited where decreasing Th/U ratios for the younger domains suggest that grains were affected by Pb-loss.

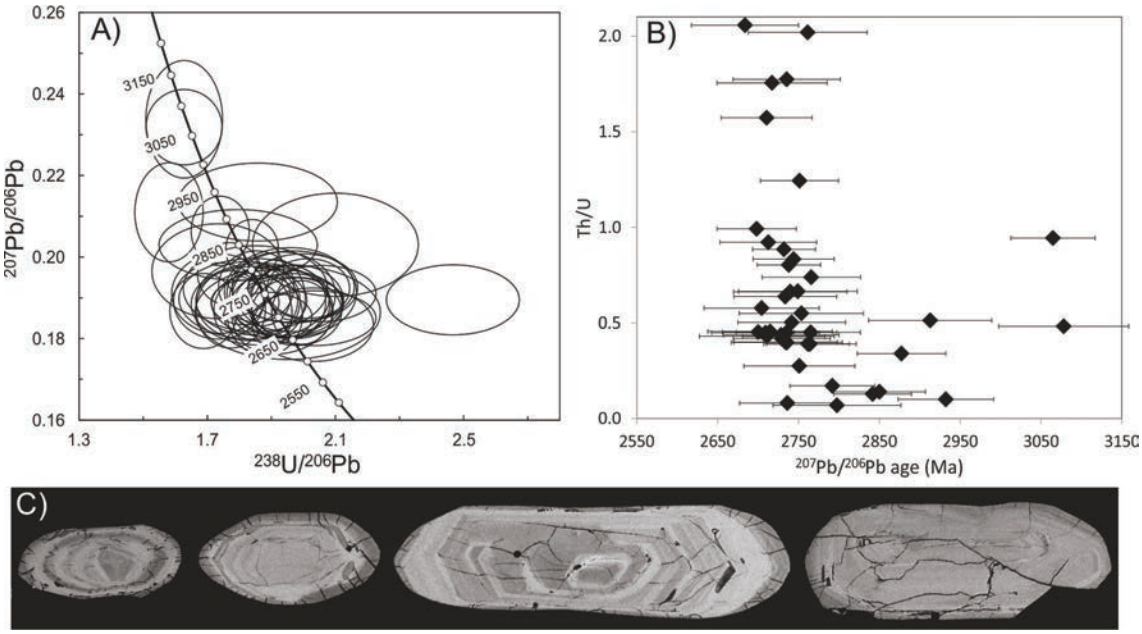

Figure 34. *Sample 527469 A) Tera-Wasserburg diagram with all data displayed. B) Th/U versus $^{207}Pb/^{206}Pb$ age diagram. C) Zircon BSE images. Errors are on 2σ level.*

Granite sheet (sample 527463)

Description: Granitic sheet intruding into mafic granulite.
Purpose: Intrusion age of granitic sheet and inheritance.
Analytical methods: BSE-imaging; GEUS LA-ICP-MS data.
Data description and interpretation: Zircon grains are mainly prismatic and from 200 to 500 µm in length. Internally most grains appear strongly altered, some with BSE-bright inclusion-rich core domains and often homogenises BSE-grey rims (Figure 35C). Core domains are homogeneous to faintly growth-zoned. Zircon U-Pb age data are generally concordant with $^{207}Pb/^{206}Pb$ ages ranging from 2686 ± 28 Ma to 2898 ± 82 Ma, where core domains plot with older ages (Figure 35A). Th/U ratios range between 0.2 and 2.6. The core domains older than ca. 2800 Ma show increasing Th/U for increasing age, whereas, younger rim domains display larger variation in Th/U with values up to 2.6 (Figure 35B). Selecting analyses from core domains yields a mean $^{207}Pb/^{206}Pb$ age of 2839 ± 17 Ma (n = 10; MSWD = 0.63), which is interpreted as an inherited population. Selecting analyses from rim domains and internal homogeneous domains yields a mean $^{207}Pb/^{206}Pb$ age of **2731 ± 9 Ma** (n = 33; MSWD = 0.85), which is interpreted as the crystallisation age of the granitic sheet.

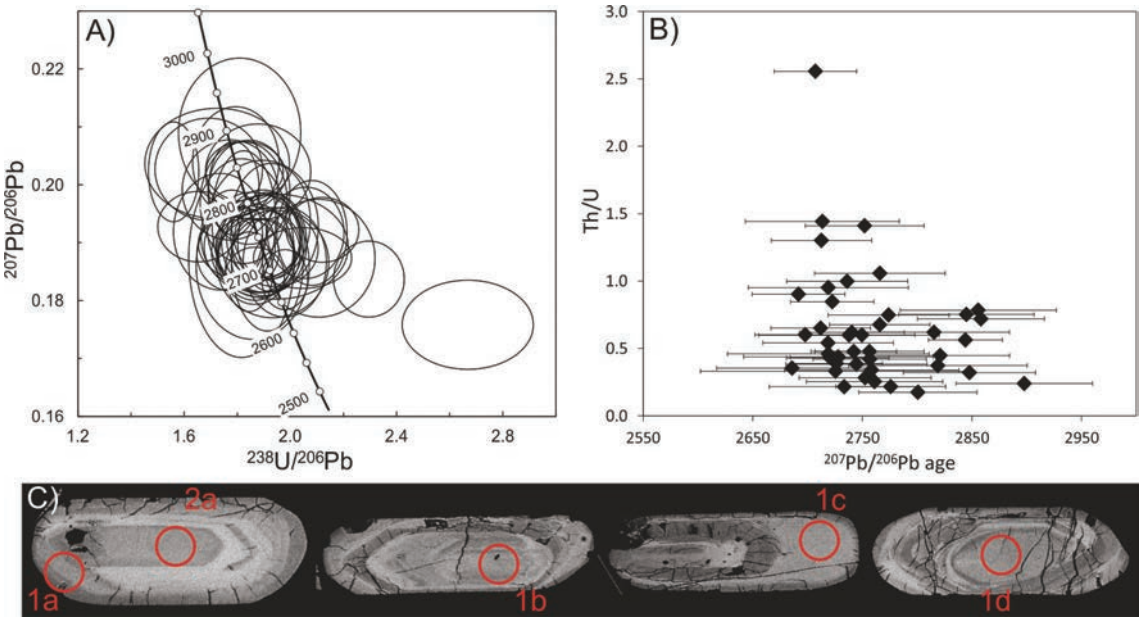

Figure 35. *Sample 527463 A) Tera-Wasserburg diagram with all data displayed. B) Th/U versus $^{207}Pb/^{206}Pb$ age diagram. C) Zircon BSE images, red circles indicate laser spots (30 µm spot size), $^{207}Pb/^{206}Pb$ ages, 1a: 2750 ± 52 Ma, 2a: 2766 ± 80 Ma, 1b: 2856 ± 62 Ma, 1c: 2745 ± 62 Ma, 1d: 2898 ± 82 Ma. Errors are on 2σ level.*

Granite sheet (sample 536537)

Description: Granitic sheet intruded into a belt composed of mainly mafic lithologies (Figure 36).
Purpose: intrusive age of granitic sheet and inheritance.
Analytical methods: CL-**i**maging; GEUS LA-ICP-MS data

Figure 36. *Outcrop images from sample 536537. A) Sample 536537 from a weakly foliated granite. B) The outcrop pattern of mafic lithologies intruded by granitic sheets; the mafic lithologies are infiltrated by orthopyroxene-bearing cm-scale felsic veins.*

Data description and interpretation: Zircon grains are oblate to prismatic and from 50 to 200 µm in length. Internally zircon textures are dominantly growth-zoned, but some grains

have homogeneous rims and internal diffuse textures (Figure 37C). Zircon U-Pb age data are largely concordant and plot in one group (Figure 37A), with $^{207}Pb/^{206}Pb$ ages ranging from 2543 ± 121 Ma to 2750 ± 50 Ma. Th/U ratios range 0.1 to 0.9 with no correlation with age (Figure 37B). Excluding the lowest age we obtain a mean $^{207}Pb/^{206}Pb$ age of **2706 ± 15 Ma** (n = 19, MSWD = 0.81), which is interpreted as the crystallisation age of the intrusive granitic sheet.

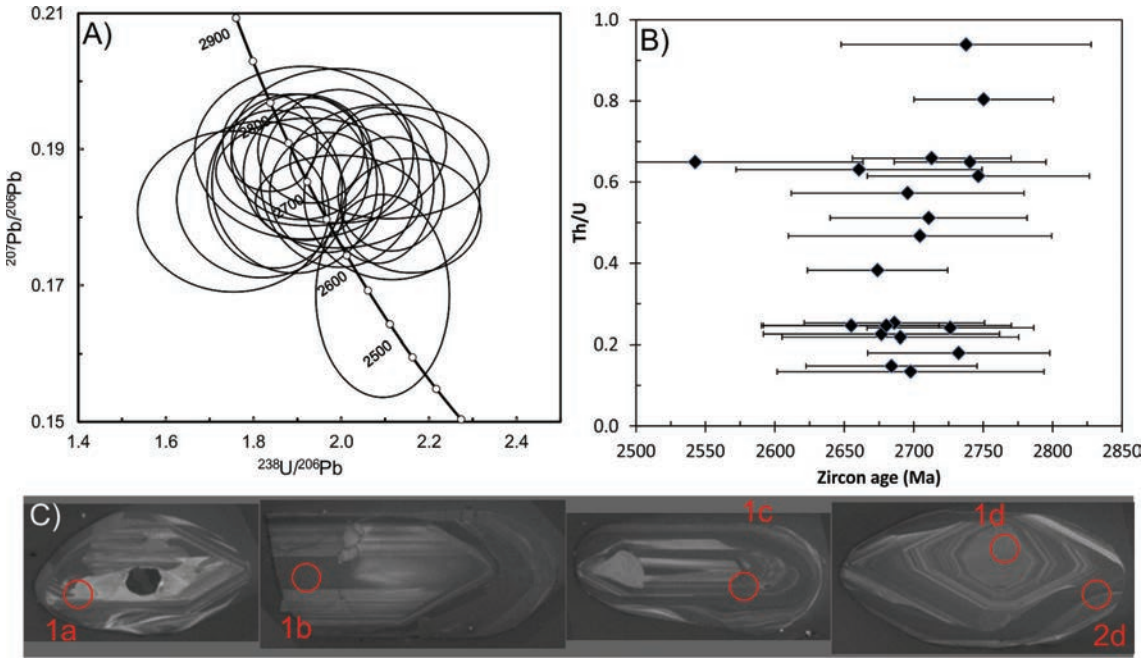

Figure 37. *Sample 536537 A) Tera-Wasserburg diagram with all data displayed. B) Th/U versus $^{207}Pb/^{206}Pb$ age diagram. C) Zircon BSE images, red circles indicate laser spots (30 µm spot size), $^{207}Pb/^{206}Pb$ ages, 1a: 2750 ± 50 Ma; 1b: 2738 ± 90 Ma; 1c: 2686 ± 65 Ma; 1d: 2741 ± 51 Ma; 2732 ± 66 Ma. Errors are on 2σ level.*

Late pegmatites

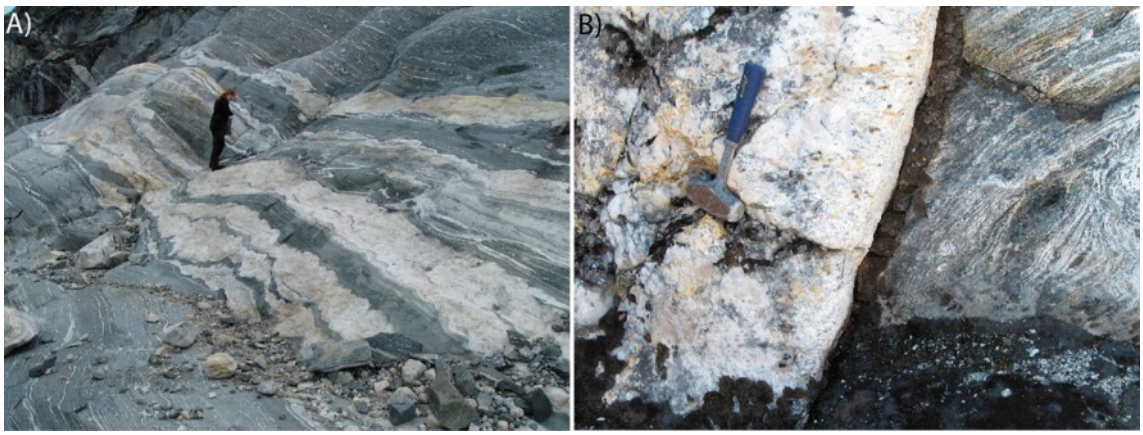

Figure 38. *A) Sample 527025 from a leucocratic pegmatite intruding into a mafic sequence of amphibolite. B) Sample 527041 from pegmatite in shear zone, the foliation in the right of the image is drawn towards parallelism with the pegmatite suggesting that the pegmatite is post tectonic and intruded into a shear zone.*

Pegmatite (sample 527025)

Description: Pegmatite with pinch-swell structures intruded into mafic sequence of amphibolite.
Purpose: Intrusive age of pegmatite
Analytical methods: BSE-imaging; GEUS LA-ICP-MS data.
Data description and interpretation: Zircon grains are strongly altered and it is uncertain to what extend the obtained ages have geological relevance (Figure 38C). The data points smear mainly along Concordia and the analyses that are within a ± 5 % discordance level display ages that range widely from ca. 2700 to 2000 Ma. The grains with the lowest $^{207}Pb/^{206}Pb$ ages display a recent Pb-loss trend with an upper intercept at 2056 ± 40 Ma (lower intercept at 485 ± 140 Ma); the geological relevance of this age is uncertain, but is interpreted as a Pb-loss age (Figure 38A). The eight oldest, concordant analyses yield a weighted average $^{207}Pb/^{206}Pb$ age of **2590 ± 48 Ma** (n=8; MSWD = 3.2), which is interpreted as the crystallisation age of the pegmatite.

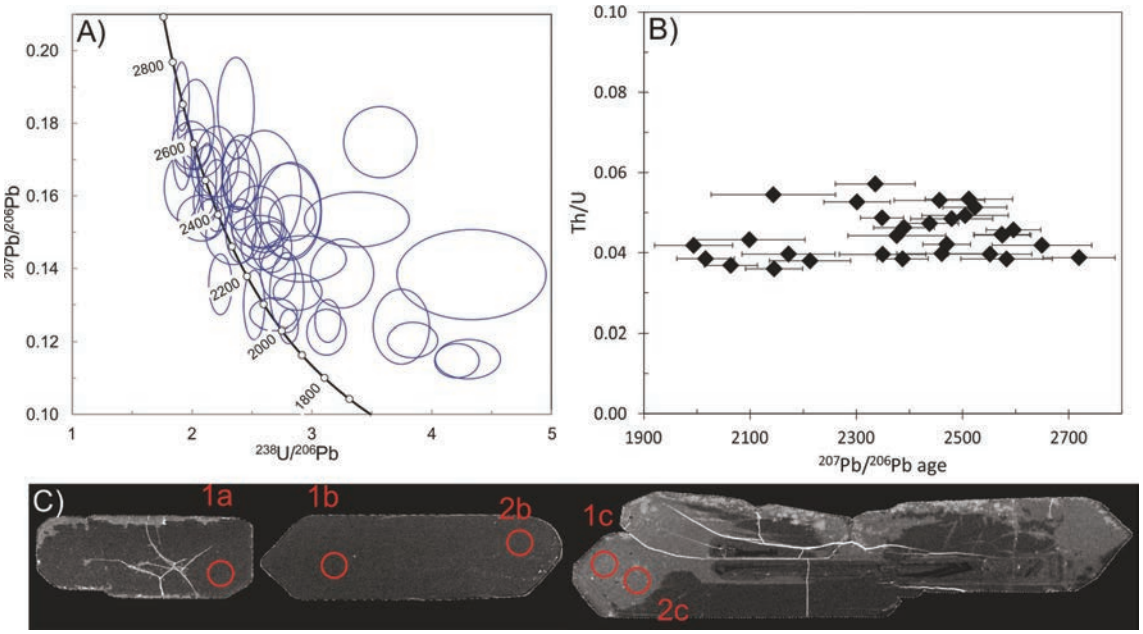

Figure 39. *Sample 527025. A) Tera-Wasserburg diagram with all data. B) Th/U versus $^{207}Pb/^{206}Pb$ age diagram. C) Zircon BSE images. Red circles indicate laser spots (spot size is 30 µm), $^{207}Pb/^{206}Pb$ ages, 1a: 2574 ± 53 Ma, 1b: 2596 ± 51 Ma, 2b: 2649 ± 94 Ma, 1c: 1993 ± 74 Ma, 2c: 2038 ± 67 Ma. Errors are on 2σ level.*

Pegmatite in shear zone (sample 527041)

Description: Pegmatite intruding into narrow (<1 m) wide shear zone. The shear zone seems to relate to the latest shearing in the area.
Purpose: Intrusive age of pegmatite and minimum age of shear zone.
Analytical methods: BSE-imaging; GEUS LA-ICP-MS data.

Data description and interpretation: Zircon grains are stubby and euhedral and from 100 to 400 µm in length. Internal textures are dominated by homogeneous, BSE-dark domains that are infiltrated by BSE-bright domains often related to fracturing (Figure 39C). Zircon U-Pb age data are mainly concordant with $^{207}Pb/^{206}Pb$ ages ranging from 2461 ± 62 Ma to 2650 ± 65 Ma and Th/U ratios from 0.3 to 0.5 (Figure 39A, B). Analyses that are more than 90 % concordant yields a weighted mean $^{207}Pb/^{206}Pb$ age of **2601 ± 9 Ma** (n = 41; MSWD = 0.87), which is interpreted as the crystallisation age of the pegmatite.

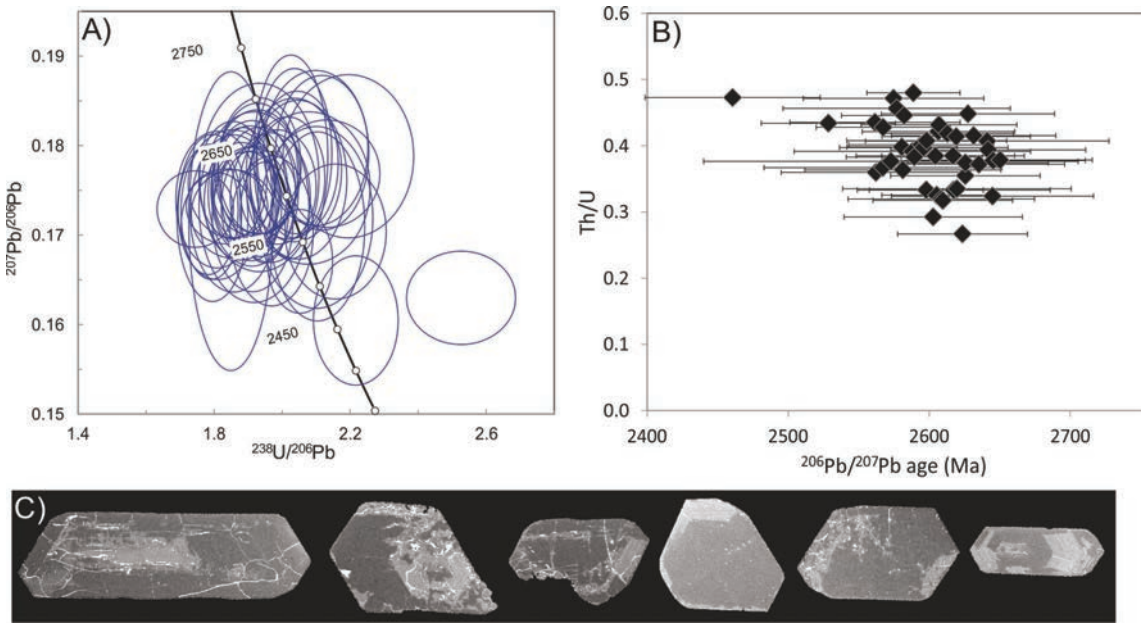

Figure 40. *Sample 527041. A) Tera-Wasserburg diagram with all data displayed. B) Th/U versus $^{207}Pb/^{206}Pb$ age diagram. C) Zircon BSE images. Errors are on 2σ level.*

Part 2: Southern section from Kong Dans Halvø to Timmiarmiut

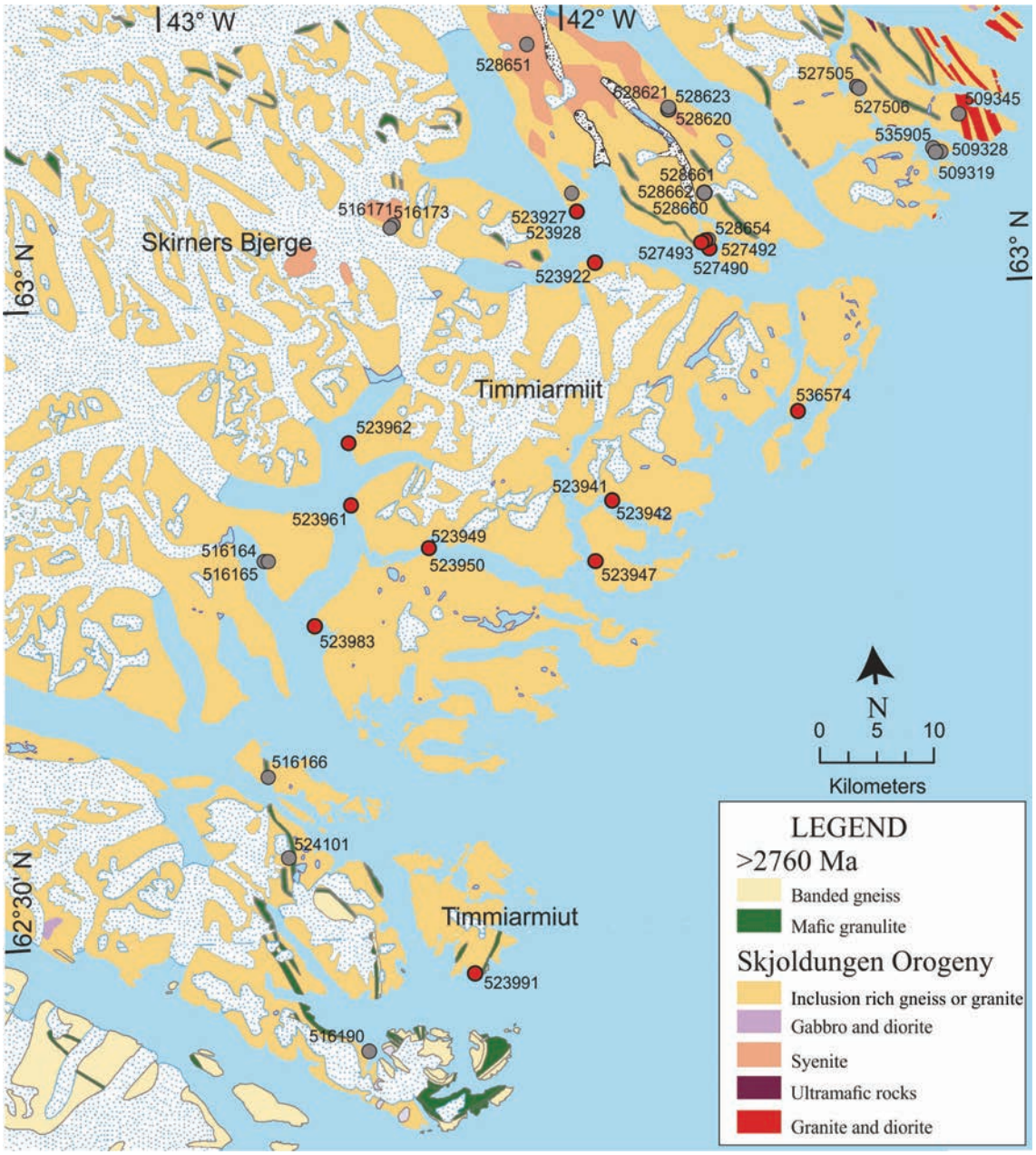

Figure 41. *Simplified geological map of the southern section of the investigated area between Kong Dans Halvø and Timmiarmiut. Red dots are locations for samples presented in this report. Grey dots are locations for samples where geochronology data have been reported either by Kolb et al. (2013) or Kokfelt et al. (2016).*

Banded gneiss basement in the southern part of the region

Banded gneisses (sample 523961)

Description: Sample is taken from banded gneiss consisting of alternating melanocratic and leucocratic cm scale layers (Figure 42A), these units are intruded by larger weakly deformed leucocratic veins that have not been dated (Figure 42A). Further the gneisses are cut by dyke that must be older than c. 2700 as this in the age of the latest felsic veining in the area (Figure 42B).
Purpose: Intrusion age of melanocratic background and felsic leucocratic veins.

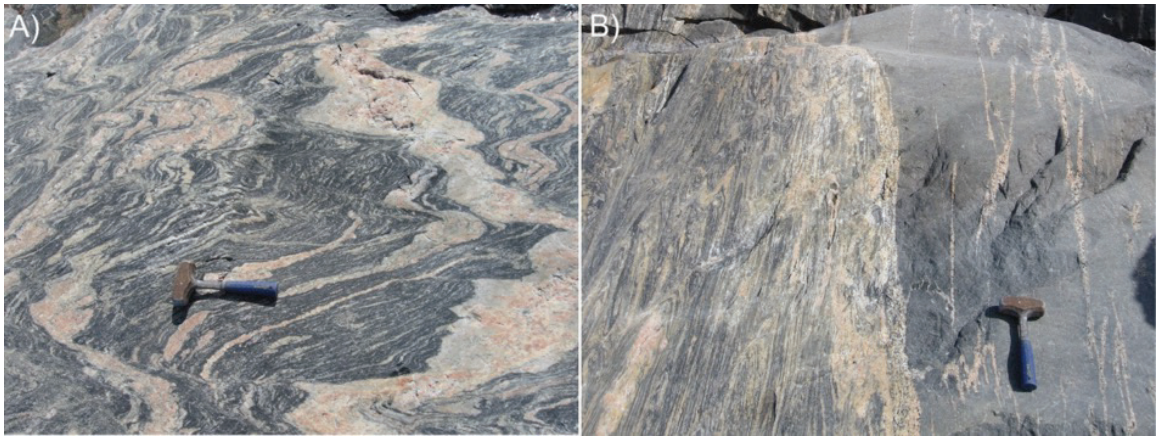

Figure 42. *Sample 523961. A) Banded gneiss composed of alternating melanocratic and leucocratic cm-scale layers that are intensely folded and cut by several generations of less deformed granitic sheets. B) Banded gneiss cut by mafic dyke that must be older than c. 2700 Ma as this is the age of the latest felsic veining in the area.*

Data description and interpretation: Zircon grains display large variations is size, from ca. 100 to 400 µm in length and are mainly rounded or oblate with only few prismatic grains. Internally zircon textures are dominated by BSE-grey core regions that are either homogeneous, growth-zoned or with diffuse textures, and BSE-brighter rim domains ranging from narrow to wide and with either growth-zoned or homogeneous textures (Figure 43C). Zircon U-Pb age data are mainly concordant and plot in two main groups (Figure 43A), with spot $^{207}Pb/^{206}Pb$ ages ranges from 2763 ± 80 Ma to 3284 ± 78 Ma. Th/U ratios range 0.2 to 2.8 with the older age population having Th/U ratios between 0.5 to 1.0, and the younger population displaying a larger range of values, up to 2.8 (Figure 43B). The old zircon population yields a mean $^{207}Pb/^{206}Pb$ age of **3231 ± 12 Ma** (n = 32; MSWD = 0.72), which we interpret as the protolith age of the melanocratic layers of the gneiss. The younger population yields a mean $^{207}Pb/^{206}Pb$ age of **2853 ± 36 Ma** (n = 10; MSWD = 2.0), which we interpret as reflecting the age of the leucocratic veins.

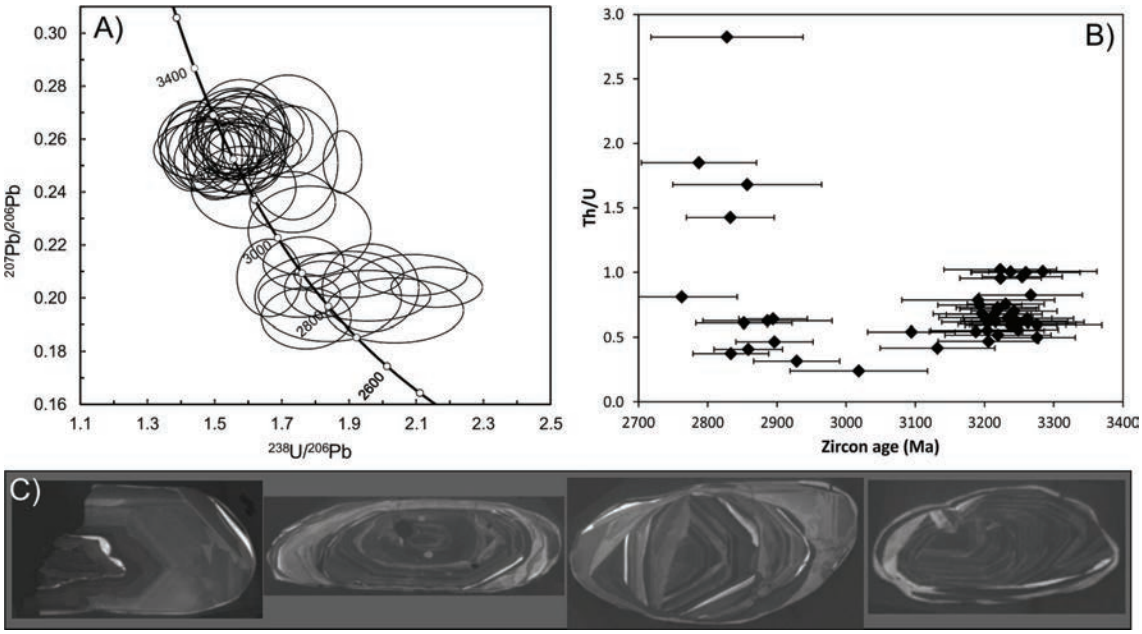

Figure 43. *Sample 523961. A) Tera-Wasserburg diagram with all data plotted. B) Th/U vs age. C) Internal zircon textures in CL. Errors are on 2σ level.*

Mingling between felsic and mafic magmas

Sample 523927 and 523928 are from a locality revealing evidence of magma mingling (Figure 44A) and strain variation (compare Figure 44A with Figure 44B).

Figure 44. *Field images from outcrops of mingling tonalitic and granitic melts (now rocks). A) Detailed view of magma mingling textures. B) Same rock types as in A, but with a larger strain. C) Tonalite sample 523927. D) Granite ample 523928.*

Tonalite (sample 523927)

Description: Fine- to medium-grained tonalite with a weakly developed foliation and mingling relation to associated granite (Figure 44C).

Purpose: Intrusion age and information on age inheritance.

Analytical methods: CL-imaging; GEUS LA-ICP-MS data.

Data description and interpretation: Zircon grains are mainly rounded or oblate and from 50 to 200 µm in length. Internally zircon textures are dominated by growth-zoned core domains that vary in intensity (CL) and homogeneous or sector-zoned rim domains (Figure 45C). Zircon U-Pb age data are mainly concordant and with one exception plot in a single group (Figure 45A) with $^{207}Pb/^{206}Pb$ ages ranging from (2453 ± 103 Ma) 2667 ± 72 Ma to 2840 ± 70 Ma. There is no apparent age difference between core and rim domains. The oldest age at 2840 Ma is from a CL bright core domain; however other core domains have younger ages. Th/U range from 0.3 to 1.5 and display a positive correlation with $^{207}Pb/^{206}Pb$ age (Figure 45B), which might reflect Pb-loss in domains with lower age. Assuming one age population that includes core and rim domains, we select all data except the young outlier, this yields a weighted mean $^{207}Pb/^{206}Pb$ age of **2725 ± 14 Ma** (n = 31; MSWD = 1.3), which is interpreted as the crystallisation of the tonalite intrusion.

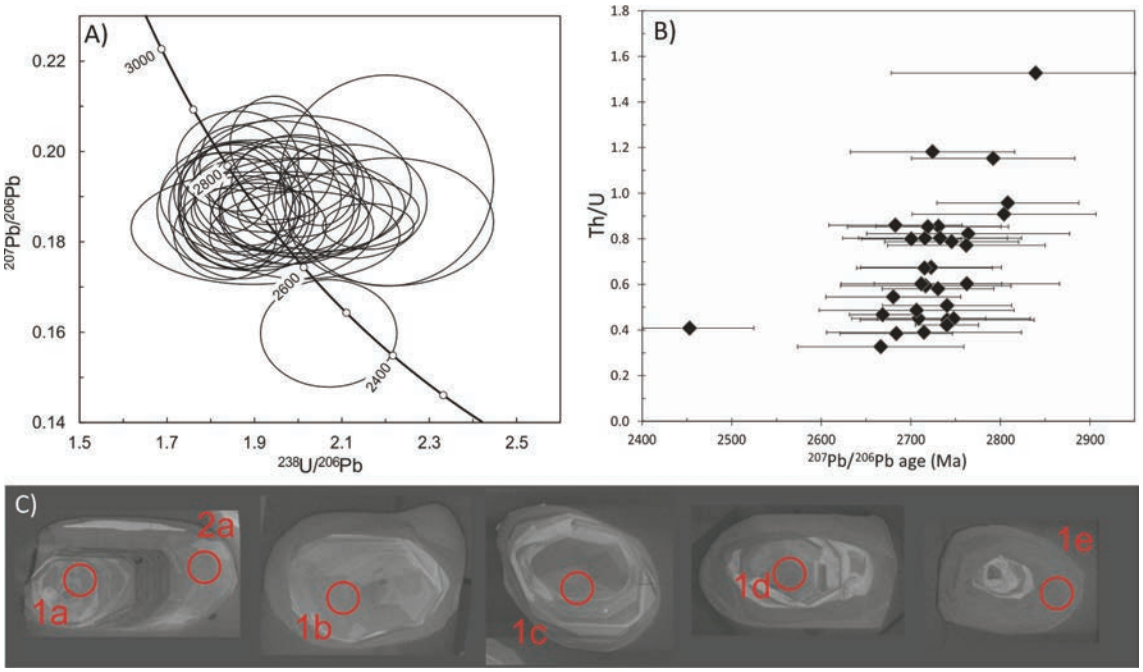

Figure 45. *Sample 523927. A) Concordia plot, all data. B) Th/U vs. $^{207}Pb/^{206}Pb$ age. C) CL images of internal textures, with indication of spot analyses for U-Pb age data: 1a: 2724 ±76 Ma, 2a: 2716 ± 109 Ma, 1b: 2701 ± 74 Ma, 1c: 2715 ± 93 Ma, 1d: 2762 ± 109 Ma, 1e: 2693 ± 103 Ma. Spots are 30 µm, $^{207}Pb/^{206}Pb$ ages. Errors are on 2σ level.*

Granite sample (523928)

Description: Medium-grained granite, locally with a weakly developed foliation, and with mingling relationship to associated tonalite (sample 523927) (Figure 44D).

Purpose: Intrusion age and information on age inheritance.

Analytical methods: CL-imaging; GEUS LA-ICP-MS data.

Data description and interpretation: Zircon grains are prismatic, rounded to oblate and range in size from 50 to 400 µm.. Internally zircon textures are dominated by growth-zoned or BSE-dark, homogeneous core domains and large sector- and growth-zoned rims (Figure 46C). Zircon U-Pb age data are mainly concordant and smear out along the Concordia (Figure 46A) with $^{207}Pb/^{206}Pb$ ages ranging from 2699 ± 61 Ma to 2951 ± 69 Ma. Th/U ratios range from 0.1 to 1.3, highest in the younger analyses (Figure 46B). Selecting analyses from rim domains we obtain a weighted mean $^{207}Pb/^{206}Pb$ age of **2740 ± 17 Ma** (n = 15; MSWD = 1.03), which is interpreted as the intrusion age. This age is within error identical to the age of the co-mingling tonalite (sample 523927), thus confirming the field observations that these melts intruded coevally. From a selection of analyses from core domains we obtain as weighted mean $^{207}Pb/^{206}Pb$ age of **2876 ± 29 Ma** (n = 15; MSWD = 2.4), which is interpreted as an inherited population.

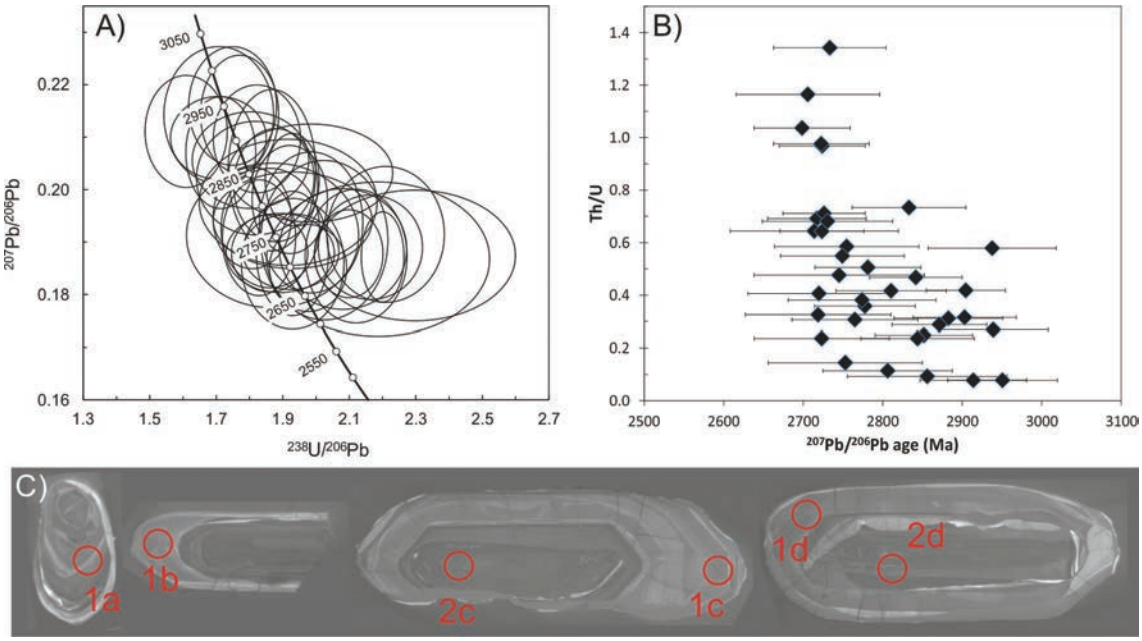

Figure 46. *Sample 523928. A) Concordia plot including all data. B) Th/U vs. $^{207}Pb/^{206}Pb$ age. C) CL images of internal textures, with position of spot analyses for U-Pb age data: 1a: 2914 ± 67 Ma, 1b: 2749 ± 78 Ma, 1c: 2724 ± 53 Ma, 2c: 2903 ± 65 Ma, 1d: 2778 ± 63 Ma, 2d: 2883 ± 68 Ma. Spots are 30 µm, $^{207}Pb/^{206}Pb$ ages. Errors are on 2σ level.*

Undeformed granite sheet (sample 523922)

Description: Medium- to course-grained granite sheet intruded into a mafic to ultramafic unit (Figure 47A, B). Both the granite sheet and the mafic to ultramafic unit are relatively undeformed, but there are some strain variations in the rocks of the outcrop.

Purpose: Intrusion age and information on age inheritance.

Analytical methods: CL-imaging; Lund LA-ICP-MS data.

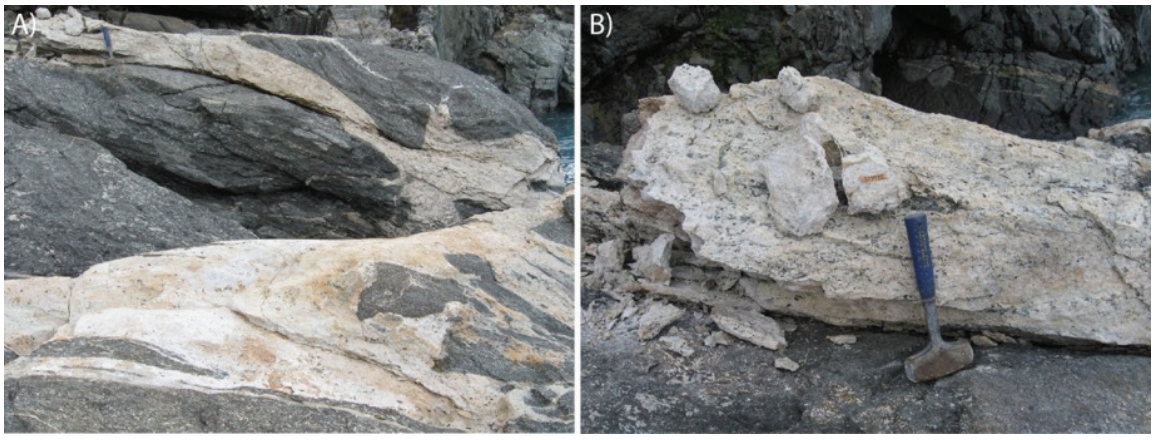

Figure 47. *Possibly magma mingling between leucocratic sheet and mafic to ultramafic intrusive*

Data description and interpretation: Zircon grains vary in size from ca. 100 to 400 µm and are mainly rounded or oblate with only few prismatic grains (Figure 48C). Internal textures are dominated by CL-bright rims with sector-zoned and homogeneous domains. The core regions seem to divide into inner sector-zoned rims/mantles and BSE-darker xenocrystic cores with a textures varying from strongly altered to growth-zoned. Zircon U-Pb age data show some spread across the Concordia, indicating either recent Pb-loss or poorly corrected instrument fractionation (Figure 48A). The $^{207}Pb/^{206}Pb$ ages range from 2678 ± 20 Ma to 2834 ± 28 Ma. Th/U ratios range from 0.6 to 4.1, with an overall increase and larger spread in Th/U ratios for the younger ages (Figure 48B). Main age population yields a mean $^{207}Pb/^{206}Pb$ age of **2736 ± 5 Ma** (n = 17; MSWD = 2.1), which is interpreted as the crystallisation age of the granite sheet. Older analyses are interpreted as xenocrystic grains.

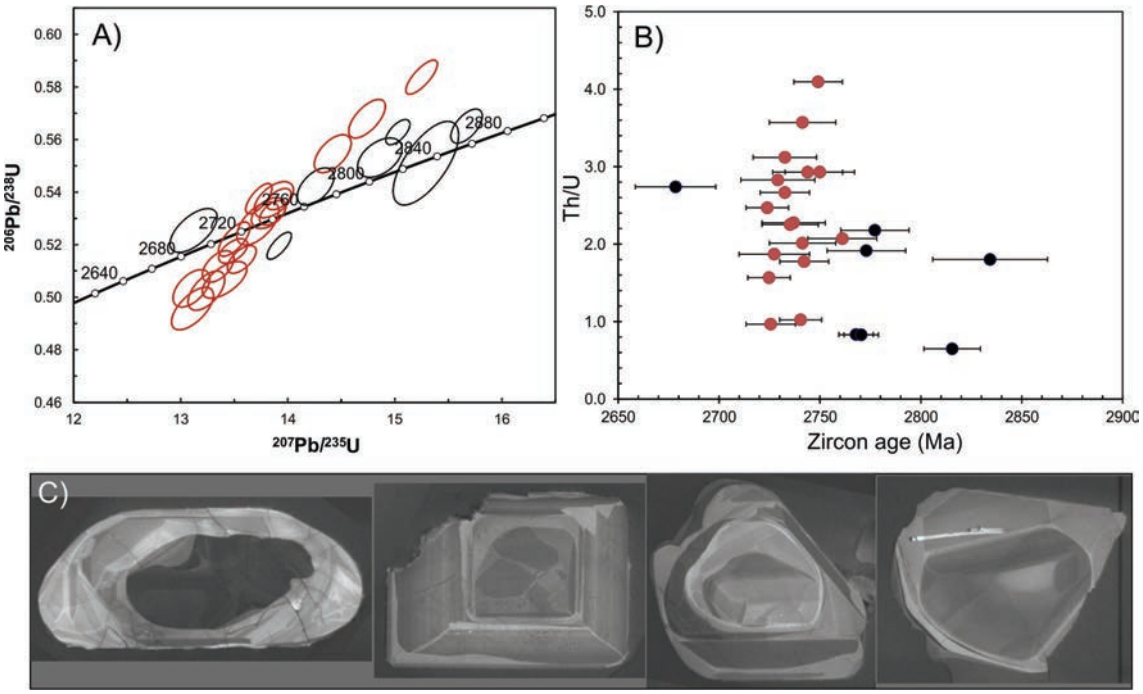

Figure 48. *Sample 523922. A) Concordia plot including all data. B) Th/U vs. $^{207}Pb/^{206}Pb$ age. C) CL images of internal textures. Errors are on 2σ level.*

Granitoids of the southern part of the region: leucocratic inclusion-rich granites with agmatitic and nebulitic textures

Granite with weak foliation (sample 527490)

Description: Leucocratic granite rich in mafic and ultramafic xenolith inclusions, at the sample site the granite has a weak foliation.
Purpose: Intrusion age and information inheritance.
Analytical methods: BSE-imaging; GEUS LA-ICP-MS data.

Figure 49. *Sample 527490, 527492 and 527493 are all from leucocratic granitoids which locally encompass two main textural types: Inclusion-rich leucocratic granitoids (A), and leucocratic granite with a nebulitic texture (B).*

Data description and interpretation: Zircon grains display large variations is size, from ca. 100 to 400 microns in length and are mainly rounded or oblate with only few prismatic grains. Internally zircon textures are dominated BSE-grey core regions that are either homogeneous or growth-zoned, and BSE-brighter mainly homogeneous rims. The cores and rims are separated by BSE-bright, metamict inner rims (Figure 50C). Zircon U-Pb age data are mainly concordant and smear out along Concordia (Figure 50A) with $^{207}Pb/^{206}Pb$ ages ranging from 2691 ± 96 Ma to 3022 ± 63 Ma, the main age population falls between 2780 and 2870 Ma and a minor population has ages ranging from 2691 to 2750 Ma. The main zircon population (2780 to 2870 Ma) represents homogeneous, BSE-grey domains and these display a positive correlation between $^{207}Pb/^{206}Pb$ age and Th/U (Figure 50B), suggesting that a metamorphic overprinting and associated Pb-loss affected the younger age domains. The minor age population is from rim domains and have Th/U ratios from 1.6 to 0.4 (Figure 50B). A selection of analyses with Th/U > 1 is taken to be the main zircon population, we obtain a mean $^{207}Pb/^{206}Pb$ age of **2833 ± 11 Ma** (n = 34; MSWD = 0.35); this age is interpreted as an inherited population. The minor population is interpreted as reflecting the intrusive age with a mean weighted $^{207}Pb/^{206}Pb$ age of **2732 ± 26 Ma** (n =6; MSWD = 0.32).

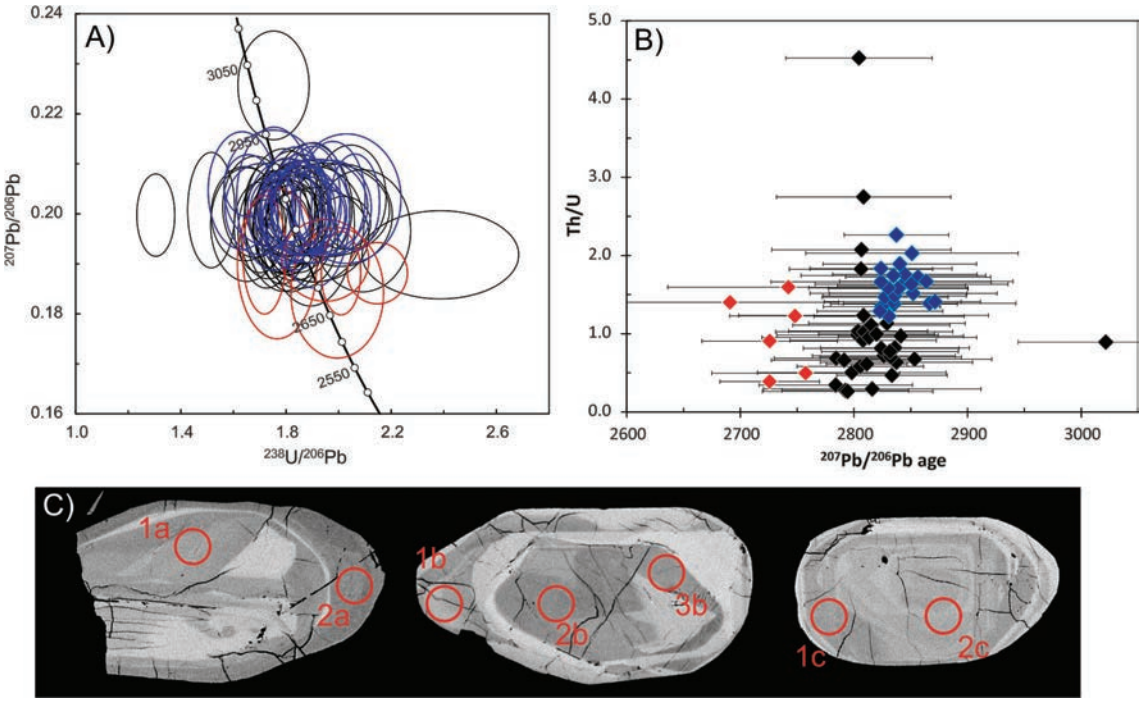

Figure 50. *Sample 527490. A) Tera-Wasserburg diagram with all data, blue ellipses: data used for calculating inherited population age; red ellipses: data used for calculating intrusion age. B) Th/U vs. $^{207}Pb/^{206}Pb$ age for analyses that are < 10% discordant. Analyses marked by blue and red colour are the selections used to calculate population ages (like in A). C) BSE images of internal textures, with indication of spot analyses for U-Pb age data: 1a: 2871 ± 40 Ma, 2a: 2748 ±58 Ma, 1b: 2784 ± 67 Ma, 2b: 2813 ± 95 Ma, 3b: 2830 ± 69 Ma, 1c: 2864 ± 76 Ma, 2839 ± 61 Ma. Spots are 30 µm, $^{207}Pb/^{206}Pb$ ages. Errors are on 2σ level.*

Granite with weak foliation and agmatitic texture (sample 527492)

Description: Inclusion-rich leucocratic granite with a weak foliation.
Purpose: Intrusion age and information about inheritance.
Analytical methods: BSE-imaging; GEUS LA-ICP-MS data.

Data description and interpretation: Zircon grains are mainly prismatic and range in size from 200 to 400 µm is length. Internally zircon textures are dominated by BSE-grey homogeneous to growth-zoned rim domains and BSE-bright core domains with metamict appearances (Figure 51C). Zircon U-Pb age data are mainly concordant and the majority of the analyses plot in one coherent group (Figure 51A) with $^{207}Pb/^{206}Pb$ ages ranging from 2697 ± 54 Ma and 2879 ± 85 Ma. The main group of analyses is from BSE-grey rim domains and have ages between 2697 ± 54 Ma and 2782 ± 42 Ma. Th/U ratios range between 0.1 and 1.5 and the main group has values above 0.52 (Figure 51B). Selecting analyses from the main group with Th/U > 0.6 yields a weighted mean $^{207}Pb/^{206}Pb$ age of **2735 ± 10 Ma** (n = 38; MSWD = 0.56), which is interpreted as the crystallisation age of the granite. Three grains with ages from 2806 to 2879 Ma are from metamict core domains and likely reflect highly altered xenocrystic cores.

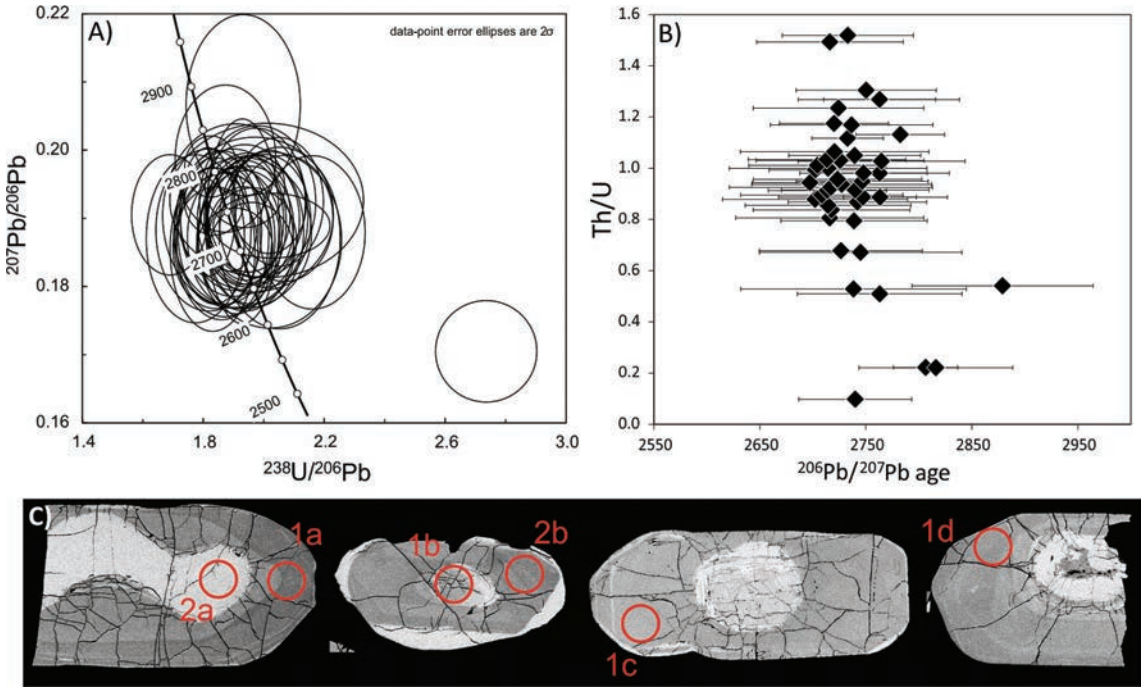

Figure 51. *Sample 527492. A) Tera-Wasserburg diagram showing all data. B) Th/U vs. $^{207}Pb/^{206}Pb$ age. C) BSE images of internal textures, with indication of spot analyses for U-Pb age data: 1a: 2742 ± 65 Ma, 2a: 2816 ± 72 Ma, 1b: 2870 ± 85 Ma, 2b: 2701 ± 65 Ma, 1c: 2765 ± 79 Ma, 1d: 2718 ± 74 Ma. Spots are 30 micron, $^{207}Pb/^{206}Pb$ ages. Errors are on 2σ level.*

Reddish granite from metasomatic zone (sample 527493)

Description: Red coloured granite related to metasomatic overprinting along a shear zone.
Purpose: Intrusion age and information on metasomatic overprinting and inheritance.
Analytical methods: BSE-imaging and GEUS LA-ICP-MS data.
Data description and interpretation: Zircon grains are mainly prismatic and oblate in morphology and vary in size from 200 to 400 µm with a few even larger grains, up to 700 microns in length. Internally the zircon textures are dominated by BSE-grey, homogeneous rim domains and BSE-brighter core domains that often appear metamict (Figure 52C). Zircon U-Pb age data are mainly concordant and smear out along the Concordia (Figure 52A) with $^{207}Pb/^{206}Pb$ ages ranging from 2605 ± 48 Ma to 2919 ± 80 Ma. Th/U ratios range from 0.01 to 4.4, where analyses with ages above 2750 Ma range between 0.01 and 0.7 and the younger analyses range from 0.01 to 4.4 (Figure 52B). Interpretation from the combined texture and age data is that zircon grains contain inherited core domains and that rim domains reflect the intrusive age. A selection of data from rim domains with Th/U > 0.5 we obtain a weighted mean $^{207}Pb/^{206}Pb$ age of **2722 ± 17 Ma** (n = 13, MSWD = 0.65). To calculate the age of the core domains, we assume that the age spread reflect Pb-loss in the core regions and we arbitrary select analyses with ages above 2850, this gives a weighted mean $^{207}Pb/^{206}Pb$ age of **2872 ± 9 Ma** (n = 13; MSWD = 0.61).

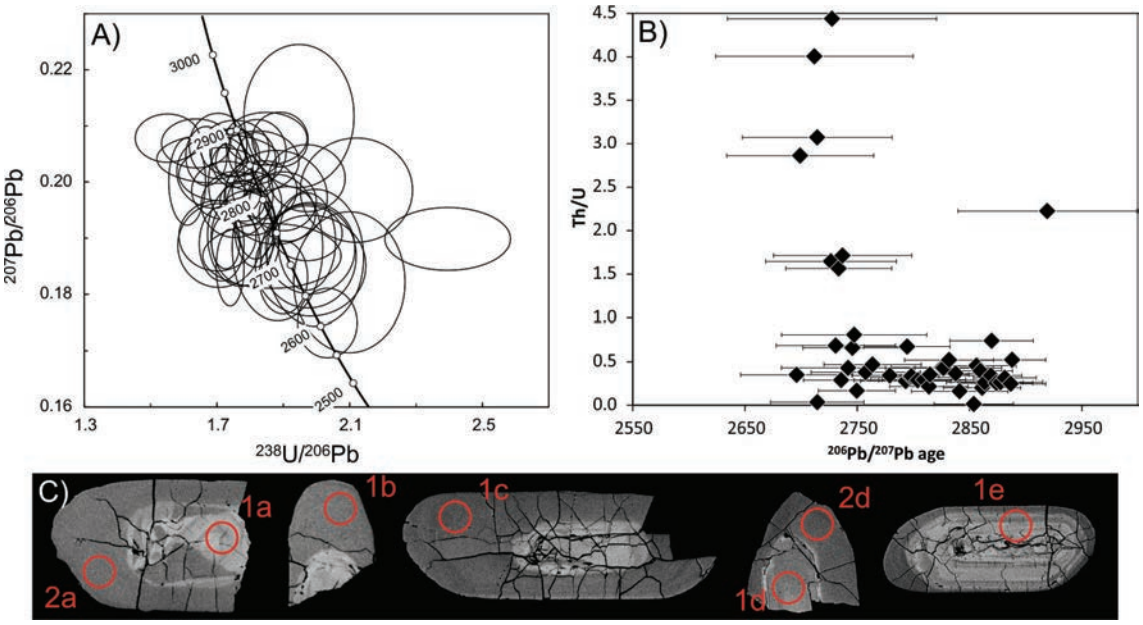

Figure 52. *Sample 527493. A) Tera-Wasserburg diagram showing all data. B) Th/U vs. $^{207}Pb/^{206}Pb$ age. C) BSE images of internal textures, with indication of spot position: 1a: 2874 ± 32, 2a: 2747 ± 65 Ma, 1b: 2714 ± 67 Ma, 1c: 2673 ± 93 Ma, 1d: 2878 ± 38 Ma, 2d: 2727 ± 58 Ma,1e: 2887 ± 31 Ma. Spots are 30 µm, $^{207}Pb/^{206}Pb$ ages. Errors are on 2σ level.*

Coarse grained and undeformed leucocratic granite (sample 536574)

Description: Undeformed, medium- to coarse-grained leucocratic granite (Figure 53C).

Purpose: Intrusion age and information on age inheritance.

Analytical methods: CL-images; Nordsim data

Data description and interpretation: Zircon grains are prismatic with aspect ratios from 1:2 to 1:3 and 200 to 400 µm in length. Internally the zircon grains have core-rim textures with bright homogeneous to sector-zoned rims and darker growth-zoned and sometimes sector-zoned cores, which also display alteration textures (Figure 53D). Zircon U-Pb analyses are concordant (Figure 53A) with $^{207}Pb/^{206}Pb$ ages ranging from 2700 ± 13 to 2775 ± 4 Ma. Th/U ratios range from 0.4 to 2.4 and display an increase with decreasing age (Figure 53B). The main data are obtained from core regions and these plots in a coherent group that show some Th/U increase for the younger analyses. Selecting eight analyses with low Th/U (< 0.8) yields an average $^{207}Pb/^{206}Pb$ age of **2765 ± 7 Ma** (n = 8, MSWD = 2.2). Only two analyses have been obtained from the bright rim domains, these have $^{207}Pb/^{206}Pb$ ages of 2700 ± 13 Ma and 2736 ± 9 Ma. The age derived from the core domains of 2765 ± 7 Ma is interpreted as an inherited igneous population. Rim domains are bright with a poorly constrained age of 2700 to 2740 Ma. The bright rims are interpreted as igneous, crystallising from a melt, an interpretation that is based on the undeformed nature of the hosting granite.

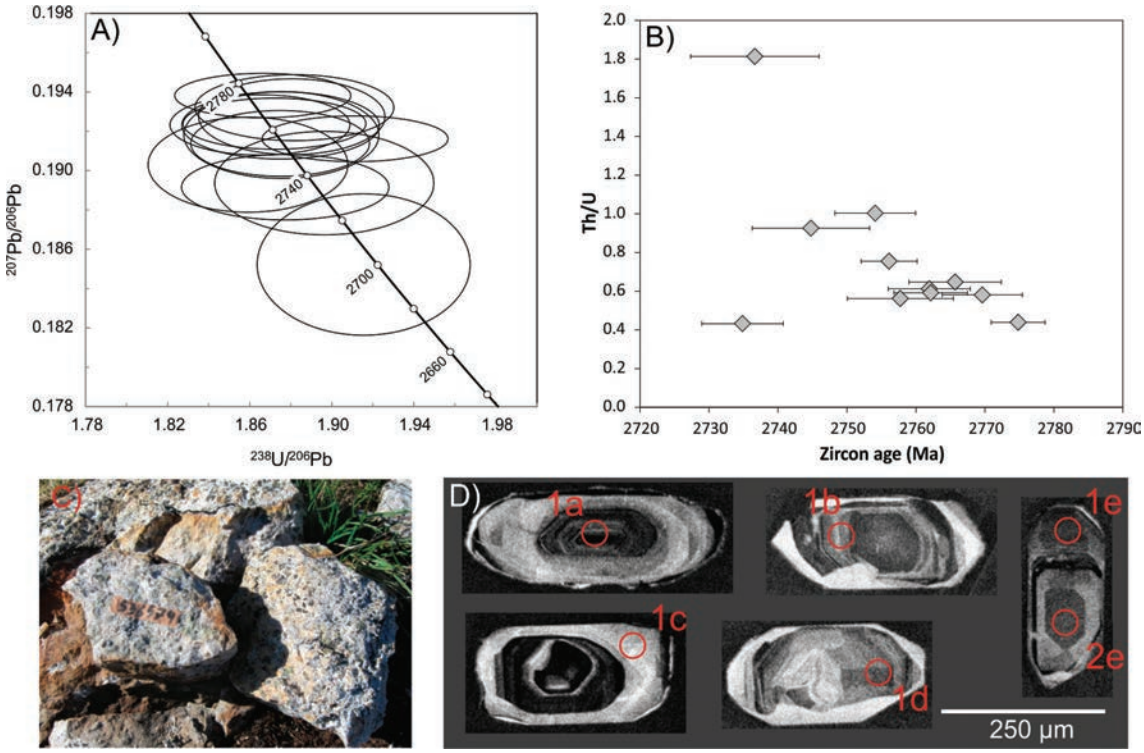

Figure 53. *Sample 536574. A) Tera-Wasserburg diagram with all data. B) Th/U versus age. C) Sample outcrop. D) CL images of analysed zircon grains, with indication of spot position. 1a: 2756 ± 4 Ma, 1b: 2766 ±7 Ma, 1c: 2700 ± 13 Ma, 1d: 2762 ± 6 Ma, 1e: 2754 ± 6 Ma, 2e: 2763 ± 5 Ma. Spots are 30 µm, $^{207}Pb/^{206}Pb$ ages. Errors are on 2σ level.*

Granitic migmatite / agmatitic gneiss (samples 523941 and 523942)

Description: Migmatitic granitic gneiss with an agmatitic texture. The enclaves are mainly mafic with a foliation that predates the weak foliation observed in the felsic matrix. There is a strain variation in the granitic matrix, where deformation is less developed in pressure shadow regions related to more competent mafic enclaves. Sample 523941 is sampled from a zone related to disintegration of mafic enclaves by felsic granitic melts (Figure 54A). Sample 523942 is from a leucocratic zone with little to no mafic enclaves (Figure 54B).

Purpose: The intrusive age of the granitic matrix, and information on zircon inheritance and to understand the difference between the different components of the agmatitic basement gneisses and granitoids.

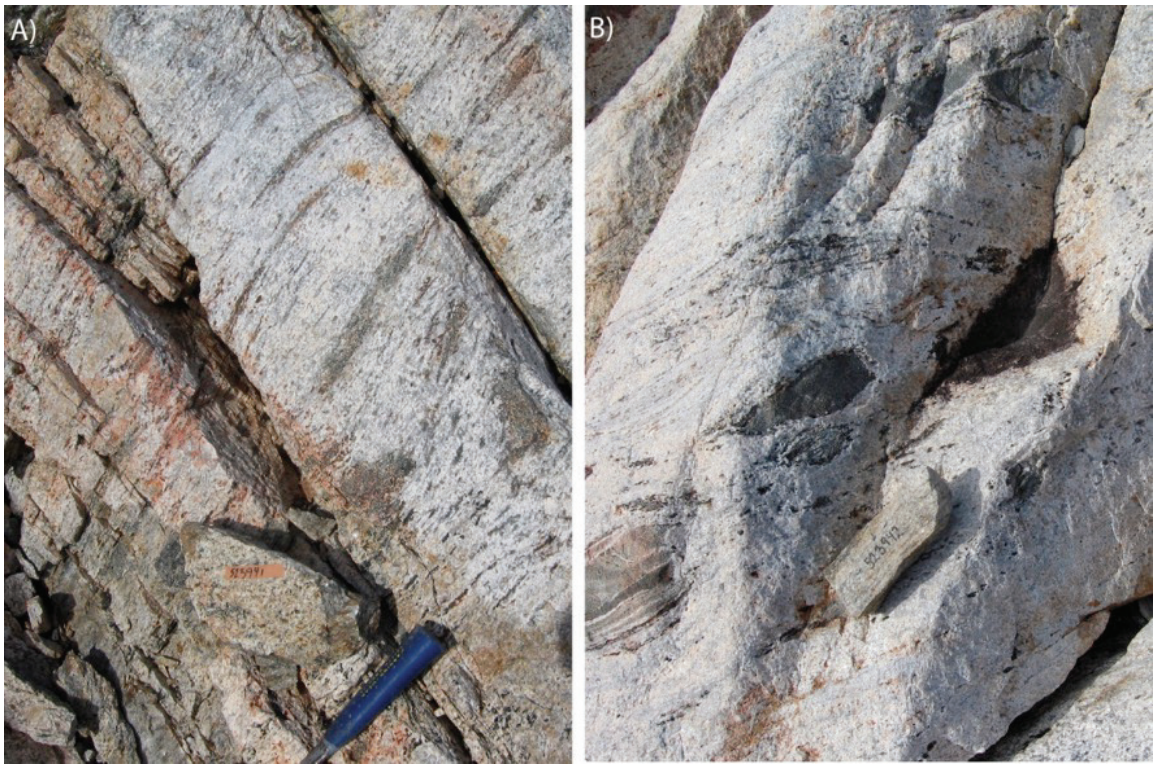

Figure 54. *Outcrop gneiss samples 523941 and 523942.*

Sample 523941

Analytical method: CL-imaging and Nordsim data.

Data description sample 523941: Zircon grains are prismatic with bright wide outer rims, growth-zoned to homogeneous inner rims (also as core) and variously altered cores (Figure 55C). Zircon grains have aspect ratios from 1:2 to 1:3 and vary from 200 to 400 µm in length. Zircon U-Pb age data are mostly concordant (Figure 55A) and $^{207}Pb/^{206}Pb$ ages range from 2718 ± 24 Ma to 2894 ± 4 Ma. The Th/U ratios range from 0.2 to 2.1 with a larger spread and higher values for the younger ages that are related to rims (Figure 55B). Analyses from the bright rims yield an average $^{207}Pb/^{206}Pb$ age of 2738 ± 14 Ma and a Concordia age of **2731 ± 7 Ma**. Analyses from inner rims and sector-zoned grains have relatively restricted Th/U ratios and we obtain an average $^{207}Pb/^{206}Pb$ age of 2809 ± 3 Ma and a Concordia age of **2808 ± 3 Ma**. One analysis from a core yields an age of 2894 ± 4 Ma.

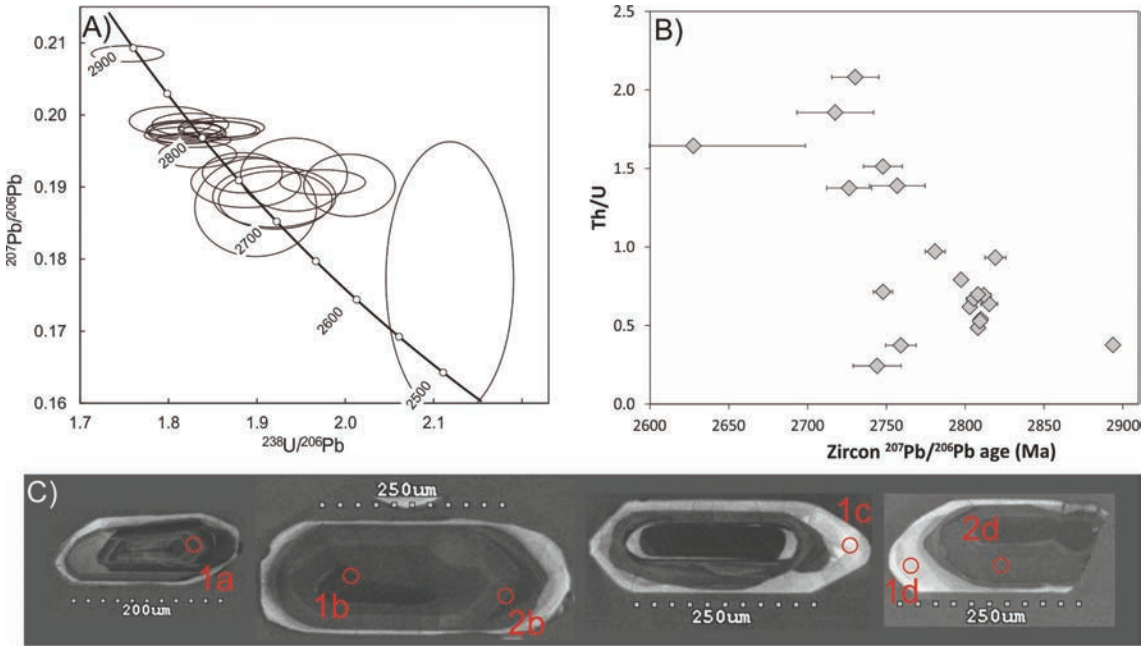

Figure 55. *Sample 523941 A) Tera-Wasserburg diagram. B) Th/U versus age diagram. C) CL images with indicated spot positions, $^{207}Pb/^{206}Pb$ ages, 1a: 2894 ± 9 Ma, 1b: 2744 ± 15 Ma, 2b: 2812 ± 5 Ma, 1c: 2718 ± 24 Ma, 1d: 2748 ± 12 Ma, 2d: 2808 ± 4 Ma. Errors are on 2σ level.*

Sample 523942

Analytical methods: CL-imaging; GEUS LA-ICPMS and Nordsim data.

Data description and interpretation: Zircon grains are prismatic rounded and oblate and 200 to 500 µm in length. Internal textures are dominated by CL-bright rims and growth- to sector- zoned CL-grey cores or inner rims and in many cases strongly altered core domains (Figure 56C) Some rounded grains are clear and transparent in normal light and have grey sector-zone cores with thin bright rims. Zircon U-Pb data have been obtained by SIMs and LA-ICPMS. The obtained data are relatively concordant, with only a few analyses being normal discordant. The $^{207}Pb/^{206}Pb$ ages vary from 2407 ± 72 Ma (2688 ± 47 Ma SIMs) to 2883 ± 70 Ma (2838 ± 9 Ma, SIMs) (Figure 56A). Th/U ratios display large scatter and vary between 0.1 and 2 with no obvious correlation with age, except that the >2800 Ma core domains (SIMs data) are mainly around 1.4 to 1.8 (Figure 56B). There is a clear relationship between textural domains and age (core-rim): Analyses in core domains yield a Concordia age of 2813 ± 12 Ma (MSWD = 0.16; SIMs age) and a $^{207}Pb/^{206}Pb$ age of **2793 ± 19 Ma** (MSWD = 0.49; LA-ICPMS), which is interpreted as the crystallisation age of an inherited population. Analyses of rims yield an intercept age of **2717 ± 28 Ma** (MSWD = 1.3; SIMs age) and a $^{207}Pb/^{206}Pb$ age of 2731 ± 34 Ma (MSWD = 1.09; LA-ICPMS), which is interpreted as the crystallisation age of the leucocratic granite.

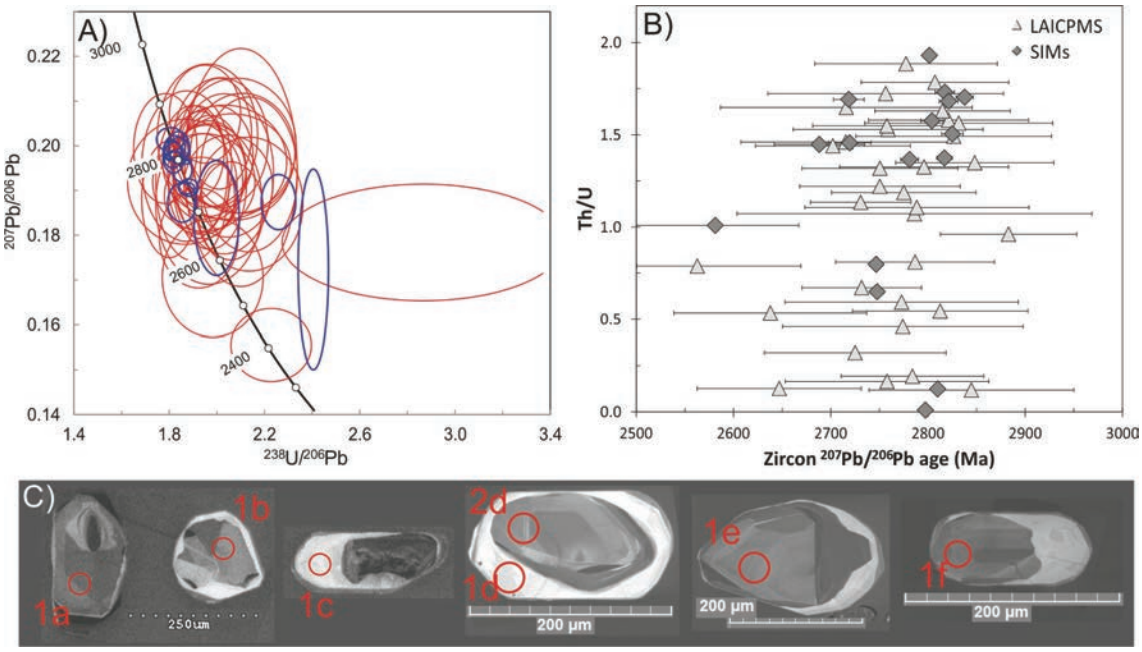

Figure 56. *Sample 523942 A) Tera-Wasserburg diagram, blue: SIMs data, red: LA-ICPMS data. B) Th/U versus age diagram. C) CL images with indicated spot positions, $^{207}Pb/^{206}Pb$ ages, 1a: 2821 ± 10 Ma, 1b: 2825 ± 11 Ma, 1c: 2719 ± 16 Ma, 1d: 2702 ± 80 Ma, 2d: 2751 ± 80 Ma, 1e: 2827 ± 101 Ma, 1f: 2815 ± 70 Ma. Errors are on 2σ level.*

Leucocratic granite (sample 523947)

Description: Similar rock types as described for sample 523941 and 523942. Sample 523947 is from a leucocratic zone that contains abundant disintegrated enclaves.
Purpose: Age of leucocratic granite and age of inheritance.
Analytical methods: CL-imaging; Nordsim data.
Data description and interpretation: Zircon grains are mainly prismatic or oblate and 150 to 300 µm in length. Internal textures are dominated by CL-bright rims with sector-zoned and homogeneous textures, and core regions that seem to consist of inner sector- zoned rims/mantles and relatively darker and small xenocrystic cores with textures varying from strongly altered to growth-zoned (Figure 57C). Zircon U-Pb analyses are relatively concordant with $^{207}Pb/^{206}Pb$ ages ranging from 2644 ± 39 Ma to 2848 ± 12 Ma (Figure 57A). There is no clear age distinction between analyses in bright rims and analyses in core domains. However Th/U ratios are clearly distinct from core and rim domains, with core values varying between 0.1 and 1 and rim values between 3.2 and 4.6 (Figure 57B). Rim analyses yield an Concordia age of **2724 ± 17** Ma (MSWD = 0.22) and a similar mean $^{207}Pb/^{206}Pb$ age of 2723 ± 24 Ma (MSWD = 3.5). This age is interpreted as the crystallization age of the granite. Core regions are complicated by the strong overprinting and core-mantle domains that are difficult to distinguish, however, selecting the concordant group of analyses (excluding a single distinctly older analysis) we obtain a weighted mean $^{207}Pb/^{206}Pb$ age of 2742 ± 8 Ma with a high MSWD (n = 10; MSWD = 14); this age likely to reflect a mixed age. One xenocrystic core is documented with an age of 2829 ± 4 Ma.

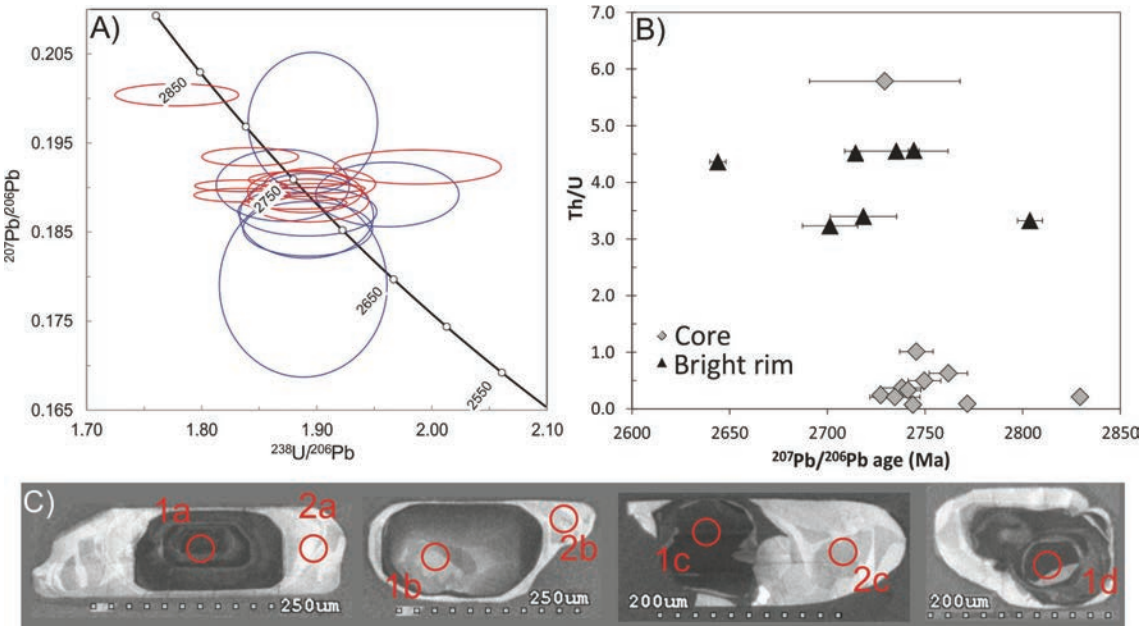

Figure 57. *Sample 523947 A) Tera-Wasserburg diagram, blue: bright rim, red: core. B) Th/U versus age diagram. C) CL images with indicated spot positions, $^{207}Pb/^{206}Pb$ ages, 1a: 2727 ± 3 Ma, 2a: 2701 ± 11, 1b: 2738 ± 8 Ma, 2b: 2719 ± 10, 1c: 2741 ± 2 Ma, 2c: 2735 ± 13 Ma, 1d: 2829 ± 4 Ma. Errors are on 2σ level.*

Leucocratic inclusion-rich granite (sample 523949 and 523950)

Description: Sample 523949 and 523950 is from the same outcrop, 523949 is leucocratic granite from a zone that contains abundant enclaves that have reacted with the leucocratic melts, sample 523950 are from a slightly more melanocratic zone (Figure 58).
Purpose: Age of leucocratic granite and age of inheritance.

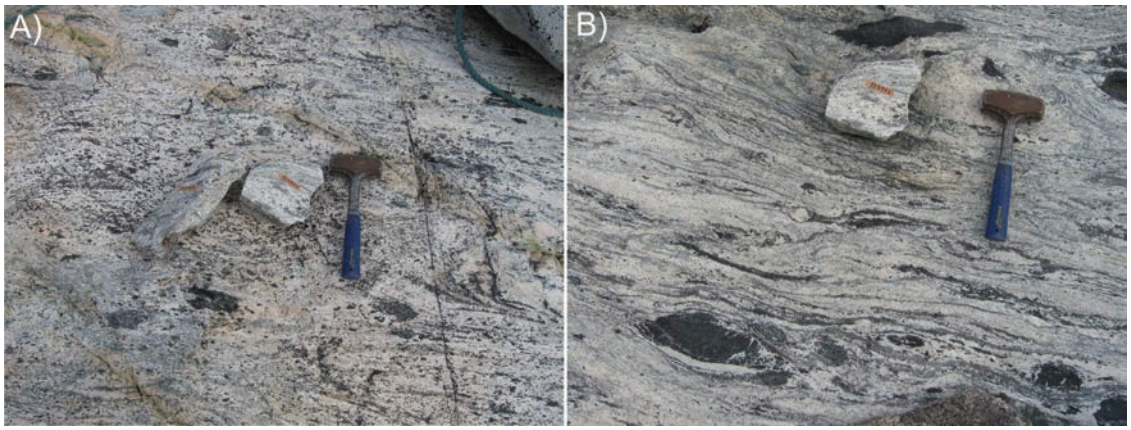

Figure 58. *Field images A) sample 523949, B) sample 523950.*

Leucocratic granite (sample 523949)

Analytical methods: CL-imaging; Nordsim data.

Data description and interpretation: Zircon grains are mainly prismatic with aspect ratios around 1:2 to 1:3 and 150 to 300 µm in length, but also include a few rounded grains. Internal textures are dominated by CL-bright rims and growth- to sector-zoned CL-grey cores and/or inner rims, and in some cases strongly altered inner core domains. Some stubby (aspect ratio ca. 1:1) grains are clear and transparent in normal light and have grey sector-zone cores with thin bright rims (Figure 59C). Zircon U-Pb data are concordant with $^{207}Pb/^{206}Pb$ ages that range from 2718 ± 13 Ma to 2915 ± 7 Ma (Figure 59A). There is an overall negative correlation of Th/U ratios (0.25 to 1.8) with age (Figure 59B). Age data fall into three groups, the youngest group that corresponds to the bright rims yields an Concordia age of **2722 ± 7 Ma** (MSWD = 0.14), inner rims and stubby grains yield a Concordia age of **2784 ± 6 Ma** (MSWD = 2.8) and the core domains yield an age of **2891 ± 11** (MSWD = 0.083). All grains have wide and bright rim domains and the Concordia age of 2722 ± 7 Ma is interpreted as magmatic, reflecting the crystallisation age of the leuco-granite. Both the inner rim (2784 ± 6 Ma) and the core domains (2891 ± 11) are interpreted as inherited and the growth-zoned texture of the inner rim domains suggest that these and the core domains are originally igneous grain.

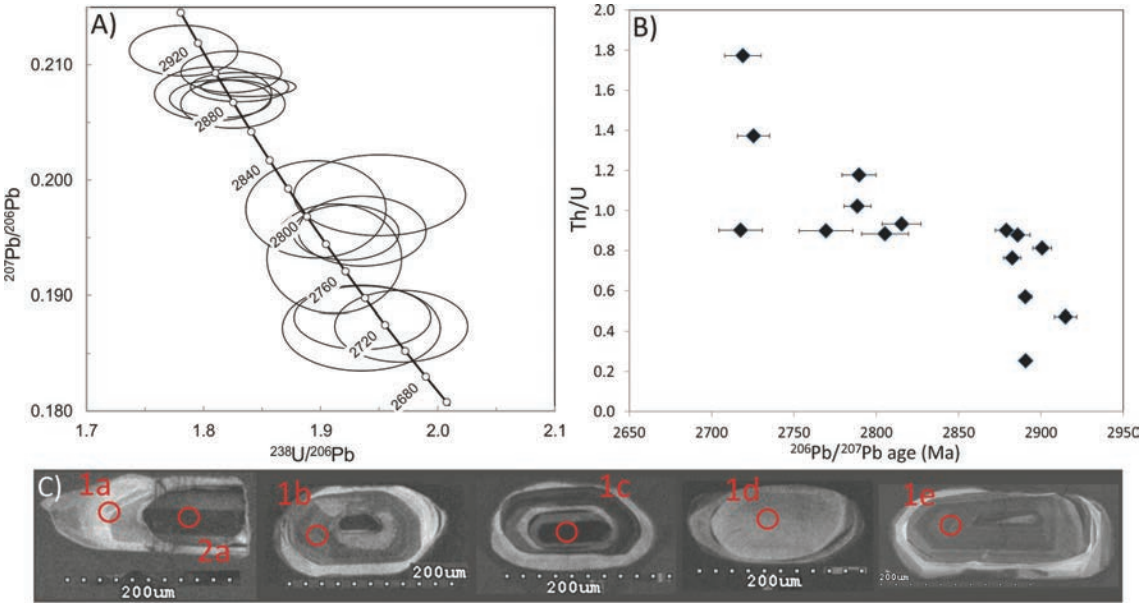

Figure 59. *Sample 523949 A) Tera-Wasserburg diagram, blue: bright rim, red: core. B) Th/U versus age diagram. C) CL images with spot position indicated, $^{207}Pb/^{206}Pb$ ages , 1a: 2727 ± 3 Ma, 2a: 2701 ± 11, 1b: 2738 ± 8 Ma, 2b: 2719 ± 10, 1c: 2741 ± 2 Ma, 2c: 2735 ± 13 Ma, 1d: 2829 ± 4 Ma. Errors are on 2σ level.*

Leucocratic granite (sample 523950)

Analytical methods: CL-imaging; SHRIMP II data.
Data description and interpretation: Zircon grains are prismatic or oblate with aspect ratios around 1:2 to 1:3 and 150 to 300 µm in length. Internal textures are dominated by CL-bright growth- and sector-zoned rim domains and CL-darker core regions that are xenocrystic and either display growth- or sector-zoned textures (Figure 60C). Zircon U-Pb data are concordant and spread out along the Concordia with $^{207}Pb/^{206}Pb$ ages ranging from

2690 ± 12 Ma to 3253 ± 7 Ma (Figure 61A). Th/U ratios show a clear relation to textural domains and to age, where the older core domains have Th/U ratios between 0.01 and 1.0 and the younger rim domains have ratios between 1 and 3 (Figure 61B). A main age population is obtained from a group of rim domains yielding a Concordia age of **2753 ± 6 Ma** (n = 11; MSWD = 0.51), which is interpreted as the crystallisation age of the leucogranite. Core domains range in age from 3253 ± 7 Ma to 2741 ± 10 Ma and are xenocrystic in origin. The three oldest core analyses yield a Concordia age of 3235 ± 20 Ma (n = 3, MSWD = 0.0027).

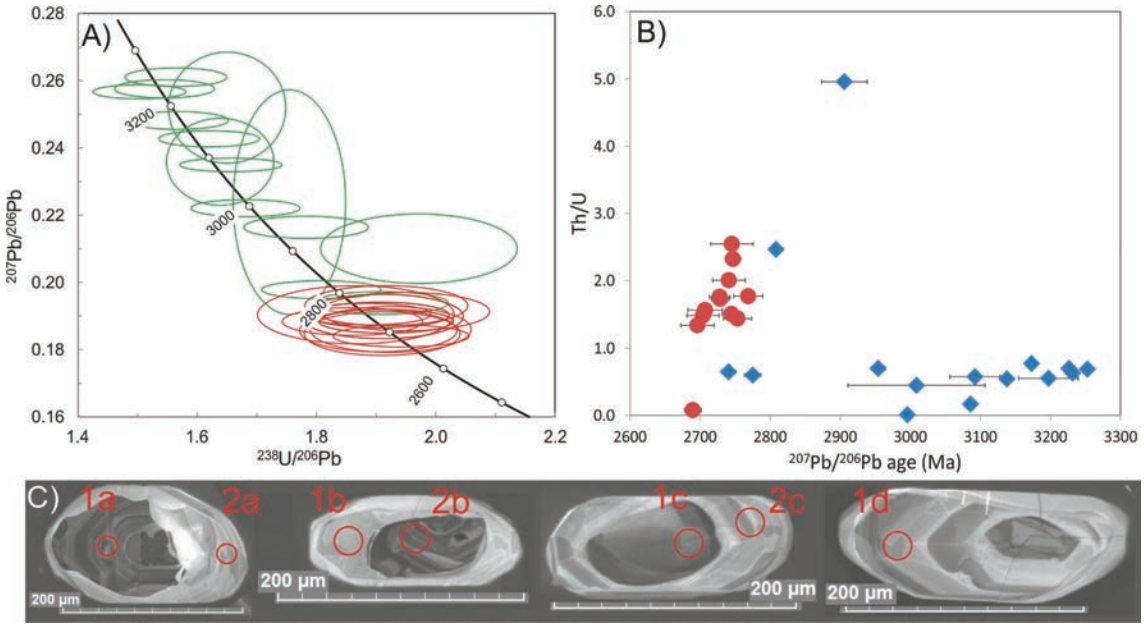

Figure 60. *Sample 523950 A) Tera-Wasserburg diagram, red: bright rim, green: core. B) Th/U versus age diagram, red: rim, blue: core. C) CL images with indication of spot positions, $^{207}Pb/^{206}Pb$ ages, 1a: 3232 ± 7 Ma, 2a: 2753 ± 21, 1b: 2906 ± 33 Ma, 2b: 3138 ± 6, 1c: 2808 ± 9 Ma, 2c: 2769 ± 21 Ma, 1d: 2728 ± 15 Ma. Errors are on 2σ level.*

Leucocratic granite (sample 523962)

Description: Similar rock types as described for sample 523941 and 523942.
Purpose: Age of leucocratic granite and age of inheritance.
Analytical methods: CL-imaging; Nordsim data.
Data description and interpretation: Zircon grains are mainly prismatic or oblate and 150 to 300 µm in length. Internal textures are dominated by CL-bright rims with sector-zoned to homogeneous textures, and core regions that consist inner sector-zoned rims/mantles and darker smaller xenocrystic cores that vary from strongly altered to growth-zoned (Figure 61C). Zircon U-Pb analyses are concordant and spread out along the Concordia (Figure 61A) with $^{207}Pb/^{206}Pb$ ages range from 2714 ± 9 Ma to 3076 ± 6 Ma. Th/U ratios range from 0.1 to 2.3 and display larger range and generally higher values for the analyses in rim domains (Figure 61B). A main age population is obtained from the rim domains and grouped together they yield a weighted mean $^{207}Pb/^{206}Pb$ age of **2728 ± 7 Ma** (n = 11, MSWD = 4.6),

which is interpreted as the crystallisation age of the leucocratic granite. Core domains are xenocrystic with $^{207}Pb/^{206}Pb$ ages ranging from 2819 ± 8 Ma to 3076 ± 6 Ma.

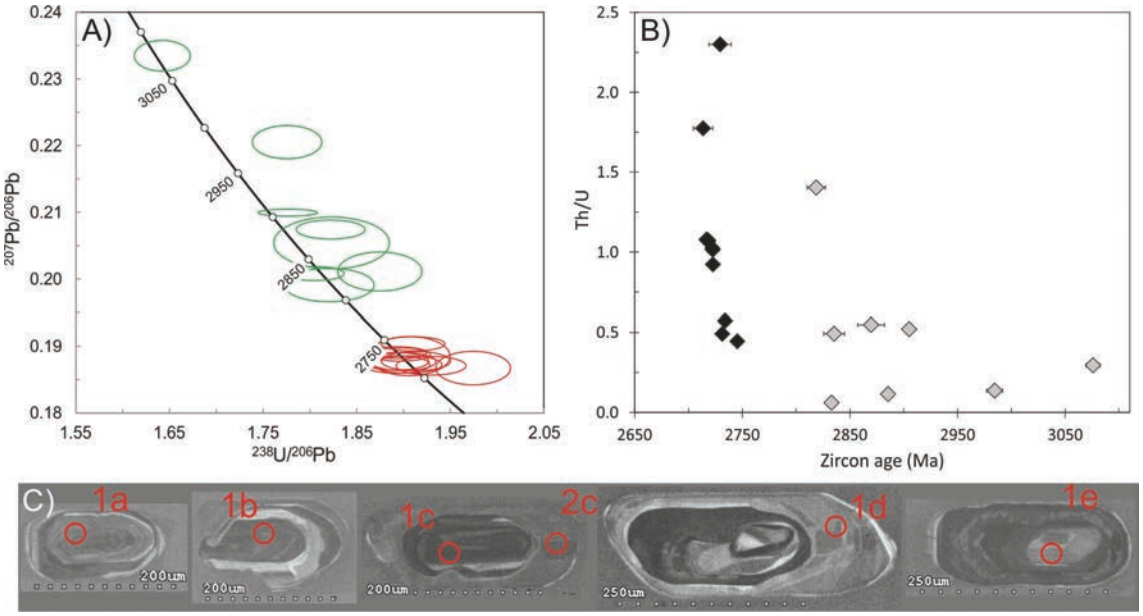

Figure 61. *Sample 523962. A) Tera-Wasserburg diagram, red: bright rim, green: core. B) Th/U versus age diagram C) CL images with indication of spot positions, $^{207}Pb/^{206}Pb$ ages, 1a: 3232 ± 7 Ma, 2a: 2753 ± 21, 1b: 2906 ± 33 Ma, 2b: 3138 ± 6, 1c: 2808 ± 9 Ma, 2c: 2769 ± 21 Ma, 1d: 2728 ± 15 Ma. Errors are on 2σ level.*

Leucocratic granite (sample 523983)

Description: Leucocratic granite with abundant mafic and ultramafic inclusion (Figure 62)
Purpose: Age of leucocratic melt and information on zircon inheritance.
Analytical methods: CL-images; Shrimp II data.

Figure 62. *Inclusion-rich granite or mafic unit intensively infiltrated by leucocratic melts.*

Data description and interpretation: Zircon grains are mainly prismatic or oblate and 150 to 300 µm in length. Internal textures are dominated by CL-bright rims with sector-zoned and homogeneous textures and core regions that include an inner sector-zoned rim/mantle and relatively darker, small cores that vary from strongly altered to growth-zoned (Figure 63D). Zircon U-Pb analyses are concordant and spread out along the Concordia (Figure 63A) with $^{207}Pb/^{206}Pb$ ages range from 2713 ± 20 Ma to 3885 ± 10 Ma. Th/U ratios range from 0.1 to 2.3 and display larger range and generally higher values for the analyses in rim domains (Figure 63B). Analyses from outer rims yield a weighted mean $^{207}Pb/^{206}Pb$ age of **2721 ± 7 Ma** (n = 8, MSWD = 0.64) which is interpreted as the crystallisation age of the leucocratic granite. Inner rim analyses yields a weighted mean $^{207}Pb/^{206}Pb$ age of **2790 ± 18 Ma** (n = 5, MSWD = 1.5), which is interpreted as inherited.

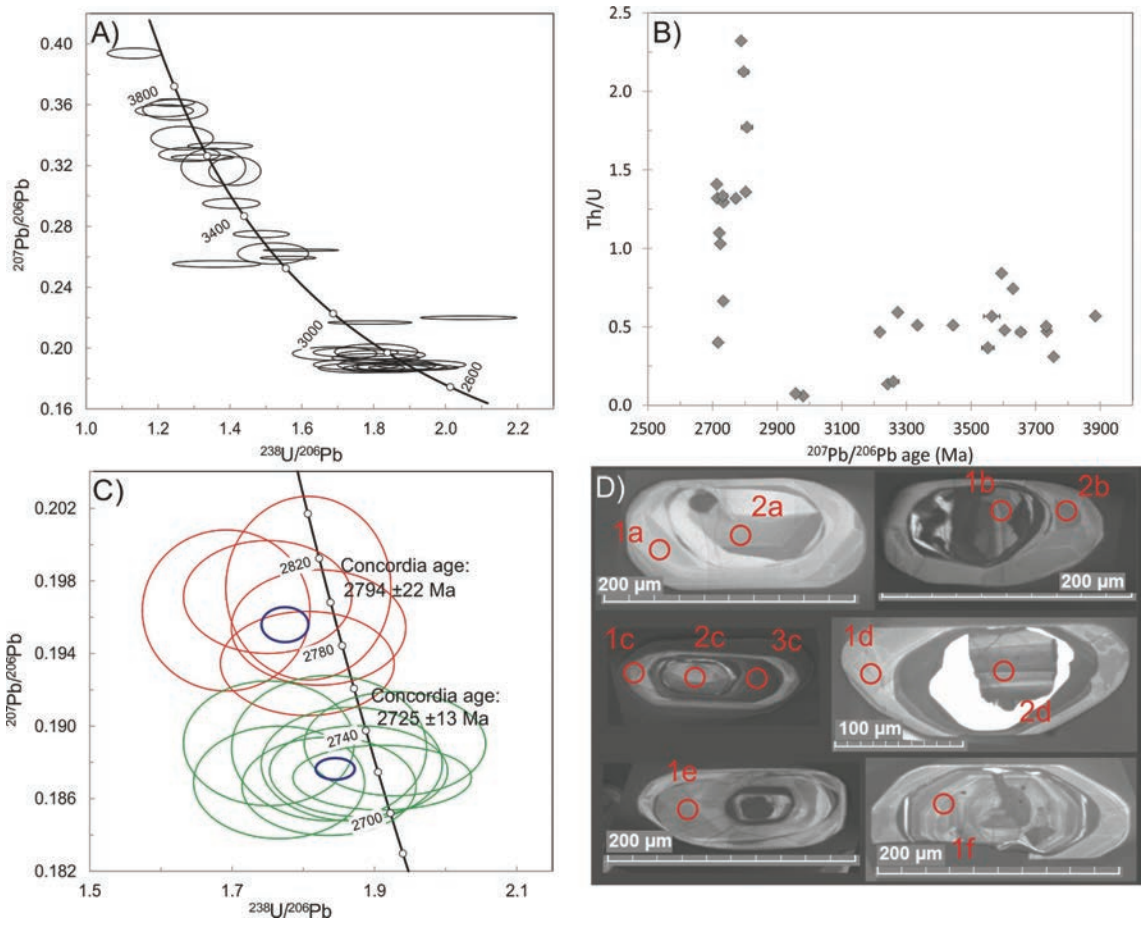

Figure 63. *Sample 523983 A) Tera-Wasserburg diagram with all data. B) Th/U versus age diagram. C) Inner (red) and outer (green) rim domains. D) CL images of analysed zircon grains: 1a: 2734 ± 12 Ma, 2a: 3654 ± 14 Ma, 1b: 3260 ± 17 Ma, 2b: 2713 ± 10 Ma, 1c: 2734 ± 10 Ma, 2c: 3885 ± 5 Ma, 3c: 2957 ± 3 Ma, 1d: 2724 ± 11 Ma, 2d: 3595 ± 4 Ma, 1e: 2788 ± 11 Ma, 1f: 3733 ± 7 Ma. Errors are on 2σ level.*

Leucocratic granite with mafic inclusion (sample 523991)

Description: Leucocratic granite with abundant mafic and ultramafic inclusion (Figure 64)
Purpose: Intrusion age and inheritance

Analytical methods: CL-images; Lund LA-ICP-MS data

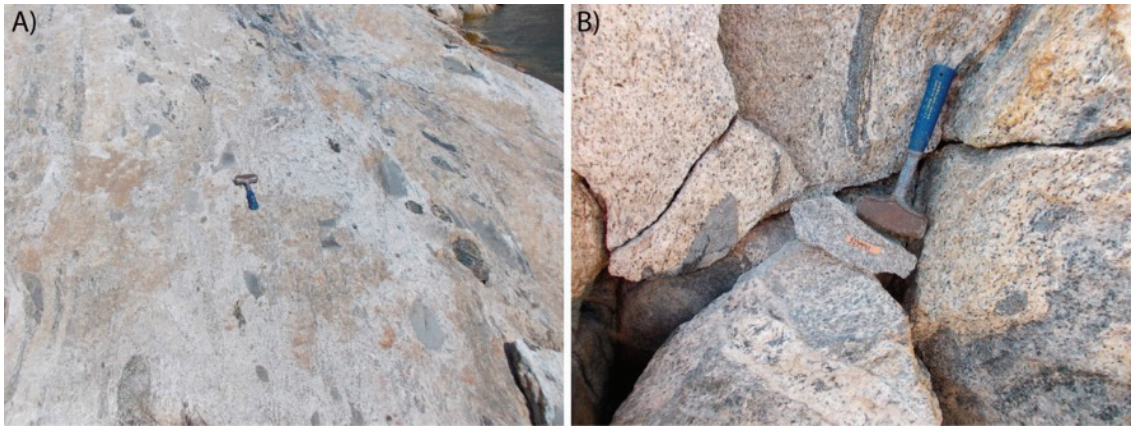

Figure 64. *Sample 523991. Field images showing the characteristic rock textures of the locality. (A) Leuco-granite with arrays of mafic inclusions making up an agmatitic texture. (B) Sample position for sample 523991, which is from a relatively undeformed and inclusion-free part of the outcrop.*

Data description and interpretation: Zircon grains are mainly prismatic, and from 100 to 300 micrometre in length. Internal textures usually consist of three domains, a core, an inner rim and an outer rim, all of which shoe growth- or sector-zoning (Figure 65C). In many grains it is however difficult to distinguish between inner and outer rim domains and inner rim and core domains. Zircon U-Pb age data display a spread along the Concordia with $^{207}Pb/^{206}Pb$ ages ranging from 2668 ± 15 Ma to 2919 ± 17 Ma (Figure 65A). A number of analyses are discordant and these do not display a well-defined Discordia intercept. Th/U ratios range from 1.3 to 0.1 (Figure 65B). From a selection of outer rim analyses we obtain a weighted mean $^{207}Pb/^{206}Pb$ age of **2740 ± 5 Ma** (n = 14, MSWD = 1.2), which is interpreted as the crystallisation age of the leucocratic granite. Analyses from inner rim domains yields a weighted mean $^{207}Pb/^{206}Pb$ age of **2801 ± 18 Ma** (n = 11, MSWD = 17).

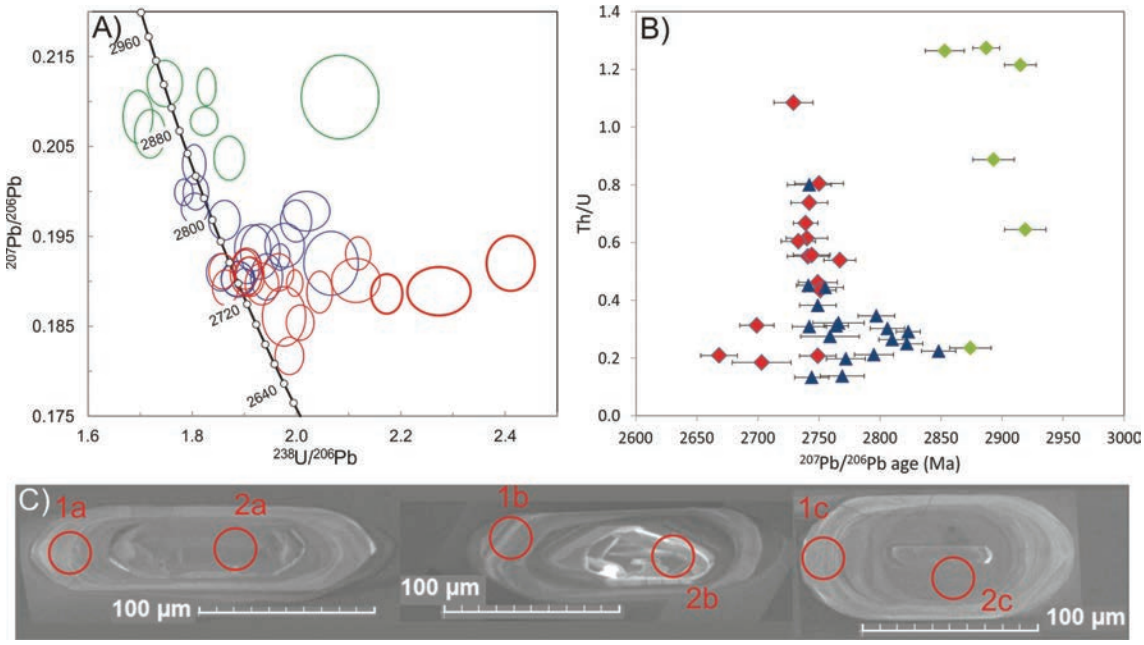

Figure 65. *Sample 523991 A) Tera-Wasserburg diagram with all data plotted, green: inner core, blue: inner rim, red: outer rim. Th/U versus age in Ma, same colour coding as in A). C) CL image of zircon textures. 1a, 2749 ± 16 Ma, 2a: 2848 ± 14 Ma, 1b: 2699 ± 14 Ma, 2b: 2874 ± 17 Ma, 1c: 2740 ± 14 Ma, 2c: 2797 ± 15 Ma. Errors are on 2σ level.*

References

Bagas, L., Næraa, T., Kolb, J., Reno, B. L., Fiorentini, M. L. 2013: Partial melting of the Archaean Thrym Complex of southeastern Greenland. Lithos 160–161, 164–182.

Bagas, L., Kolb, J., Fiorentini, M. L., Thebaud, N., Owen, J., Rennick, S., Stensgaard, B. M. 2016: On the processes that formed Archaean Ni-Cu sulfide mineralisation in the deep continental crust, Thrym Complex, southeastern Greenland. Precambrian Research 277, 68-86.

Berger, A., Kokfelt, T. F. and Kolb, J. 2014: Exhumation rates in the Archean from pressure–time paths: Example from the Skjoldungen Orogen (SE Greenland). Precambrian Research 255, 774-790.

Blichert-Toft, J., Rosing, M. T., Lesher, C. E., and Chauvel, C. 1995: Geochemical Constraints on the Origin of the Late Archean Skjoldungen Alkaline Igneous Province, SE Greenland. Journal of Petrology 36, 515-561.

Claoué-Long J. C., Compston W., Roberts J., Fanning C. M. 1995: Two Carboniferous ages: a comparison of SHRIMP zircon dating with conventional zircon ages and 40Ar/39Ar analysis. In: W.A. Berggren, D.V. Kent, M.-P. Aubrey, J. Hardenbol (Eds.), Geochronology Time Scales and Global Stratigraphic Correlation, Special Publication, Vol. 54, SEPM (Society for Sedimentary Geology), Tulsa, OK (1995), pp. 3–21.

Compston, W., Williams, I. and Meyer, C. 1984: U-Pb geochronology of zircons from lunar breccia 73217 using a sensitive high mass-resolution ion microprobe Journal of Geophysical Research: Solid Earth (1978–2012) 89, B525-B534.

Frei, D. and Gerdes, A. 2009: Precise and accurate in situ U–Pb dating of zircon with high sample throughput by automated LA-SF-ICP-MS. Chemical Geology 261, 261-270. doi:10.1016/j.chemgeo.2008.07.025.

Jackson, S., Pearson, N. J., Griffin, W. L. and Belousova, E. A. 2004: The application of laser ablation - inductively coupled plasma - mass spectrometry to in situ U-Pb zircon geochronology. Chemical Geology 211, 47-69.

Kalsbeek, K. and Taylor, P. N. 1993: Sm-Nd isotope age data from the Archaean Skjoldungen area, South-East Greenland. Internal GGU report, 159, 89-92.

Kokfelt, T. F., Næraa, T., Thrane, K. and Bagas, L. 2016: New zircon U-Pb and Hf isotopic constraints on the crustal evolution of the Skjoldungen region, South-East Greenland. Geological Survey of Denmark and Greenland Bulletin 35, 55-58.

Kokfelt, T.F., Thrane, K., Næraa, T., Klausen, M.B. and Tegner, C., 2016. Geochronology of the Skjoldungen Alkaline province, South-East Greenland, Geological Survey of Denmark and Greenland Report, 2016/11, 122 pp.

Kolb, J., Thrane, K., and Bagas, L. 2013. Field relationship of high-grade Neo- to Mesoarchaean rocks of South-East Greenland: Tectonometamorphic and magmatic evolution. Gondwana Research 23, 471-492.

Ludwig, K. 2008. Isoplot/Ex 3.70. A Geochronological Toolkit for Microsoft Excel. Berkeley Geochronological Center, Berkely, Special publication 4, 76 pp.

Ludwig, K. 2009. Squid2: A User Manual, rev. 12 Apr, 2009. Berkeley Geochron. Ctr. Spec. Pub. 5, 110 p

Nasdala L., Hofmeister W., Norberg N., Martinson J.M., Corfu F., Dörr W., Kamo S.L., Kennedy A.K., Kronz A., Reiners P.W. 2008. Zircon M257-a Homogeneous Natural Reference Material for the Ion Microprobe U-Pb Analysis of Zircon. Geostandards and Geoanalytical Research 32, 247-265.

Nielsen, T.F.D., Rosing, M. T. & Vasudev, V.N. 1988. Archaean gneisses of the Skjoldungen area, South-East Greenland. In Nielsen T. F. D (eds.): The Archaean terrains in South-East Greenland. Internal GGU report, 17-32.

Nutman, A.P., Rosing, M.T. 1994. SHRIMP U–Pb zircon geochronology of the late Archaean Ruinnæsset syenite, Skjoldungen alkaline province, South-East Greenland. Geochimica et Cosmochimica Acta 58, 3515–3518.

Paton, C., Woodhead, J., Hellstrom, J., Hergt, J., Greig, A. & Maas, R. 2010. Improved laser ablation U-Pb zircon geochronology through robust down-hole fractionation correction. G Cubed, 11, doi:10.1029/2009GC002618

Paton, C., Hellstrom, J., Paul, B.,Woodhead, J. and Hergt, J. 2011. “Iolite: Freeware for the visualisation and processing of mass spectrometric data.” Journal of Analytical Atomic Spectrometry. doi:10.1039/c1ja10172b.

Sláma, J., Košler, J., Condon, D.J., Crowley, J.L., Gerdes, A., Hanchar, J.M., Whitehouse, M.J. 2008. Plešovice zircon – a new natural reference material for U–Pb and Hf isotopic microanalysis. Chemical Geology 249, 1-35.

Stacey, J.S. and Kramers, J.D. 1975. Approximation of terrestrial lead isotope evolution by a two-stage model. Earth and Planetary Science Letters 26, 207-221.

Stern, R.A., Bodorkos S., Kamo S.L., Hickman A.A., Corfu F. 2009. Measurement of SIMS instrumental mass fractionation of Pb isotopes during zircon dating. Geostandards and Geoanalytical Research 33(2), 145–168.

Tusch, J. 2013. Lu–Hf Granatdatierung an Granuliten der Helge – Halbinsel in der Skjoldungen Alkaline Province, Süd – Ost – Grönland. Universität zu Köln, Institut für Geologie und Mineralogie, Bachelor thesis.

Whitehouse, M.J., Kamber, B.S., Moorbath, S. 1999. Age significance of U–Th–Pbzircon data from early Archean rocks of west Greenland – a reassessment basedon combined ion microprobe and imaging studies. Chem. Geol. 160, 210–224.

Whitehouse,M. J.& Kamber, B. S. 2005. Assigning dates to thin gneissic veins in high-grade metamorphic terranes: a cautionary tale from Akilia, Southwest Greenland. Journal of Petrology, 46, 291–318.